An Introductory Course in SubQuantum Mechanics

Alberto Ottolenghi

An Introductory Course in SubQuantum Mechanics

Alberto Ottolenghi*
Department of Computer Science, University College London, WC1E 6BT London, United Kingdom
(Dated: August 6, 2018)

Taking a reverse engineering approach in the search for simulations of Quantum Mechanics, a (re)formulation of SubQuantum Mechanics is proposed. The case of the one-dimensional free particle is analysed using a class of mathematical physics toy models proposed in the 1990s and based on interlaced diffusion processes, hereby identified as a key underlying source of the symplectic Hamiltonian synthesis. Such toy models are recalculated and reinterpreted within the context provided by the physics intuition proposed. Such approach suggests that higher contemporary arithmetics, combinatorics and probability-theory techniques should emerge as a natural mathematical language for SubQuantum Mechanics. A meaningful connection is identified between these ideas and the experimental work done in micro-fluid-dynamics to reproduce features of Quantum Mechanics with experimental classical micro-physics. Selected concepts are then discussed which can support the structuring of a broad SubQuantum Mechanics mathematical physics program based on this highly contextual realistic framework.

CONTENTS

* alberto.ottolenghi@hotmail.com, a.ottolenghi@ucl.ac.uk

I. DO WE REALLY UNDERSTAND CLASSICAL MECHANICS?

At the beginning of the 19th Century, Hamilton identified the symplectic relationships in geometric optics. These were embedded in the lens optical table analysis resulting from the work of many talented scientists during the previous 150 years, starting with Galileo, Kepler and Newton. At the same time of Hamilton's work, the formulation of classical thermodynamics was finding its coherent form, also resulting from the previous 150 years of work on the subject, starting from the Otto-Carnot cycle and the experimental work of Hooke and Boyle, which initiated the theoretical formulation of thermodynamics with the ideal gas law. The culmination of this theoretical process, in parallel with the theory of geometric optics, did highlight that classical thermodynamics is also mathematically structured according to the same symplectic geometry. It was in parallel found that many other theories did encapsulate the same symplectic geometry, which due to its braided features perfectly and synthetically formalises at once also all of Newton's Laws of Mechanics. This led to the formulation of rational mechanics in its Hamiltonian form. The formal convergence of all these fields led to the omnipresence of the Hamiltonian and Lagrangian formalism.

Because of the early realisation by Legendre that such formalism is an optimisation methodology, as e.g. between mechanical and potential energy in mechanics, the Hamiltonian and Lagrangian formalism has also become almost omnipresent well outside the domain of physics. Most notably in optimal control theory, starting with Maxwell formalism for steam engine powered mechanical controls in the 19th Century. Then structured through much of R.Bellman work in the '50s, through which the classical action can be rediscovered from its formal connection to the concept of differential human action, and even as a *choice* of action, i.e. a decision, linking up to the formalism of decision making theory (see [1]). Therefore also closing the loop back to the original motivations to call the optimisation choice between kinetic energy and potential energy an *action*.

Although in time, it is the Hamiltonian formalism from geometric optics which has provided the abstract *a posteriori* justification for such unified approach, it would now seem more in line with the contemporary information theorists' approach to physics if we took the view that all these different theories are thermodynamics of some kind. Therefore the action of mechanics should be looked at as an inverted sign analogue of a form of entropy, which in turn needs to be thought of as a source of action. As a matter of fact, Quantum Field Theory tells us something close to this view, in a less straightforward way. Similarly the variational principle formulation for Hamiltonian systems effectively hints to the same idea. The natural use of opposite signs to be arising from the inverse relative context between macroscopic and microscopic, which are formally bridged by the logarithmic and the exponential functions. Classical position and momentum are therefore to be considered thermodynamical macroscopic variables. Averages in Quantum Mechanics do not precisely clarify in what sense they are thermodynamical variables, but can help in seeing how this could be. By looking back, we are led to recognise that there is an *a priori* natural conceptual unification of action and entropy, of inertia and entropy, already embedded in 19th Century physics. A NeoClassical reading of Classical Mechanics.

I.Kant formulated much of his philosophical framework largely motivated by the need of foundational concepts for the laws of mechanics as settled by the Newtonian synthesis. On the other side, Quantum Mechanics was formulated at the peak of the NeoKantian philosophy period, which boomed towards the end of the 19th and spilled well into the 20th Century, quite strongly in Germany. The NeoKantian school therefore tried to repeat for Quantum Mechanics what Kant did for Classical Mechanics, including through the work of E.Cassirer, who was born 8 years before M.Born in the same city and within the same social environment. Such work seems to remain unfinished. And the prevailing approach of our days seems to suggest that such framework cannot be completed at all. It would be quite appropriate if SubQuantum Mechanics could be understood as a base for a NeoClassical reading of Newtonian Mechanics. In time, it could become then a pre-Newtonian cognitive tool enabling to close the philosophical loop as well, while providing a base for a reformulation of Kant's philosophical structure beyond the NeoKantian approach, which had to stop at the Quantum Mechanical level.

The evolution equations of Quantum Mechanics need here to be considered as the result of an intermediate linear effective theory, whereby such equations' algebraic-combinatorial features reflect the combinatorial nature of the processes generating them. A class of combinatorial dynamics. The non-linear measuring process and its repetition provide the sampling process which leads to the Born rule statistics: they need to become additional parts of the same theory. We will draw an analogy with the statistical formalism and with the linear versus non-linear alternating techniques used in a large part of classical Machine Learning. This identifies an underlying statistical mechanics of a different kind from those studied in more established physical theories. In this sense we should use the term *Sub-Quantum Mechanics*. While the term *Combinatorial Mechanics* seems preferable to indicate its study independently from Quantum Mechanics.

In order to try to apply any Bell-like no-go theorem analysis to such framework, one has first to extend Bell-like hidden variables to a broader formalism, time-dependent and structured, which describes the sampling process and

its context. This would allow for example to discuss and analyse the evolution dynamics of the different samplings involved. Any additional variable involved in the sampling would then impact only at the sampling process level and should be considered as latent-only variables, rather than hidden, in the sense of very short lived, as discussed further below. Their cumulative effect would be zero by the conservation laws imposed by the persistency of the calibration. Therefore at least one set of hidden variables are themselves hidden at Bell's usual analysis level. In other words, at Bell-analysis level there has to be no visible or detectable inference causal effect. But during the sampling process there can be a temporary cross-balanced causal inference, local both in time and space, the balancing (double) bookkeeping of which, is kept by the calibration. Such an extension would enable the structuring of part of SubQuantum Mechanics and would seem to represent a separate area on its own, which has not been developed yet to the best of our knowledge. In this course, we will then sketch what seems to be the right approach and what conceptual reasons one can see for the Bell-like no-go theorems not to strictly apply to this framework. As such, SubQuantum Mechanics is not saying that anything that we know is wrong, on the opposite: it is taking all what we know as right, in order to improve the reverse engineering. The approach is to learn from Quantum Mechanics all that can be learned. In order to shape the path beyond the epistemological barrier which we seem currently to be in the slow process of trying to break through.

This conceptual methodology provides the need to quantise *from below*, in the sense of a deconstruction and reconstruction formalism, scaling down to SubQuantum level and back up all the way to Classical Mechanics level. The bridge between the different scale levels should start from an interlacing of Brownian-like processes, which generates a double symplectic structure, which in turn provides a physical *raison d'être* for the metaplectic group, the Maslov index and their formal link to hyperbolic geometry. This in turn provides a discretised source of Lorentz-boost invariance, to be discussed in this context with respect to a differential variation of physical strain, also arising through the deconstruction and reconstruction of the photon at absorption and emission. This in turn seems to intuitively clarify why gravity is difficult to quantise *from above*, whereby a quantisation *from below* might identify more naturally how gravity and other fields interconnect, as well as what is inertia and the dynamical nature of the equivalence principle. Quantum theories are hereby positioned as structures at intermediate scales. For the sake of providing intuition through analogies, quantum strings should be thought more as DNA, proteins or other ribbon like structures in molecular biochemistry, whereby SubQuantum building blocks are enormously smaller and initially will have to be excessively oversimplified. Such building blocks are likely to be quasi-one-dimensional objects, but they should not be confused with the strings of Quantum String Theories. A similar warning would apply if we were to compare the SubQuantum web discussed below and Loop Quantum Gravity formalism.

The study of the foundations of Quantum Mechanics becomes then ultra-high energy physics. SubQuantum Mechanics appears to be a pre-Newtonian structured statistical mechanics whereby the Born rule can be thought of as related to the first principle of thermodynamics, while the Lorentz-boost invariance can be thought of as related to the second principle of thermodynamics. Therefore unifying entropy and inertia. Entropy as inertia in transforming energy into work. Inertia as a form of SubQuantum entropy. Therefore the equivalence principle becomes the bridge for the link between entropy through to gravity and back.

When the complexity of the semi-classical limit becomes effectively untreatable with other techniques, it might be possible to study it by taking a direct limit from SubQuantum Mechanics to Classical Mechanics, bypassing Quantum Mechanics in a way (see also the discussion in the first paragraph of Section XI). This might prove relevant in order to deform accurately hyperbolic dynamics into elliptic or mixed, and vice-versa, at the semi-classical limit.

Can ANY description of physical reality be considered complete?

Whereby the word *reality* is here understood in relation to the word *real* in the sense of *royal*. Reality being what is imposed on us without the possibility of not accepting it, as a royal decision of the King.

II. ELEMENTS OF SUBQUANTUM PHYSICS

The early Bohr's and Schrödinger's hope of linking quantum and life encouraged many physicist and other scientists at trying to explain life with quantum mechanics. This failed. But lead to modern genetics and proteomics (see [2]). We will reverse such approach and draw analogies and ideas from genetics and life-related sciences to try to sketch the SubQuantum world. We will also draw from the physical intuition arising from the study of macroscopic quantum phenomena.

In addition to its *a posteriori* practical usefulness, this *macro-to-micro* approach presumes effectively that there is a hierarchical structure in nature, such that features at smaller scales are partially reproduced at some stage of higher complexity at higher scale. And that we can observe nature to infer ideas which can help us to guess how to reverse engineer matter structure at scales where our technology can not probe, yet. *Subtle is the Lord ...*

FIG. 1. Simplified representation of a straightened monomer chain. The toothpick schematically represents the axis of the chain. A coil of metal wire schematically represents a monomer. The full wire represent the chain. The colour is a proxy for the charge. The handedness is a proxy for the helicity. The handedness is the same whatever direction one looks at. The model shown here is a right-handed monomer chain. A double chain can be composed in several ways on this basis.

We will consider as SubQuantum building blocks quasi-one-dimensional objects which can organise themselves into chains, similarly to how each helix of DNA is built out of monomers units. The size and inertia of the building block of a chain's coil is related to Plank's action constant through the speed of light at which it propagates. Any coiled coil structure is likely to be related to the frequency of vibration of a double helix as it propagates, as a tentative very rough SubQuantum structural description of the photon.

To avoid confusion with quantum strings we will call such building blocks *SubQuantum monomers*, also to implicitly suggest that they should have further structure, such naming being prone to evolution. An early and much less structured prototype of such concept was introduced in 1964 by J.J.Fleming in [3] who called them *Sub-Quantum Entities*. We have preferred to take the hyphen away to clarify the holistic nature of the theory (wholistic as well, because of its unification potential), whereby the name SubQuantum is chosen only to structurally relate it to Quantum Mechanics, following Fleming's choice over fifty years ago. It should nevertheless be noted that, despite the choice of name, our approach has nothing to do with J.Grea's approach [4] in the years shortly after Fleming's paper, both of them developing in their own way de Broglie's ideas of that time. In fact, Grea started his analysis from Hamiltonian mechanics: in our context his approach appears like starting from the laws of classical thermodynamics to derive statistical mechanics, rather than the other way around; any analysis on such basis can therefore only lead to an impossibility conclusion because of the reversed logic. Other later uses of the term also do not seem to be in line with our framework.

For simplicity, each SubQuantum monomer is assumed to have two internal binary properties. We might think at them as SubQuantum dyons, and we might be tempted to use this as an alternative name, by analogy to the Schwinger-Zwanziger concept of dyons, the evolution of Dirac's concept of monopole which led to Seiberg-Witten theory of particles' electric charge arising from a condensation of quantum dyons (see [5] and references therein). For the benefit of our physical intuition, we will think that their internal properties are *(i)* positive or negative charge, whereby charge interaction is to be understood only by contact, and *(ii)* positive or negative helicity. This can be thought in analogy to the way DNA monomers can hold positive or negative bases and then twist, aligned with one or the opposite direction along one of the two DNA chains. An oversimplified single chain, straightened on a line, is represented by the model in Figure 1.

Chains of monomers can organise themselves into double chains, similarly to the DNA. Or they can organise in other ways. Including into a quadrupolar web, by linking up through quadrupolar junctions, similarly to the Holliday junction intermediate structure observed in genetic recombinations (see [6]). Such quadrupolar web will be called the *SubQuantum web*. In its simplest form, it can be pictured as building up a diamond like structure in three-dimensional space, as very schematically sketched in Figure 2. This would be the topology corresponding to an isotropic, case.

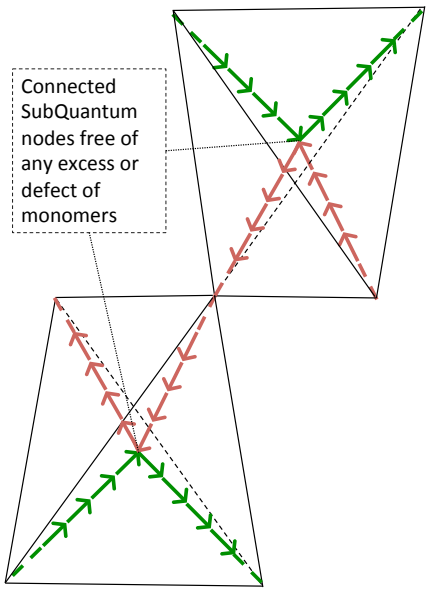

FIG. 2. Very schematic sketch of the simplest diamond-like configuration of the SubQuantum web of monomer chains, in quadrupolar coordination at each node. Monomers in green (red) can be thought of as positive (negative) charge. Arrows up (down) can be thought of as right (left) handed. Real $3D$ models can be build as art-work by using polystyrene balls as connectors and the toothpick model of Figure 1 in different colours and handedness.

The stabilisation of a double helix vibration moving through such a SubQuantum web is to be enabled by the relative structure of web and photon. When the four chains meeting at a node have each a different combination of charge and helicity, the node can be seen as neutral of both binary internal properties. It can be intuitively thought of as formed through a condensation during cosmological inflation, the inflation speed-up to be intuitively related to a volume increase similar to the one observed from the inverse sublimation of water vapour into ice. It could also be considered in the search for a modelling of Modified Newtonian Dynamics semi-empirical formulas and as a contributor to dark energy.

The SubQuantum web can decompose and recompose through a superplasticity which provides a key ingredient for the understanding of inertia and can be thought of as a self-correcting combinatorics of its components. Such a web is not an ether for the transmission of electromagnetic waves, but it can be an ether for the transmission of gravitational waves. It is an enabling medium for other physical features. For example, its degrees of freedom do contribute to any wave function and therefore it participates in quantum interference. Its physical limits would naturally imply a correction to the gravitational force in very extreme cases. It could cause a weakening correction to the gravitational force with respect to current theoretical levels, intuitively in the case of excessive stretch. It could also cause an opposite correction to the gravitational force, intuitively in case of reaching the limits to compression, or melting at the core of a black hole, or in case of re-condensation as a source of black hole very high energy jets, or in a pre-inflationary cosmology swampland quasi-melted state. Just like diamond it can be thought of as formed or melted out of very high pressure environment, in this case understood in the sense of a quantum-gravity-like strong-force regime. C.Rovelli white hole proposal (see [7]), as an alternative to black hole full evaporation, seems more natural from this perspective, whereby Beckenstein-Hawking formulas (see [8]) should be seen as a Bohr-Sommerfeld kind of approximation coming from the semi-classical formalism used to derive them, which has an asymptotic character.

By analogy with the macroscopic quantum physics of electronic instabilities in solids (see [9]), couples with both monomers of the same charge and opposite helicity will be called positive or negative Coopers pairs ($cp\pm$). Monomers couples of opposite charges and same helicity will be called positive or negative helicity virtual-photon-like pairs ($ph\pm$). We can see here how comes D.Bohm could hardly have considered such an approach, despite his initial motivations were in line (see quote from the Bohm-Einstein correspondence in [10]). It would have been certainly emotionally unsettling for D.Bohm to start from the ideas used by the Bardeen-Cooper-Schrieffer team to beat him and D.Pines to the superconductivity theory, and therefore to the Nobel, just about on the finish line.

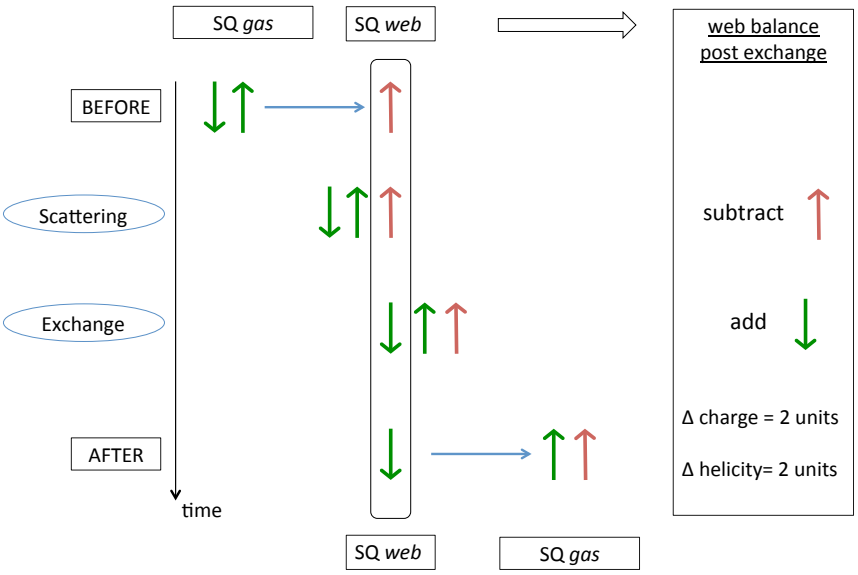

FIG. 3. Exchange of monomer between a couple in the SubQuantum gas and a node in the SubQuantum web.

We will not consider the other couples at this stage, as in this framework they would be either deemed to be unstable or being neutral of both charge and helicity. Such a restriction is made at this stage for the purpose of discussing the Quantum limit of SubQuantum Mechanics.

SubQuantum monomers can couple into pairs and can diffuse and scatter within the SubQuantum web, whereby we will here consider the scattering to be limited to the nodes of the web. We will assume at this stage that the pair coupling is stable if the charges or if the parities are opposite, effectively taking some very-ultra-small mechanical property as responsible for the couple formation. When a monomer couple hits a node, it can exchange one of the monomers with the web chains, therefore resulting in a change of monomer type as shown in Figure 3.

We would then like to build a wave function from these pairs and their dynamics, just like in macroscopic quantum phenomena one builds Ginzburg-Landau complex order parameters which satisfy quantum evolution equations. In the case of electronic instabilities, both the degrees of freedom of the couples of charge carriers and the degrees of freedom of the atomic structure of the solid do contribute to the mathematical construction of the complex order parameter (see [9]). In a similar way, the SubQuantum gas of coupled monomers and the SubQuantum web will have to contribute degrees of freedom enabling the construction of the wave function. Among the differences it should be recalled that in the case of macroscopic quantum phenomena, a non-linear term might appear in the evolution equation. This arises typically from the fact that the "wave function" is actually a complex Ginzburg-Landau parameter resulting from a collective effect, whereby the non-linear term is related to the direct interaction among each constituent. It should also be noted that in quantum optics, as photons have no mass, the difference between *(i)* the Ginzburg-Landau complex order parameter of the laser collective state and *(ii)* a quantum wave function, is very small if not observable at all. In this case the physics can often be confused to the study of a wave function, despite the physical density under scrutiny is the result of a collectively generated complex order parameter. Nevertheless, as the systems become more complex, such difference can become relevant, as in the calibration of numerous Qubit-like or Quantum-Logic-Gates-like devices, whereby the difference with the theoretical Qubit will start to show up because of the difference between a complex order parameter and a wave function. Similarly, decoherence theorists can often forget to be dealing with a quantum condensate.

Because of the structure of the couples above, either the couples do not change in type, or the scattering generates a combinatorial dynamics as in Figure 4. The continuous line corresponds to a circular dynamics (1) $\rightarrow$ (2) $\rightarrow$ (3) $\rightarrow$ (4) and the dotted line corresponds to a circular dynamics (1) $\rightarrow$ (4) $\rightarrow$ (3) $\rightarrow$ (2). We will call these *Ord-process* and *Reversed Ord-process* respectively because, to the best of our knowledge, the first one was first introduced in [11] at a strictly formal and less general reverse engineering level. The most general dynamics from Figure 4 mixes these $3D$ sub-process, although after a maximum of 8 steps part of the process is always repeated.

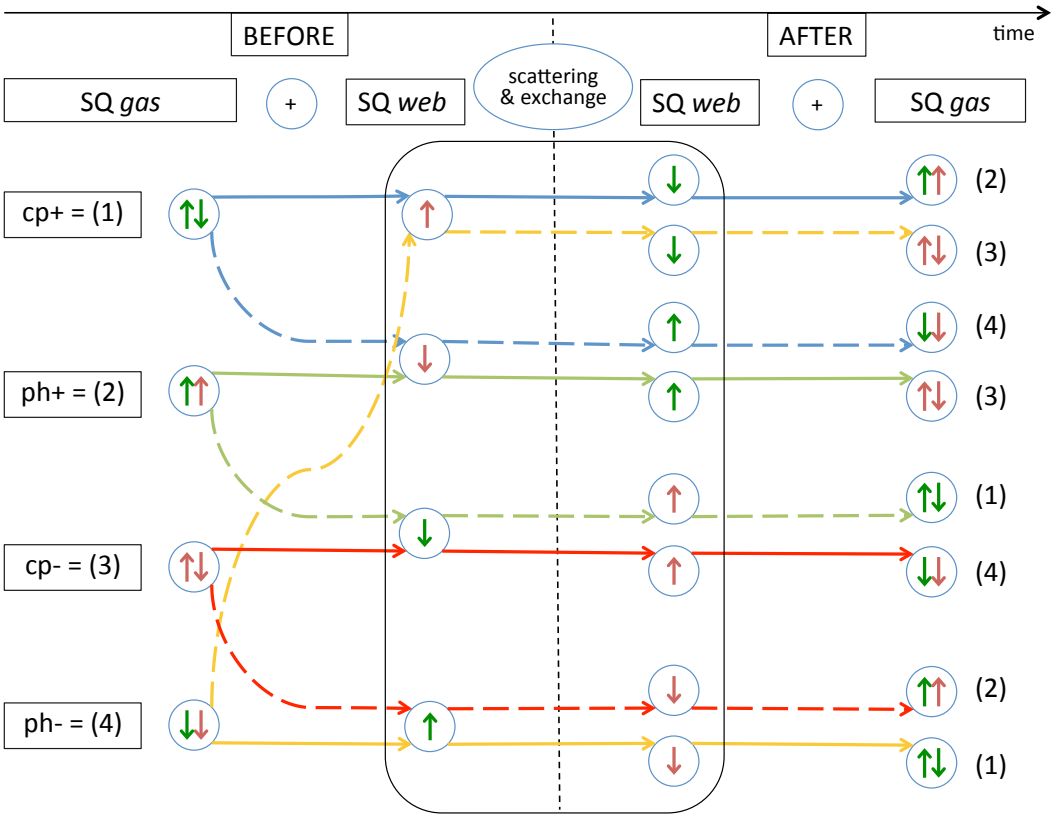

FIG. 4. Schematic representation of $3D$ combinatorial dynamics relevant for a discussion of the Quantum limit of SubQuantum Mechanics for the linear time evolution. Identified by analogy to macroscopic quantum phenomena arising from electron instabilities. The central area shows the evolution of the relevant monomer in the SubQuantum web, following a scattering by a couple of the SubQuantum gas, which in turn induces an exchange of monomer between SubQuantum web and SubQuantum gas, generalising the exchange process of Figure 3. The couples in the SubQuantum gas are shown on the left before the scattering and on the right after the scattering. There are two types of event which reproduce the same post scattering SubQuantum gas couple, which causes each type of SubQuantum gas couple to be observed on the right twice: a double-covering-like feature. By iterating the dynamics, there is a path of states for both the SubQuantum gas couple and the SubQuantum web monomer which one chooses to follow. There is then more than one path which leads to periodic dynamics of different kind. Each of the four colours corresponds to one of the four types of SubQuantum couples at the beginning of each iteration. The path following the continuous lines is closed and corresponds to a periodic dynamics. The same is true for the paths with dashed lines only.

These circular subprocesses appear to be mimicking a double realisation of the Klein group V. The quaternion group of order 8, Q_8, provides a double cover of the Klein group and seems to be embedded in such dynamics. From the diagram of Figure 4 one can actually build aperiodic or quasi-periodic words, but also all the words realising any subgroup of the quaternion group Q_8.

It should further be noticed that trough both the dotted and un-dotted periodic cycles, the accumulated variation of helicity and charge of the SubQuantum web is nil. This seems to be true for quasi-periodic words of this combinatorial dynamics. An example of the single step web variation is sketched in Figure 3. Looking at the web balance along these paths, the doubling process can model the evolution at the SubQuantum web level, with respect to the deficiencies caused by the exchanges with the SubQuantum gas. This in turn models the complex conjugate wave function.

In the semi-classical limit of Quantum Mechanics, classical periodic orbits tend to concentrate over themselves the key contribution to the wave function density. Similarly at SubQuantum level we can expect that it is mainly the cyclical processes and their effective intermittence which contribute in the Quantum limit. There would be then an ouroborology (in the sense of M.Berry, see [12]) allowing to take the Quantum limit of SubQuantum Mechanics. The discrete groups V and Q_8 seem then to be selecting the processes whose (quasi)periodicity provide the scale bridge from SubQuantum to Quantum Mechanics.

This approach looks similar to the ouroborology which appears in many features of the semi-classical limit of Quantum Mechanics. It will be by choosing and selecting such circular periodic processes that the reverse engineering of the evolution equations of Quantum Mechanics can be built. As for the semi-classical limit of Quantum Mechanics, the intuition is that the non-periodic or non-quasi-periodic dynamics tend to reduce to a white noise which becomes of low relevance in the limit, while the recurring dynamics stabilises and reinforces in the limit. To model the SubQuantum web, we need to take into account: *(i)* the complementary dynamics of the SubQuantum gas; *(ii)* some form of bookkeeping record system; and *(iii)* the auto-interacting features of the quadrupolar web. The pure auto-interacting features of the web might possibly be represented with a combinatorial proxy of the Satchdev-Ye-Kitaev model (see [13]), whereby one needs to extend the $1D$ lattice of the SYK model to the diamond lattice, then treat the randomness as a representation of the complementary diffusion process, and so on. Autocorrection should be an additional feature, requiring a SubQuantum version of the Pastawski-Yoshida-Harlow-Preskill model (see [14]), providing the dynamical link between inertia and gravity, but from a purely combinatorics pre-classical point of view.

In D=1, the SubQuantum web is reduced to a set of equally spaced points on a line and the couples can be simplified to two kinds of SubQuantum monomers, positive and negative charge, whereby the helicity is replaced by the direction of movement on the line. The kinematics and part of the dynamics are merged and the mathematical treatment can be highly simplified, whereby the SubQuantum monomers can be treated as point-like entities. The global circular dynamics above can then be easily formalised in D=1 as discussed in the next Sections.

The *it from bit* conceptualisation which appears to be quite useful in the study of the relationship between Quantum Mechanics, Information Theory and Quantum Gravity, is then reversed at SubQuantum level into a *bit from it* approach. It being the monomer, bit being the combinatorial codification of the dynamics. And due to the base-eight structure of the combinatorics for the Schrödinger case below, in such case we should call this a *byte from it* approach.

III. NON-RELATIVISTIC SUBQUANTUM FREE PARTICLE FOR D=1

In one dimension one can take helicity as the direction of movement. We will therefore use R and L to denote the helicity state. It is also possible to keep the $(+)$ and $(-)$ notation in Figure 4, but we should note that for the types $(1),(3)$ the $(+),(-)$ have a coherent physical meaning, and also for $(2),(4)$, but not for any other choice of pairing. It makes therefore sense to take the net density between (1) and (3) or between (2) and (4) but not otherwise. For the sake of discussing the $1D$ case we will consider that $(+)$ and $(-)$ relate to charge. Other equivalent realisations of the $3D$ combinatorial dynamics in Figure 4 can be compatible with this choice. If we classify the possible circular combinatorial dynamics which one can generate in $1D$ with this approach, as graphically shown in Figure 5, it will be clear that the only two Cases which allow to reverse engineer what we are after are the two we have immediately identified in $3D$ through Figure 4. In $1D$ we will then identify (1) with $(R,+)$, (2) with $(L,+)$, (3) with $(R,-)$ and (4) with $(L,-)$. These considerations allow to clarify the mapping of the combinatorial dynamics in Figure 4 with the one of [11], which is Case I in Figure 5. Differently from here, in the context of [11] the circular dynamics $(1)\rightarrow(2)\rightarrow(3)\rightarrow(4)$ had no physical motivation, not even tentative, other than its *a posteriori* practical formal use. We will compare this choice of combinatorics against the other five options of circular dynamics among four elements and clarify why we fall back on the two options singled out from Figure 4 anyways.

We therefore consider a regular one-dimensional lattice of period δ. We look at it every ϵ units of time in a stroboscopic reconstruction of time evolution. We therefore follow as much as possible the notations of [11]. We write first the time unit evolution of the densities of SubQuantum monomers over a time ϵ. At this stage, it is assumed that each of the possible events has equal probability. We choose Ord-process. Because of the circularity of the dynamics, at each node there is only one kind of monomer coming from the right and one kind from the left. We then count the number of monomers of each type at each node and each time-step with the densities p_i.

$$\begin{cases} p_1(m\delta,(s+1)\epsilon) = \frac{1}{2}p_1((m-1)\delta,s\epsilon) + \frac{1}{2}p_4((m+1)\delta,s\epsilon) \\ p_2(m\delta,(s+1)\epsilon) = \frac{1}{2}p_2((m+1)\delta,s\epsilon) + \frac{1}{2}p_1((m-1)\delta,s\epsilon) \\ p_3(m\delta,(s+1)\epsilon) = \frac{1}{2}p_3((m-1)\delta,s\epsilon) + \frac{1}{2}p_2((m+1)\delta,s\epsilon) \\ p_4(m\delta,(s+1)\epsilon) = \frac{1}{2}p_4((m+1)\delta,s\epsilon) + \frac{1}{2}p_3((m-1)\delta,s\epsilon) \end{cases} \tag{1}$$

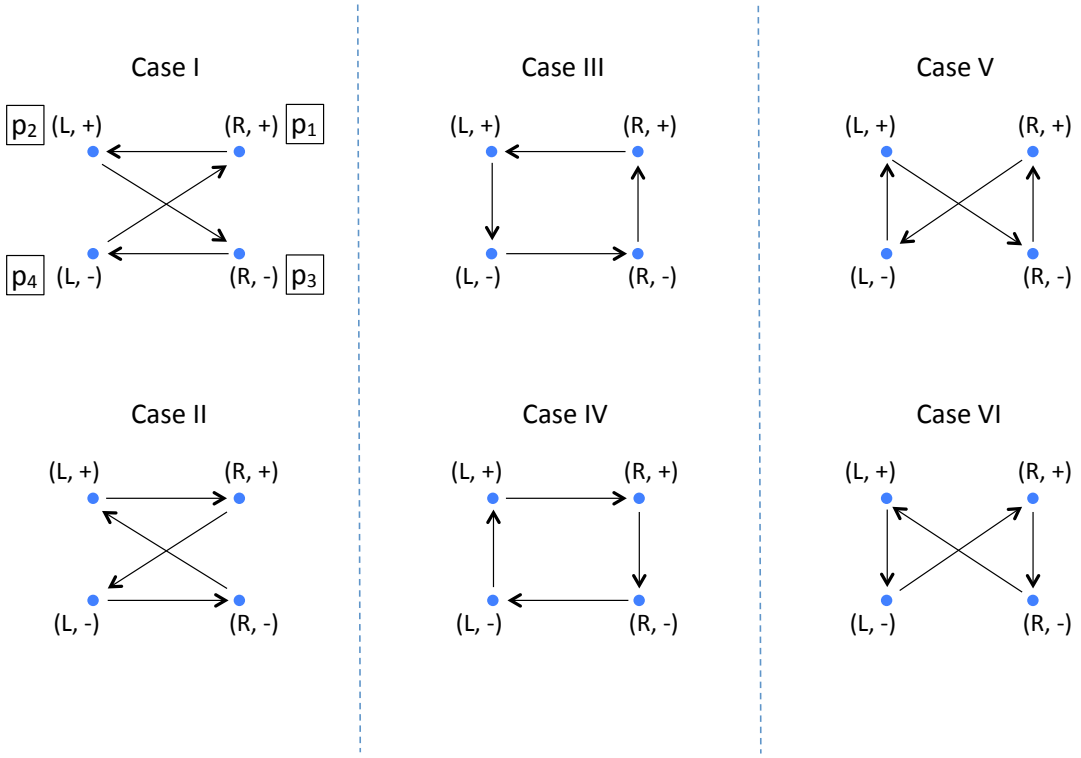

FIG. 5. Six options of combinatorial rotational dynamics for four elements. For simplicity, the arrows starting from each of the points and returning on themselves are not drawn: these correspond to the no-change of state events. Vertical arrows prevent the dynamics for the net densities to be a closed dynamic. Only Case I (the *Ord-process*) and Case II (the *Reversed Ord-process*) are free of vertical arrows. Each Case at the bottom is the reversed of the corresponding Case at the top.

For simplicity of notation we will omit the δ and ϵ until it is relevant to reintroduce them. Therefore we rewrite the process above with the following notation:

$$\begin{cases} p_1(m, s+1) = \frac{1}{2}p_1(m-1, s) + \frac{1}{2}p_4(m+1, s) \\ p_2(m, s+1) = \frac{1}{2}p_2(m+1, s) + \frac{1}{2}p_1(m-1, s) \\ p_3(m, s+1) = \frac{1}{2}p_3(m-1, s) + \frac{1}{2}p_2(m+1, s) \\ p_4(m, s+1) = \frac{1}{2}p_4(m+1, s) + \frac{1}{2}p_3(m-1, s) \end{cases} \tag{2}$$

At this point we consider only the net densities between the (1) and (3) and the net densities between the (2) and (4), as it is natural from the discussion above. In the $1D$ case this is equivalent to consider that the only relevant variables are the net charge density going to the right and the net charge density going to the left.

We totally discard all the other variables as not relevant for the reverse engineering, the net densities already encapsulating all the relevant information in the Quantum limit with respect to the linear time evolution. We are therefore performing a coarse graining and all processes with equal net values of the densities will be indistinguishable. The probability of transition (1/2) above will then have to be renormalised by a constant $\tilde{\alpha}$ to take into account indistinguishable paths.

We will not calculate the numerical value of $\tilde{\alpha}$ at this stage, because we will do more coarse graining later on and because it does not seem straightforward. The coarse graining required in this reverse engineering can be intuitively understood by the fact that in the Quantum limit, the periodic features dominate. The effective information sufficient for the description of the linear evolution equations at the Quantum scale is then concentrated around such periodic features. The evolution equations of Quantum Mechanics are therefore complete, if *complete* is to be understood in this specific way.

The way that this is achieved is by packaging together all that is indistinguishable because of the circularity enabling the scale change. It will be only when optimisation conflicts are maximal, typically at the semi-classical limit (a ionisation threshold, a ballistic transport regime, etc.), that any other degree of freedom might need to reappear locally in the form of a conflict resolution parameter: the Maslov index.

Therefore we retain only the net densities' process. Because we did throw away information, this is formally a new different process, derived from the initial process for the p_i, and as clarified by the introduction of the constant $\tilde{\alpha}$.

$$\begin{cases} \tilde{\phi}_1 = p_1 - p_3 \\ \\ \tilde{\phi}_2 = p_2 - p_4 \end{cases} \tag{3}$$

$$\begin{cases} \tilde{\phi}_1(m, s+1) = \frac{\tilde{\alpha}}{2}\tilde{\phi}_1(m-1, s) - \frac{\tilde{\alpha}}{2}\tilde{\phi}_2(m+1, s) \\ \\ \tilde{\phi}_2(m, s+1) = \frac{\tilde{\alpha}}{2}\tilde{\phi}_1(m-1, s) + \frac{\tilde{\alpha}}{2}\tilde{\phi}_2(m+1, s) \end{cases} \tag{4}$$

$\tilde{\alpha}$ is a normalisation constant, which we will not evaluate until all the steps of coarse graining are completed. In the case of the choice of Ord-process, the rotational dynamics is such that the net densities variable have their own closed dynamics. This turns our to be true also for the Reversed Ord-process, which is Case II in Figure 5, whereby Ord-process is Case I. When considering the other possible rotational dynamics of four elements, which are Case III to VI in Figure 5, the net densities do not result into a closed dynamics (see also Appendix A). This is because it is the transitions along the vertical lines that prevent a closed dynamics. If we write the corresponding net densities on the left hand side, in fact, the terms on the right hand side which should be netted in order to get $\tilde{\phi}_1$ now depend one on $(m+1)$ and the other on $(m-1)$ rather than both from $(m-1)$, and the same for the terms related to ϕ_2 rather than both from $(m+1)$. Therefore the combinatorics form Case III to VI do not allow to express the $\tilde{\phi}_i$ in terms of themselves.

The only two closed dynamics resulting into a closed net densities' form, correspond to the two cases identified from Figure 4, by using continuous lines only or dotted lines only respectively. One can also check easily that Case III to VI do not appear within the overall combinatorial dynamics in Figure 4.

We then look at the complex combination $\tilde{\psi} = \tilde{\phi}_1 + i\tilde{\phi}_2$. As we will be taking the limit for ϵ and δ going to 0, we can look at the $\tilde{\phi}_i$ as continuous functions. We can then take the zeroth-order approximation in the development of the space variable around the value m, $\tilde{\phi}_i(m \pm 1, s) \sim \tilde{\phi}_i(m, s)$, and therefore:

$$\tilde{\psi}(m, s+1) \simeq \frac{\tilde{\alpha}}{2}\tilde{\psi}(m, s) + \frac{i\tilde{\alpha}}{2}\tilde{\psi}(m, s) = \frac{1+i}{\sqrt{2}}\frac{\sqrt{2}}{2}\tilde{\alpha}\ \tilde{\psi}(m, s) = e^{i\frac{\pi}{4}}\frac{\tilde{\alpha}\sqrt{2}}{2}\tilde{\psi}(m, s) \tag{5}$$

The evolution over 8 steps of time is then:

$$\tilde{\psi}(m, s+8) \simeq \left(e^{i\frac{\pi}{4}}\right)^8 \left(\frac{\tilde{\alpha}\sqrt{2}}{2}\right)^8 \tilde{\psi}(m, s) \tag{6}$$

We can now keep our eyes closed and open them briefly and periodically so to look at the dynamics only at each multiple of 8 of the discrete time unit. Which means that we are throwing away more information: we are performing a second coarse graining. More diffusion paths would become indistinguishable. We would then be looking at a further new process whereby a new constant α would need to be introduced. We will also need to introduce a new integer time step index $\hat{s} = s/8$ whereby for s we can retain values only equal to multiples of 8.

To clarify that we are actually now considering a third further renormalised process derived from the previous one, we will use the notation ψ to replace $\tilde{\psi}$:

$$\psi(m, \hat{s}+1) \simeq \left(e^{i\frac{\pi}{4}}\right)^8 \left(\frac{\alpha\sqrt{2}}{2}\right)^8 \psi(m, \hat{s}) \tag{7}$$

It can be observed then that by taking $\alpha = \sqrt{2}$, at order zero the function ψ does not evolve at all after a step in the new time variable $\hat{s}$ (and therefore modulo 8 with respect to s):

$$\psi(m, \hat{s}+1) \simeq \psi(m, \hat{s}) \tag{8}$$

This choice of α makes the net densities stationary at order zero. Such a choice of renormalisation constant α after two coarse graining steps appears to be the appropriate value as discussed below (see also Appendix A) and will be retained in the following.

We then look for a higher order development, whereby we similarly use the notation ϕ_i to replace $\tilde{\phi}_i$. We reintroduce the δ and ϵ which had been omitted and we develop in powers of δ. From Appendix A we see that the first-order contribution is nil, as in the usual diffusion equation setting, because of the closed nature of the dynamics in the ϕ_i.

At the second order of the development the two diffusion dynamics appear interlaced in a symplectic-like way:

$$\begin{cases} \phi_1(m, \hat{s}+1) \simeq \phi_1(m, \hat{s}) + 4\delta^2 \frac{\partial^2 \phi_2}{\partial x^2}(m, \hat{s}) \\ \\ \phi_2(m, \hat{s}+1) \simeq \phi_2(m, \hat{s}) - 4\delta^2 \frac{\partial^2 \phi_1}{\partial x^2}(m, \hat{s}) \end{cases} \tag{9}$$

One can then take the ϕ_i terms on the right to the left and divide all by ϵ. We wish to take the continuum limit with $\delta \to 0$, $\epsilon \to 0$, while keeping constant the diffusion constant (or viscosity coefficient) $(\delta^2/\epsilon) = D$ and keeping constant (x, t) where $m\delta = x$ and $\hat{s}\epsilon = t$ (therefore this is also a limit modulo 8 in s).

We then get:

$$\begin{cases} \frac{\partial \phi_1}{\partial t}(x,t) = \frac{D}{2} \frac{\partial^2 \phi_2}{\partial x^2}(x,t) \\ \\ \\ \frac{\partial \phi_2}{\partial t}(x,t) = -\frac{D}{2} \frac{\partial^2 \phi_1}{\partial x^2}(x,t) \end{cases} \tag{10}$$

One can then set the diffusion constant as the ratio of Plank's constant and another constant which will turn out inevitably to be the inertial mass carried by the wave function. To avoid confusion with the integer m we will call the inertial mass m_I. And by setting $D = (\hbar/m_I)$, the interlaced diffusion process above can then be written in compact form, using $\psi = \phi_1 + i\phi_2$, as:

$$\frac{\partial \psi}{\partial t} = \frac{D}{2} \frac{\partial^2}{\partial x^2}(\phi_2 - i\phi_1) = \frac{\hbar}{2m_I} i \frac{\partial^2 \psi}{\partial x^2} \tag{11}$$

And by multiplying by $i\hbar$:

$$i\hbar \frac{\partial \psi}{\partial t} = -\frac{\hbar^2}{2m_I} \frac{\partial^2 \psi}{\partial x^2} \tag{12}$$

This is the free particle Schrödinger equation which in this context deserves a number of observations.

Observation I. The transition to a continuum function for the ϕ_i is well justified formally within the equivalent formalism of the probability description of random walks. Because we have here taken the view that we have a unbounded population of SubQuantum monomers, each of the p_i is a density function. One can then switch to the single particle view, whereby one asks what is the probability that at time $s\epsilon$ and place $m\delta$ a given monomer is of type i. The formalism is equivalent and the two ϕ_i become differences of probabilities, which are renormalised to take into account the multiple indistinguishable processes leading to the same configuration.

Within the probability formalism, the passage from discrete to continuum is straightforward and formally equivalent. It looses nevertheless the physical intuition which is more natural in our view by associating the content of densities to the functions involved. On the other hand, it is when discussing the measurement process that the numerical and formal equivalence between the two approaches might become useful.

Observation II. As detailed in Appendix A, we can analyse the evolution before taking the continuum limit at Discrete Fourier Transform level: $\tilde{\phi}_j(p,s) = \sum_{i=-\infty}^{+\infty} \tilde{\phi}_j(m,s)e^{-ipm\delta}\delta$. We use the mathematical notation p of [11], although k, the wave vector symbol, would be physically more correct. To keep the dimensional analysis correct, we can then consider that p is actually short for $(p/\hbar)$.

The ϵ time step evolution is then given by applying the transfer matrix T_ϵ as follows:

$$\begin{pmatrix}\tilde{\phi}_1(p,s+1)\\ \tilde{\phi}_2(p,s+1)\end{pmatrix} = \frac{1}{2}\begin{pmatrix}e^{-ip\delta} & -e^{ip\delta}\\ e^{-ip\delta} & e^{ip\delta}\end{pmatrix}\begin{pmatrix}\tilde{\phi}_1(p,s)\\ \tilde{\phi}_2(p,s)\end{pmatrix} = T_\epsilon\begin{pmatrix}\tilde{\phi}_1(p,s)\\ \tilde{\phi}_2(p,s)\end{pmatrix} \tag{13}$$

T_ϵ has then eigenvalues:

$$\lambda_\pm = \frac{\cos p\delta \pm \sqrt{\cos^2 p\delta - 2}}{2} \simeq (1 \pm i) + \frac{(p\delta)^2}{2}(1 \mp i) = \frac{\sqrt{2}}{2}e^{i\frac{\pi}{4}}\Big(1 \mp i\frac{(p\delta)^2}{2}\Big) \tag{14}$$

And eigenvectors at order zero $\tilde{\psi} = \tilde{\phi}_1 + i\tilde{\phi}_2$ and $\tilde{\psi}^* = \tilde{\phi}_1 - i\tilde{\phi}_2$.

The evolution over 8 steps of time is given by the matrix:

$$\begin{aligned} T_\epsilon^8 = {} & \tfrac{1}{256}\begin{pmatrix}e^{-8ip\delta} & -e^{8ip\delta}\\ e^{-8ip\delta} & e^{8ip\delta}\end{pmatrix} - \tfrac{6}{256}\begin{pmatrix}e^{-6ip\delta} & -e^{6ip\delta}\\ e^{-6ip\delta} & e^{6ip\delta}\end{pmatrix} + \tfrac{6}{256}\begin{pmatrix}e^{-4ip\delta} & -e^{-4ip\delta}\\ e^{4ip\delta} & e^{4ip\delta}\end{pmatrix} + \tfrac{2}{256}\begin{pmatrix}e^{-2ip\delta} & -e^{2ip\delta}\\ e^{-2ip\delta} & e^{2ip\delta}\end{pmatrix} \\ & -\tfrac{2}{256}\begin{pmatrix}1 & 1\\ -1 & 1\end{pmatrix}\cos 6p\delta + \tfrac{2}{256}\begin{pmatrix}3 & -1\\ 1 & 3\end{pmatrix}\cos 4p\delta + \tfrac{2}{256}\begin{pmatrix}3 & -1\\ 1 & 3\end{pmatrix}\cos 2p\delta + \tfrac{3}{256}\begin{pmatrix}1 & -1\\ 1 & 1\end{pmatrix} \end{aligned} \tag{15}$$

This shows that there are 8 groups of diffusion paths in the $\tilde{\phi}_i$ each distinguished by the wave vector magnitude and its combination among the positive and negative modes. To each of these groups it belongs a set of indistinguishable processes in the p_i variables. The renormalised probability $\frac{\alpha}{2}$ will then have to take into account the 8 groups of paths and the 8 time steps skipped at each time:

$$\big(\#\ of\ groups\big) \times \big(Renormalised\ Probability\big)^{(s=8)} = \frac{1}{2} \tag{16}$$

Therefore:

$$\frac{\alpha}{2} = \sqrt[8]{\frac{1}{2\times 8}} = \frac{\sqrt{2}}{2} \tag{17}$$

From the perspective of this renormalisation approach, it would as well be natural to look at the four Bell states for Bell-like experiments to be representing at quantum level the features of the local interlaced double diffusion process of SubQuantum mechanics. The $2\sqrt{2}$ factor which characterises quantum correlations could then be seen to arise from this renormalisation of probabilities. And the 4 factor of non-physical theories would appear to be related to the the full $1D$ SubQuantum degrees of freedom, which do not all impact upon the evolution equations at quantum level and are in this sense non physical at Quantum level. The SubQuantum web is a contextual structure with respect to the net density.

The form of T_ϵ seems to suggest that we are dealing with a specific group of matrices and that there might be an algebraic structure behind the time dynamics and its modulo 8 structure. The signs structure is also similar to a $1D$ version of the change of basis matrices relating the two mostly used representations for the Dirac matrices. The appearance of the row with 3 and 1 is similarly reminiscent of the bottom non dyadic rows in the Leech lattice generation matrix, whereby the 3 tend to arise in connection to the three E_8 lattice embeddings into the Leech lattice. The modulo 8 structure seems to replicate in a similar way the counting of some kind of embedded triple, as if we were looking at a lower dimensional projection of the Leech lattice.

Observation III. $|\psi|$ is a renormalised probability combining the effect of the renormalised densities ϕ_1 and ϕ_2. But because of the renormalisation above, $|\psi|$ **looks like** a square root of a probability. It is then natural if Quantum Mechanics shows features which appear as square root like versions of what found in Classical Mechanics. Spinors are square root of vectors and Dirac operators are square roots of Klein-Gordon operators. In the Schrödinger context this means that the Born rule probability is actually the product of two independent probabilities, each with the same numerical value. This is then the signature that the collapse of the wave function should be the result of a two-steps process, each being weighted by a probability of the same numerical value.

Observation IV. The SubQuantum web plays here the role of an infinite-like reservoir. Its deficiency from being neutral in internal variables can be modelled by matching dynamics by replacing ψ with ψ^*, or ϕ_2 with $-\phi_2$. Therefore $|\psi|^2$ represents the combined contribution of the product of *(i)* the probability of having net SubQuantum monomers of the SubQuantum gas at x, and *(ii)* the probability of net SubQuantum monomers excess or defect in the SubQuantum web also at x. The two probabilities are numerically matching because of the conservation of monomers exchanged, while any interaction of gas or web with an external agent is independent nevertheless. From Figure 4 we can see that both the Ord-process and the Reversed Ord-process are cases where the net impact on the SubQuantum web is nil at each rotation cycle. The implicit infinite-like reservoir assumption on the SubQuantum web seems then justified by the fact that the net flow is zero on average. If the net effect on the web is zero with a high frequency and without interruption, we only really need to use a finite part of the reservoir anyways. ψ^* provides then the complementary (double) bookkeeping and the balancing diffusion accounting at the SubQuantum web level.

Observation V. If we use the Madelung, also called hydrodynamic or semi-classical, customary notation $\psi = |\psi|e^{i\theta}$, then

$$\tan\theta = \frac{\phi_2}{\phi_1} \quad \Rightarrow \quad \partial_x\theta = \frac{\phi_1\partial_x\phi_2 - \phi_2\partial_x\phi_1}{\phi_1^2+\phi_2^2} = \frac{1}{|\psi|}\left[\frac{\phi_1}{|\psi|}(\partial_x\phi_2) + \frac{\phi_2}{|\psi|}(-\partial_x\phi_1)\right] \tag{18}$$

One can then think at the current of density $|\psi|\partial_x\theta$ (and not $|\psi|^2\partial_x\theta$) as the composition of two opposite currents, each with diffusion coefficient provided by the density of the other current, with the appropriate normalisation. This is a natural interpretation of the quantum phase of the Schrödinger equation in this setting. Therefore ϕ_2 plays the role of a local diffusion coefficient for the (net) diffusion of ϕ_1 and vice-versa. Each sub-current carrying the relevant algebraic sign. One can then similarly relate the quantum potential in the evolution equation for $|\psi|$ to the Fisher information of the probability distribution $|\psi|$ (or possibly of $|\psi|^2$ by taking into account Section V), whereby the control parameter of the Fisher formula is the value $\bar{x}$ AFTER the measure of x. A *self Fisher information* of the net monomer density, with respect to the post-measure collapsed value, which contributes to the interpretation of the quantum potential.

Observation VI. If we were to take the semi-classical limit directly from the SubQuantum process and without taking first the Quantum continuum limit, when close to a singularity and in the presence of an external potential, one would expect locally to be able to use a similar process but not necessarily to be able to match the circular dynamics on the two sides of the singularity. Any mismatch will then need to be reconciled in term of multiples of the quarter of a circular process at SubQuantum level. Because of the double covering resulting from the two kind of net densities this reconciliation is done in terms of eighth of unity, which is the correspondent factor to the modulo 8 renormalisation. This provides a SubQuantum physical meaning of the Maslov index. The double process at ψ and ψ^* level would similarly be the basis for the double cover of the symplectic group, the metaplectic group. We hope therefore with this to shed some additional light on the nature of the symplectic group and its double covering. The well known relation between the double covering of the symplectic group and quadratic forms, should provide a mapping between quadratic reciprocity and a class of SubQuantum combinatorial dynamics to be identified.

Observation VII. If one considers the possibility of vibration and deformation of the SubQuantum web, as well as the propagation of the respective modes, this would be the natural candidate for a SubQuantum version of the gravitational field. The diffusion process would then be a key source of such vibrations or deformations. At the same time one can see from above that the gas diffusion length, or the frequency of interaction between the gas and the web, is here the dynamical source of inertia. One can immediately see that the same dynamical process is always and inevitably the source of both the inertial mass and gravitational force generated by the mass. The need for an equivalence principle is therefore dynamic and inevitable in this context.

Observation VIII. If we look at the $3D$ dynamics in Figure 4 and at its physical meaning, ϕ_1 would then be related to the net charge, while ϕ_2 would be related to the net helicity carried by the photon like monomer couples. This is an intriguing physical interpretation as the imaginary part of the wave function would appear to be related to a virtual dissipation which is recycled on an ongoing basis without overall dissipation, i.e. globally, but not locally, preserving conservation laws.

This reverse engineering encourages then to bring in more arithmetics and number theory to generalise this kind of models.

IV. RELATIVISTIC SUBQUANTUM FREE PARTICLE FOR D=1

We now consider a modified Ord-process as follows:

$$\begin{cases} p_1(m,s+1) = (1-\tilde{\mu}\epsilon)\ p_1(m-1,s) + (\tilde{\mu}\epsilon)\ p_4(m+1,s) \\ p_2(m,s+1) = (1-\tilde{\mu}\epsilon)\ p_2(m+1,s) + (\tilde{\mu}\epsilon)\ p_1(m-1,s) \\ p_3(m,s+1) = (1-\tilde{\mu}\epsilon)\ p_3(m-1,s) + (\tilde{\mu}\epsilon)\ p_2(m+1,s) \\ p_4(m,s+1) = (1-\tilde{\mu}\epsilon)\ p_4(m+1,s) + (\tilde{\mu}\epsilon)\ p_3(m-1,s) \end{cases} \tag{19}$$

If we take the probabilistic view of Observation I at the end of Section III, this is the standard technical way to formally introduce the transition from discrete process to the continuum. We will discuss below the differences with the previous approach and what we can learn from them. We use the letter $\tilde{\mu}$ rather than the λ used in probability theory of diffusion processes, to avoid here the confusion with the eigenvalues of the previous Section. $\tilde{\mu}$ represents then a frequency of interaction with a node and therefore $\tilde{\mu}\epsilon$ is the number of scattering events over a time ϵ. At the same time, $\tilde{\mu}$ acts as a renormalisation parameter, which can be reset at any coarse graining step, therefore simplifying the equivalent renormalisation discussion done in the previous Section.

We then proceed to get rid of all variables but for the net densities, whereby $\tilde{\mu}$ is changed into μ to remind us that we are looking at a different process derived from the one above.

$$\begin{cases} \phi_1 = p_1 - p_3 \\ \phi_2 = p_2 - p_4 \end{cases} \tag{20}$$

$$\begin{cases} \phi_1(m,s+1) = (1-\mu\epsilon)\ \phi_1(m-1,s) - (\mu\epsilon)\ \phi_2(m+1,s) \\ \\ \phi_2(m,s+1) = (1-\mu\epsilon)\ \phi_2(m+1,s) + (\mu\epsilon)\ \phi_1(m-1,s) \end{cases} \tag{21}$$

Which is equivalent to the following, where we have also reinserted δ and ϵ in the arguments:

$$\begin{cases} \epsilon^{-1}\Big[\phi_1\Big(m\delta,(s+1)\epsilon\Big) - \phi_1\Big((m-1)\delta,s\epsilon\Big)\Big] = -\mu\Big[\phi_1\Big((m-1)\delta,s\epsilon\Big) + \phi_2\Big((m+1)\delta,s\epsilon\Big)\Big] \\ \epsilon^{-1}\Big[\phi_2\Big(m\delta,(s+1)\epsilon\Big) - \phi_2\Big((m+1)\delta,s\epsilon\Big)\Big] = -\mu\Big[\phi_2\Big((m+1)\delta,s\epsilon\Big) - \phi_1\Big((m-1)\delta,s\epsilon\Big)\Big] \end{cases} \tag{22}$$

We develop then in powers of δ. We can see that on the left hand side there will be a leading term in ϵ^{-1} for the time derivative and a leading term in (δ/ϵ) for the space derivative, all the remaining terms being of order $(\delta/\epsilon)\delta^n$ with $n \geq 1$. Similarly on the right there will be a difference of the ϕ_i and then terms in δ^n with $n \geq 1$. It is then natural to take the limit for $(\delta/\epsilon) = constant = c$ the speed of light, while $\epsilon \to 0$, $\delta \to 0$, $s\epsilon = constant = t$, $m\delta = constant = x$ and $m, s \to \infty$ (see also Appendix B).

By identifying μ with $(m_I c^2/\hbar)$ we get:

$$\begin{cases} \Big[\frac{1}{c}\frac{\partial}{\partial t} + \frac{\partial}{\partial x}\Big]\phi_1(x,t) = -\frac{m_I c}{\hbar}\big[\phi_1(x,t) + \phi_2(x,t)\big] \\ \\ \Big[\frac{1}{c}\frac{\partial}{\partial t} - \frac{\partial}{\partial x}\Big]\phi_2(x,t) = -\frac{m_I c}{\hbar}\big[\phi_2(x,t) - \phi_1(x,t)\big] \end{cases} \tag{23}$$

Or also:

$$\begin{cases} \frac{1}{c}\Big[\frac{\partial}{\partial t} + \frac{m_I c^2}{\hbar}\Big]\phi_1 = -\frac{\partial \phi_1}{\partial x} - \frac{m_I c}{\hbar}\phi_2 \\ \\ \frac{1}{c}\Big[\frac{\partial}{\partial t} + \frac{m_I c^2}{\hbar}\Big]\phi_2 = \frac{\partial \phi_2}{\partial x} + \frac{m_I c}{\hbar}\phi_1 \end{cases} \tag{24}$$

Where we have not made explicit the dependency on (x,t) of the ϕ_i just to simplify the notation. We can now eliminate any time transient effect of frequency $(m_I c^2/\hbar)$ by introducing the variables $\psi_i = \phi_i e^{\frac{m_I c^2}{\hbar}t}$ so that we get the symplectic-like interlaced linear wave equations:

$$\begin{cases} \Big[\frac{1}{c}\frac{\partial}{\partial t} + \frac{\partial}{\partial x}\Big]\psi_1 = -\frac{m_I c}{\hbar}\psi_2 \\ \\ \Big[\frac{1}{c}\frac{\partial}{\partial t} - \frac{\partial}{\partial x}\Big]\psi_2 = \frac{m_I c}{\hbar}\psi_1 \end{cases} \tag{25}$$

By applying them in sequence one can see that each of the ψ_i satisfies the Klein-Gordon equation. The ordered pair $\Psi = (\psi_1, \psi_2)$ is then a square root of a vector (i.e. a spinor) and the partial differential operator corresponding to the action on the left is the square root of the Klein-Gordon operator. Therefore this is the Dirac equation for the $1D$ free-particle. It can also be multiplied by $\hbar$ and then rewritten using Pauli matrices as:

$$i\hbar\partial_t\Psi = ic\sigma_z\hbar\partial_x\Psi + m_I c^2\sigma_y\Psi \tag{26}$$

where $\sigma_z = \begin{pmatrix} 1 & 0 \\ 0 & -1 \end{pmatrix}$ and $\sigma_y = \begin{pmatrix} 0 & -i \\ i & 0 \end{pmatrix}$.

Observation A. When we compare to the non-relativistic case, instead of two real functions ϕ_1 and ϕ_2 which combine into a complex function ψ, we have here two real functions ψ_1 and ψ_2. If one was to retain the full combinatorial dynamics of Figure 4, one would expect to obtain four such functions. In addition, in $3D$ one can not merge the combinatorial and the cinematic description as it is the case for $1D$. One can therefore expect such functions to have some features like the non-relativistic ψ, which make them complex in general. The gradients of the phases will then originate the cross diffusion currents.

Observation B. At this level of discussion we do not use the intermediary functions $\tilde{\psi}_i$, as in the Schrödinger case, because it is only a matter of taking a different numerical value for the constant μ, which in turn is set at the end.

Observation C. The form of the $1D$ Dirac equation for the ψ_i above can be seen as-if ψ_1 acted as a source for the movement to the right of ψ_2 waves, which in turn acted as a source for the movement to the left of ψ_1 waves. A bit like the main spring in the barrel and the hair spring at the balance wheel of a mechanical clock (see [15]), but without dissipation, so that there is no damping factor for the oscillatory dynamics.

Observation D. In the relativistic case $\phi_i = \psi_i e^{-\mu t}$. The ψ_i represent the oscillating net densities once the transient is over. The ϕ_i represent therefore two net densities which go to zero, while oscillating. The SubQuantum network would be then absorbing the charge and helicity on average. The spinor and its conjugate represent the oscillatory part of the dynamics post-transient.

Observation E. The SubQuantum web contributing to the wave function is standing still with respect to the SubQuantum gas of the particle (local-web). The SubQuantum gas is moving at the speed of light in opposite directions between scattering events. It seems less straightforward what a Lorentz boost corresponds to. If the reference system from which a measure is made moves with respect to the reference system of the particle, there should be a broader web, co-contextual with the measuring reference system, which is standing still with respect to the moving reference system (contextual-web). The particle local-web can then be "moving" through the broader contextual-web, for example by diffusion of the excess and deficit monomers. This implicitly assumes that there is a process which, at least at high energy, can confine the SubQuantum diffusion process of the particle to a finite area or boundary. This could be arising as a result of the web being reversibly charged only in the area relevant for the diffusion process, as well as by a process of interaction with the surrounding environment similar to inertial confinement. The particle is therefore implicitly seen as carrying an Anti-de-Sitter-like hyperbolicity barrier at its boundary.

Observation F. If we consider a SubQuantum web moving locally at the limit at a speed of c with respect to the larger contextual SubQuantum web, the monomers locally moving in the same directions are fixed in the reference system of the web. The others are pushed towards them at double the speed. This creates a strain which can be the catalyst for the formation of composite structures to model the photon reconstruction process. This suggest that there should be also contextual forms of the emission theories for Special Relativity, which to the best of our knowledge do not seem to have been considered in the past, probably because incompatible with the ether hypothesis as medium for the propagation of electromagnetic waves, which was erroneously assumed to be a necessary feature.

Observation G. The exchanges between gas and web can facilitate our search for an heuristic of the collapse of the wave function as a two step process, in line with Observation III in the previous paragraph.

Observation H. The fact that the ϕ_i go to zero correspond to an on-average neutralisation process of the SubQuantum gas which takes place modulo the oscillatory modes encoded in the ψ_i. Neutralisation processes of this kind can also facilitate our search for an heuristic of the collapse process.

This class of models do provide a **linear** version of the models used to study non-linear chemical oscillators, such as the Belousov-Zhabotinsky reaction system, the Brusselator model, derived from the Turing ring morphogenesis model leading to Turing waves (see [16] which provides an early prototype of the Ord-process). The very important difference is that the interlacing of Brownian processes and the gas-web balanced exchange do enable a linear non-dissipative analogous model, which is not at all the same dynamics. The SubQuantum web reservoir is here locked into a linear rotational exchange dynamics, non-dissipative. This is different to the multiple reservoirs and the net give or net take mode of chemical oscillations, which are eventually dissipative. Similar comments apply to Activate Random Walk models, whereby the non-linearity arises from the direct interaction among particles.

One can certainly build models with the two features at once. To provide a structured image for the complex order parameter of selected macroscopic quantum phenomena, intermediary between the mean-field theory and the quantum field theory pictures. Which is interesting in its own sake. Although it is a case where the non-linearity is not very relevant, as a simplified example of such a modelling approach one can take the Josephson effect. In this case we could ask if there is, at the insulating (or bad-superconductor) barrier, a Cooper pairs scattering and exchange process of the kind used for monomers couples in this course, from which a rotational dynamics would follow. This would simplify and clarify the dynamical reason for the Josephson current to be an alternate current, rather than just by calling on the formal calculated phase difference of the complex order parameters (wave-functions-like) on the two sides of the junction. Such approach would put the Josephson effect on a similar basis of Bekenstein-Hawking radiation and the Unruh effect, which in turn should be seen as macroscopic quantum effects. In each case, one can consider that some form of couple breaking dynamics is mediated by an interface, respectively by the black-hole horizon, at the boundary of validity of non-global Rindler coordinates region and at the Josephson barrier. Bogolyubov transformations providing the hyperbolic geometry formal link among them. Black hole evaporation might therefore be seen as the effect of a Josephson-like alternate current to infinity.

V. AN HEURISTIC FOR THE SINGLE MEASUREMENT PROCESS

Starting from Observations G and H at the end of the previous Section, as well as Observations III and IV in Section III, we are led to consider a two-steps process for the collapse of the wave function. In general such two steps might be merged into one, as for example if we were to discuss spontaneous emission. Or they could lead to almost no net effect, as if we were to discuss weak measurement processes. In the following, we will limit ourselves to a very schematic description of the measure of position for a free-particle in one dimension. We then compare in a way the degrees of freedom of gas and web which contribute to the wave function to the two subunits of the Ribosome. We further compare the incoming photon to the transmission RNA which is read by the Ribosome and brings information into the Ribosome. We then compare the outgoing photon to the DNA which is generated by the Ribosome to encode the genetic information to carry away. The analogy is only to generate an image, where we usually have none. But there is no close analogy other than in the broad approach. The key steps of such process are sketched in Figure 6. If we look at the Ribosome as a two-subunits zip, the RNA is un-zipped in and DNA is then zipped out.

We will call then *un-zipping* and *re-zipping* the two steps used to sketch the collapse process in Figure 6. Re-zipping because, contrary to the molecular biochemistry analogy, the entity before and after in our case is of the same nature. We use the idea that the charge is carried by the network on average and that the oscillatory modes can be discarded for the conceptual discussion below illustrating the steps in Figure 6.

Before the un-zipping process we consider separately SubQuantum web and gas, whereby the wave function can be thought of as an effective composite field resulting from key degrees of freedom of both gas and web. This is our asymmetric two-parts zip. The incoming photon in schematised as a double helix of positive and negative monomers. The web is charged positive in the schematisation of Figure 6. Upon un-zipping, the negative helix of the photon decomposes into the web to neutralise it. By reaction a comparable amount of positive monomers in the gas are pulled towards the area where the double helix has un-zipped.

The concentration of positive monomers in the gas needs then to go to zero through a transient process like the one that drives the $\phi_i = \psi_i \exp(-\mu t)$ to nil in the evolution equation of the relativistic case. The web therefore releases the required negative monomers for the neutralisation of the concentrated positive monomers in the gas. Such process is balanced by the re-zipping of the photon whereby the positive helix picks up the excess negative charges in the gas. The net result is that the web is charged in the area where the un-zipping took place. The conservation of momentum requires therefore an exchange of momentum between the relevant degrees of freedom of the gas-web system (effectively the wave function) and the photon. The charge distribution has collapsed.

Each of the un-zipping and re-zipping processes are independent. The probability of exchange of momentum for each step of the process is related to the net densities, of the gas and the web respectively, involved in the evolution equation before the un-zipping takes place. In the Schrödinger case for simplicity, they will be proportional to the numerical values of $|\psi|$ and $|\psi^*|$. The amount of momentum exchanged should then be proportional to the value of $|\psi|^2$ at x, where x is the location where the un-zipping and re-zipping takes place. Note that this does not yet imply the Born rule, which will be discussed in Section VII. The two topics are separate. This Section is also required for a discussion of the Lorentz boost in the next Section, which in turn completes the relativistic case analysis of the previous Section. This interrelationship among each topic is behind the order chosen for the exposition and should not be overlooked.

Observation (i). A formal description of the un-zipping and re-zipping processes is likely to be connected to the combinatorics of partitions, which should allow to take into account the multiple ways to decompose a very long chain. The number of partitions $p(n)$ is the number of distinct ways of representing n as a sum of natural numbers, with order irrelevant. The partitions generating function $g(u)$ is the power series with $p(n)$ as coefficients. Its analytical properties encrypt then the cross-combinatorics among the $p(n)$, which generates the decomposition channels for the zipping processes. By Euler formula:

$$g(u) = \sum_{n=0}^{\infty} p(n) u^n = \prod_{k=1}^{\infty} \left(\frac{1}{1-u^k} \right)$$

Observation (ii). The u in $g(u)$ from Observation *(i)* can be extended to $w = u + iv$ in the complex plane and we can use the variable τ with $w = e^{2\pi i \tau}$, therefore $|w| = \sqrt{u^2+v^2} = e^{-2\pi Im(\tau)}$ and $(w/|w|) = e^{-2i\pi Re(\tau)}$. The imaginary part should provide a modelling for the deconstruction mechanism, a bit like dissipation can be modelled by the imaginary part of a complex variable for other physical systems. The partitions generating function is also

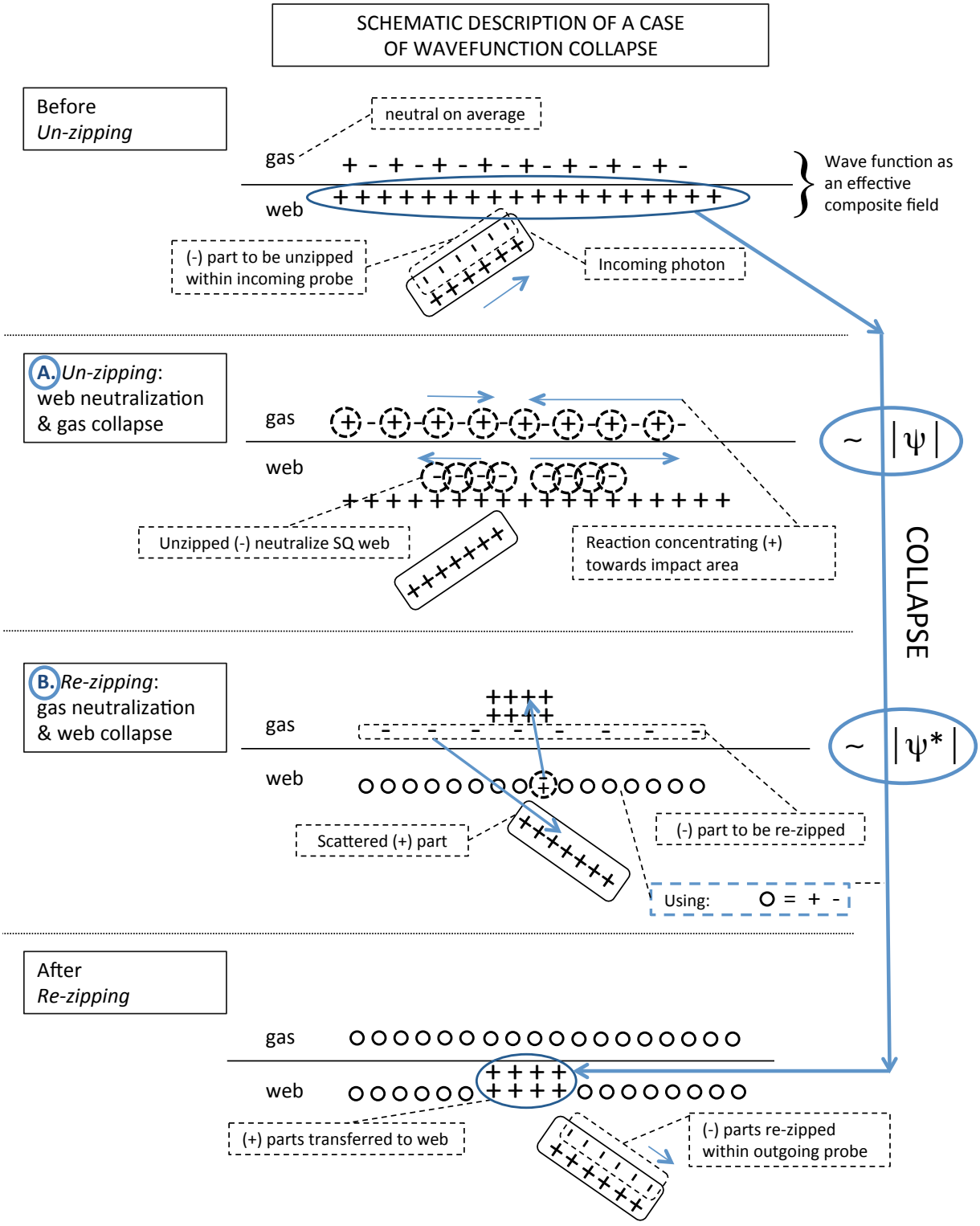

FIG. 6. Rudimental un-zipping and re-zipping scheme for a case of wave function collapse. By analogy to RNA-Ribosome-DNA biochemistry of double helices deconstruction-reconstruction processes. The process is the composition of two parts, A and B, independent from each other. The amount of conjugate observable exchanged by both gas and web is related to the value of $|\psi|^2$ at the point of un-zipping and re-zipping x. This does not imply the Born rule, which arises only through the accumulation of the sampling over numerous collapses. In this framework, Wigner does not play any role in the single collapse of a wave function. Only Wigner's friend is involved.

closely related to the Dedekind η function, the well known modular function of weight $(1/2)$ arising in the study of elliptic curves, elliptic functions and modularity (see [17]):

$$\eta(\tau) = e^{\frac{2\pi i\tau}{24}} \prod_{k=1}^{\infty}(1 - e^{2\pi ik\tau}) = \frac{e^{\frac{2\pi i\tau}{24}}}{g(e^{2\pi i\tau})}$$

This relationship uses the analytic extension of the partitions generating function and is an important element to derive the Rademacher formula for the number of partitions $p(n)$, which arises from the calculation of the n^{th} residue integral of $g(w)$ (see [17]):

$$p(n) = \sum_{k=1}^{\infty} \left\{ \frac{d}{dn} \frac{\sinh\left[\frac{2\pi}{2k}\sqrt{\frac{2}{3}\left(n - \frac{1}{24}\right)}\right]}{\frac{2\pi}{2k}\sqrt{\frac{2}{3}\left(n - \frac{1}{24}\right)}} \right\} \frac{A_k(n)}{\sqrt{3k}}$$

Whereby:

$$A_k(n) = \sum_{0 \le m < k,(m,k)=1} e^{2\pi i(\frac{s(m,k)}{2} - \frac{m}{k}n)}$$

We have used here the notation (m, k) for relatively primes integers. The Dedekind sums $s(m, k)$ are defined using $\lfloor\ \rfloor$ for the nearest lower integer function ($\frac{m}{k} < 1$):

$$\frac{s(m,k)}{2} = \sum_{r=1}^{k-1} \frac{r}{2k}\left(\frac{m}{k}r - \left\lfloor \frac{m}{k}r \right\rfloor - \frac{1}{2}\right)$$

Such a formula shows dependence of $p(n)$ from hyperbolic functions, as amplitudes, times exponential sums. It is a bit like a strange discrete quantum transform. It might be useful to search for a combinatorial dynamics of the kind used in this course which could be generating such a functional form. The hyperbolicity can be thought of as a strain arising from the constraint of n for the total of each given partition. While the Dedekind sums arise to clockwork-like match the different integration paths related to the structure of each group of partitions for a given n. Such clockwork originates from the modular-related, Farey-sequence-aligned Ford cycles, the partial boundaries of which form the integration path used in the complex plane to derive the formula. This is intuitively similar to a mechanical clock where on one side one has the mechanism which controls, regulates and delays the release of potential energy (the balanced strain between the main spring in the barrel and the hair spring by the balance wheel, see [15]) and on the other side one has an anchor retarding the de-multiplication clockwork to get each pointer to slow down in order to turn at the right rate (which is effectively the inverse mechanical feature of the piston chamber, where the sparkle generated explosion makes the piston go faster to make the wheel turns faster). The Dedekind sums dependent exponentials in the formula for the amplitudes can be thought as some generalisation of the exponential of the Maslov index and might be used as a linking factor to the linear evolution SubQuantum circular dynamics.

Observation (iii).

If $\theta(z;\tau) = \sum_{n=-\infty}^{\infty} e^{(\pi in^2\tau + 2\pi inz)}$ is the standard Jacobi Theta function, then (see [18]):

$$\theta(0;\tau) = \frac{\eta^2(\frac{\tau+1}{2})}{\eta(\tau+1)} = \frac{g(e^{2\pi i\tau})}{g^2(-e^{2\pi i(\frac{\tau}{2})})}$$

For imaginary arguments $\tau = it$, we have $u = e^{-2\pi t}$ and, except for a sign factor in the argument of one of the g, the Theta is essentially the ratio of two partitions generating functions, quadratically scaled and with quadratic related arguments:

$$\theta\big(0; \frac{\log u}{2\pi i}\big) = \frac{g(u)}{g^2(-\sqrt{u})} = \prod_{k=1}^{\infty} \frac{\left[(1 - (-\sqrt{u})^k\right]^2}{1 - u^k} = \frac{g(e^{-2\pi t})}{g^2(-e^{-\pi t})}$$

Furthermore:

$$g^2(-\sqrt{u}) = (\sum_{n=0}^{\infty} p(n)(-\sqrt{u})^n)^2 = \sum_{n,m=0}^{\infty} p(n)p(m)(-\sqrt{u})^{(n+m)} =$$

$$= \sum_{n}^{\infty} p^2(n)u^n + \sum_{(m+n)=l=0}^{\infty} (-1)^l u^{\frac{l}{2}} \sum_{n=0,2n\neq l}^{l} p(n)p(l-n)$$

Such a relationship between the $z = 0$ boundary values of the Jacobi Theta and the ratio of permutations generating functions might provide hints to identify a connection to the relationship between the combinatorics of un-zipped and re-zipped configurations. The product of the number of two sets of permutations might be interpreted as the number of possible pairing of each possible permutation component, which would suggest that these formulas could lead to a formal model. $\theta(0; it)$ is also a solution for the heat equation. The modularity and Heisenberg group relevance of Jacobi's Theta might arise in connection to a combinatorial dynamics similar to those discussed in the previous paragraphs.

Observation (iv). For imaginary arguments the Jacobi Theta function is also well known to act as a kernel element for a relevant integral representation of the Riemann zeta function (see [19]). We will use the notation $\tilde{\theta}(t) = \frac{1}{2}[\theta(0; it) - 1]$ rather than the Riemann notation ψ to avoid confusion with the wave function:

$$\frac{\Gamma\Big(\frac{s}{2}\Big)\zeta\Big(2\Big(\frac{s}{2}\Big)\Big)}{\pi^{(s/2)}} = \int_0^{\infty} \tilde{\theta}(t) t^{\frac{s}{2}} \frac{dt}{t}$$

This is a Mellin transform which can be inverted as:

$$\theta(0; it) = 1 + \frac{1}{2\pi i} \int_{\frac{c}{2}-i\infty}^{\frac{c}{2}+i\infty} \Gamma\Big(\frac{s}{2}\Big)\zeta(s)(\pi t)^{-\frac{s}{2}} ds$$

The logarithm of the ζ function is in turn well known to be an integral transform of the counting function for prime powers $f(t)$:

$$\zeta(s) = \exp\ \Big\{\frac{1}{s}\int_1^{\infty} f(x)x^{-s}\frac{dx}{x}\Big\}$$

Where:

$$f(x) = \sum_{n=1}^{\infty} \frac{1}{n} F(x^{\frac{1}{n}})$$

And where, by using the Heaviside step function θ_H with the value at the jump equal to (1/2) (i.e. the average of the two sides of the single step), and by denoting P the set of primes:

$$F(x) = \sum_{p\in P} \theta_H(x - p)$$

The function f incorporates appropriately normalised step functions at each power of a prime. This can be seen as a set of input signals like those used in Heaviside's electric circuit theory (see [20]). These impulses located at the powers of the primes, generate a transient signal feeding into a complex circuitry represented by the integral

transforms which relates f to the Jacobi Theta function, and therefore to the permutations combinatorics. Which seems to represent some post-transient or pre-transient current. In fact, if the $p(n)$ are given by Rademacher formula, then the link is a bit of an extravagant multi-bridging of analytic number theory:

$$\frac{\sum_{n=0}^{\infty} p(n)e^{-2n\pi t}}{\sum_{n,m=0}^{\infty} p(n)p(m)(-1)^{n+m}e^{-(n+m)\pi t}} =$$

$$= 1 + \frac{1}{2\pi i}\int_{\frac{c}{2}-i\infty}^{\frac{c}{2}+i\infty} \Gamma\Big(\frac{s}{2}\Big)\Big[\exp\ \Big\{\frac{1}{s}\int_1^{\infty}\sum_{m=1}^{\infty}\frac{1}{m}\sum_{p\in P}\theta_H(x^{\frac{1}{m}}-p)x^{-s}\frac{dx}{x}\Big\}\Big]\frac{ds}{(\pi t)^{\frac{s}{2}}}$$

Or also:

$$\sum_{n,m=0}^{\infty} p(n)p(m)(-1)^{n+m}e^{-\frac{n+m}{2}2\pi t} =$$

$$= \sum_{n=0}^{\infty}\frac{p(n)e^{-2n\pi t}}{1+\frac{1}{2\pi i}\int_{\frac{c}{2}-i\infty}^{\frac{c}{2}+i\infty}\Gamma\big(\frac{s}{2}\big)\Big[\exp\ \Big\{\frac{1}{s}\int_1^{\infty}\sum_{m=1}^{\infty}\frac{1}{m}\sum_{p\in P}\theta_H(x^{\frac{1}{m}}-p)x^{-s}\frac{dx}{x}\Big\}\Big]\frac{ds}{(\pi t)^{\frac{s}{2}}}}$$

Loosely speaking it is as-if we had some kind of un-zipping propagator. Note that the π as a "time" factor in the exponential is related to the damping cycles of the convection loops in the heat convection equation between two plates. And that on the left of the equation above there are also half cycles whereby on the right there are full cycles only. But on the right there is a highly structured t dependence at the denominator, while on the left there is a clean composition of permutation counts, which should be expressed through the Rademacher formula. We are not going to explore this further at this stage, as it seems to require a thorough separate investigation. What we want to stress it that normally one looks at the inter-dependence of $\zeta(s)$ on $f(x)$. If we look at the prime powers as a signalling source instead, we are naturally led to continue the series of formulas towards the left and therefore to see the Rademacher formula as a result of a chain of reactions which starts with the primes.

Observation (v). The Observations above suggest that the prime numbers and their distribution might be involved in the un-zipping and re-zipping processes. In the sense that they provide base modes for the analysis of the combinatorial options corresponding to the physical decomposition of SubQuantum chains. The $\zeta(s)$ function and its generalisations are involved in the translation between prime-indexed impulses and deconstruction-reconstruction combinatorics. The cinematic of the out of equilibrium evolution between initial and final states should be then formalised within the appropriate probability functional space, for example to include Tallis distributions as well as Gaussian distributions. The Rademacher formula might allow to say something about the space clockwork through the number analytic functional form of the $p(n)$, while the primes might provide time-to-space analytics of the process trough the structure of $\zeta(s)$. For $s = [(1/2)+it]$, the $\zeta(1/2+it)$ function very large t asymptotic properties are known to be quite different from the currently computable sector of the $\zeta(s)$ domain (see [21] and references therein). There might be then a value on the critical line whereby a phase transition between two asymptotic behaviours occurs: a proxy of an Avogadro Number for number theory, which could be the result of a reciprocity-like symmetry between 0 and $\pm\infty$ on the critical line. Or some other transitional set which facilitate the modelling of an emission and absorption process in line with this physical intuition. If F.Dyson idea of connecting PV numbers to ζ zeros proves correct in some way (see [22]), Pisot-Vijayaraghavan numbers and their $1D$ quasi-crystal signature could also play a role in the zipping processes. A quasi-crystalline-like geometry related to the ζ zeros might provide a tentative model of some first order purely numerological justifications of the quasi-reverse-integer nature of the fine structure constant. It might be that nature is once again ahead of us and is performing ultra-high speed prime factorisations of very large n at each absorption and emission process. To properly calculate any structured quantities for this part of SubQuantum mechanics, powerful Quantum Computers will probably be needed.

Observation (vi). If we take the clock and piston analogy from Observation (ii) above, the mechanical clock retardation is intuitively identified with the absorption process and the piston acceleration by the sparkle is intuitively identified with the emission process, which seems biologically natural. For the piston, the simplest model is the ideal

gas law $PV = nRT$. V can be restated as $V = xS$, with S the constant section of the piston and x the direction of movement. P can be restated as $P = p\Delta$, with p the unit of momentum exchanged at given pressure and volume and Δ a constant taking into account the gas density and other features of the thin surface of gas by the piston head. Except for constants to be reabsorbed by each variable, the energy $nRT = PV$ can be then restated as $H = px$. This analogy seems in line with the name of dilatation operator used for the quantised version of such Hamiltonian, such naming inspired by the functional effect on the eigenfunctions by the operator. The quantisation of this hamiltonian generates difficulties, but can be discussed within the framework of the Berry-Keating model [23]. As a first step, to get real formal eigenvalues the Hamiltonian operator is symmetrised in the form $\hat{H} = \hat{x}\hat{p} + \hat{p}\hat{x}$, introducing then both the emission-like and the absorption-like channels. There have then been various attempts to regularise the quantisation procedure for this model: by compactifying the phase space, introducing cut-offs or modifying the Hamiltonian functional form (see [24]). Because its symmetrised version has $(1/x^s)$ as formal eigenfunctions with eigenvalues $Im(s)$, the connections to the study of the Riemann hypothesis naturally arise. The interpretation of some of its features as some form of emission-like or absorption-like mechanisms is well known. Including more recently the idea to regularise using non-Hermitian operators (see [25]), already used in the study of open radiative process in Quantum Mechanics (pseudo-Hermitian operators in the sense of G.W.Mackey). In this context, the SubQuantum physical intuition would suggest that the van der Waals real gas equivalent Hamiltonian might provide an alternative regularisation option for the Berry-Keating operator. We also hope that the observations in this section do provide an additional intuitive reason for linking Berry-Keating models to emission and absorption. And will encourage to revisit these models to question if they can be seen as an effective tool to model part of SubQuantum Mechanics at the Quantum limit, but for a process that Quantum Mechanics does not model: the time evolution between when the pre-measure initial state starts to evolve and the time at which the post-measure final state is formed and stabilised. Such dynamics being currently modelled to the best of our knowledge only for systems immersed into a collective quantum condensate, such as a laser or maser fields (decoherence theory) which are systems where the quantum coherence is among infinite particles. If since the 1990s femto-chemistry can single out and identify separately a metastable state which is intermediary for the transition between different stable configurations of sizeable molecules (see [26]), then a similar stroboscopic structure can in principle be identified for the single particle transition. Rather than asking which Hilbert space is defined by the $\hat{H} = \hat{x}\hat{p} + \hat{p}\hat{x}$ operator alone, it might be more appropriate to apply $\hat{H}$ to the Hilbert space which naturally arises in the study of different problems, for example the harmonic oscillator Hilbert space, or the hydrogen atom Hilbert space. This corresponds to consider $\hat{H}$ as an external interaction operator, environment-like. Therefore mimicking the Bath to Quantum-Object formalism of Lindbladian theory for quantum-condensate-environments open-quantum-systems.

Observation (vii). The only way we can see for coexisting dynamics to be defined on the same web is to use non-coincident time processes, each based on a different time-step modulus, each modulus co-prime with the others. Therefore the primes connection seems necessary also to model multiple particle states.

Observation (viii). Shor algorithm is schematically split in two parts (see [27]). The first one is the classic number theory connection between prime factors and periods of the appropriate arithmetic function. The second one is the use of the Quantum Fourier Transform to statistically single out the periods, and therefore the prime factors. It seems possible that Quantum Computing might be mimicking SubQuantum processes. The Quantum Fourier Transform would then correspond to the statistical sampling process discussed later in Section VII, while the arithmetic function would correspond to structural features at SubQuantum level, possibly something about the combinatorial dynamics behind the un-zipping and re-zipping processes.

VI. LORENTZ BOOST

Starting with the $1+1D$ Dirac equation for the free particle, a Lorentz boost can be applied along the only direction to get the $1D$ free-particle Dirac equation in the boosted reference system. By Lorentz invariance of the Dirac equation, the boosted equation has the same mathematical form. The transformation linking the initial two bi-spinors in $1+1D$ to the boosted bi-spinors is diagonal (see [28]), which is an extreme simplification observed uniquely in $1+1$ dimensions. The Lorentz boost in $1+1D$ in fact does not show the counter-diagonal terms of the general case. Furthermore, the single spacial dimension implies no rotations, the complex-variable features of the Lorentz group action on spinors are absent, as it is also absent the complex-variable character of the spinors involved. This is often seen as a trivial aspect of the $1+1D$ case. Nevertheless, as we are ambitiously seeking a reverse engineering *learning* path, this fact seems fortuitous. One can then take a reversed point of view, by trying to leverage on such simplicity in order to identify features of the SubQuantum physics of the Lorentz boost. A first exploration in higher dimensions would be probably quite hard. In fact, rotations and the extra dimensions make coefficients complex-valued. The

impact on the boost algebraic structure is that we also get the counter-diagonal terms. In $3+1D$ relativistic spinors have $d+1=4$ components, being the square root of a $d=3$ dimensional vector. The transformation for 4-spinors in $3+1D$ for a Lorentz boost along the x direction (an *xBoost*, as in $3D$ we also need to specify the direction), is given by (see [29]):

$$L_{4spinor}^{xBoost}=\begin{pmatrix}\sqrt{\frac{\gamma+1}{2}} & 0 & 0 & \sqrt{\frac{\gamma-1}{2}}\\ 0 & \sqrt{\frac{\gamma+1}{2}} & \sqrt{\frac{\gamma-1}{2}} & 0\\ 0 & \sqrt{\frac{\gamma-1}{2}} & \sqrt{\frac{\gamma+1}{2}} & 0\\ \sqrt{\frac{\gamma-1}{2}} & 0 & 0 & \sqrt{\frac{\gamma+1}{2}}\end{pmatrix} \tag{27}$$

Whereby $\gamma=(1/\sqrt{1-\beta^2})$ is the Lorentz factor. $\beta=(v/c)$ and v is the constant speed in the x direction at which the non primed system is moving with respect to the primed measuring system's frame. If $\Psi=(\psi_1,\psi_2,\psi_3,\psi_4)$ is the Dirac 4-spinor in the reference system moving at speed v and $\Psi^{'}=(\psi_1^{'},\psi_2^{'},\psi_3^{'},\psi_4^{'})$ is the Dirac 4-spinor in the measuring system frame, then:

$$\Psi^{'}=L_{4spinor}^{xBoost}\quad\Psi \tag{28}$$

The transformation which relates $\Psi^{'}$ to Ψ is a **linear** transformation. Nevertheless, the dependence of its coefficients from the rapidity is hyperbolic. The rapidity being defined as ϕ_r such that $\tanh\phi_r=(v/c)$. We have used the index r to avoid confusion with the ϕ_i in the diffusion process while keeping the usual notation for the rapidity ϕ. As a function of the rapidity, the coefficients of the linear transformation for the Lorentz boost for spinors can be restated to show more clearly the hyperbolic dependence.

Now $\gamma=\cosh\phi_r$ and $\beta\gamma=\sinh\phi_r$. Therefore $\sqrt{(\gamma+1)/2}=\cosh(\phi_r/2)$ and $\sqrt{(\gamma-1)/2}=\sinh(\phi_r/2)$,. This shows further in what sense spinors are square root of vectors: spinors transform according to linear coefficients which are hyperbolic functions of half of the rapidity, while vectors transform according to linear coefficients which are hyperbolic functions of the full rapidity. For example the (ct,x) coordinate vector, under a Lorentz boost in the x direction, transforms as:

$$\begin{pmatrix}ct\\ x\end{pmatrix}=\begin{pmatrix}\cosh\phi_r & \sinh\phi_r\\ \sinh\phi_r & \cosh\phi_r\end{pmatrix}\begin{pmatrix}ct'\\ x'\end{pmatrix}=L_{2vector}^{xBoost}(\phi_r)\begin{pmatrix}ct'\\ x'\end{pmatrix} \tag{29}$$

In $1+1D$ spinors have $d+1=2$ components. Despite the coordinates still transform under a Lorentz boost as the equation above, the matrix $L_{2spinor}^{Boost}$ for the transformation of the 2-spinors simplifies to become (see appendix C):

$$L_{2spinor}^{Boost}=\begin{pmatrix}\sqrt[4]{\frac{c-v}{c+v}} & 0\\ 0 & \sqrt[4]{\frac{c+v}{c-v}}\end{pmatrix} \tag{30}$$

The coefficients on the diagonal of the matrix above are the square root of the relativistic Doppler coefficients. The use of the rapidity as a variable is a bridge to the natural coordinates used in the study of hyperbolic geometry where the Poincaré equivalent form of the operator L belongs in general to $PSL(2,\mathbb{C})$. The more general angle corresponding to the rapidity is then complex valued: the complex hyperbolic angle introduced by F.Klein, L.Fuchs and H.Poincaré. The complexification allows to include the other transformations in the Lorentz group other than the Lorentz boosts. We will come back in Appendix E on this hyperbolic complex angle formalism to discertization in $3D$. We can write:

$$\begin{cases}\psi_1^{'}(x',t')=\sqrt[4]{\frac{c-v}{c+v}}\ \psi_1\Big(\Big[\frac{v}{\sqrt{c^2-v^2}}ct'+\frac{c}{\sqrt{c^2-v^2}}x'\Big],\Big[\frac{c}{\sqrt{c^2-v^2}}t'+\frac{v}{\sqrt{c^2-v^2}}\frac{x'}{c}\Big]\Big)\\ \psi_2^{'}(x',t')=\sqrt[4]{\frac{c+v}{c-v}}\ \psi_2\Big(\Big[\frac{v}{\sqrt{c^2-v^2}}ct'+\frac{c}{\sqrt{c^2-v^2}}x'\Big],\Big[\frac{c}{\sqrt{c^2-v^2}}t'+\frac{v}{\sqrt{c^2-v^2}}\frac{x'}{c}\Big]\Big)\end{cases} \tag{31}$$

When we look for example at ψ_1, the factor arising from the linear transformation L can be also written as

$$\psi_1^{'} = e^{\frac{1}{4}\log(1-\frac{v}{c})}\ e^{-\frac{1}{4}\log(1+\frac{v}{c})}\psi_1 \tag{32}$$

The ϕ_i in turn are the result of the oscillatory dynamics of the ψ_i and the transient given by $e^{-\mu t}$, whereby μ is not modified by a Lorentz boost. The effect of the square root of the relativistic Doppler coefficient arising from L can then be seen in two different ways. Either it is a reduction (increase) for the numerical value of ψ_1 (ψ_2). Or it is a shift in the reference point in time for the transient factors, which is advancing (delaying) time for ψ_1 (ψ_2). This equivalent interpretation can probably be easily identified only in $1+1D$, as the complication arising from the interference of the other two dimensions is removed and L is so simple. In formulas:

$$\begin{cases} \psi_1^{'} = e^{\frac{1}{4}\log(1-\frac{v}{c})}\ e^{-\frac{1}{4}\log(1+\frac{v}{c})}\phi_1(x,t)e^{\mu t} \\ \\ \psi_2^{'} = e^{-\frac{1}{4}\log(1-\frac{v}{c})}\ e^{\frac{1}{4}\log(1+\frac{v}{c})}\phi_2(x,t)e^{\mu t} \end{cases} \tag{33}$$

We can develop the square root of the relativistic Doppler factor as an exponential and in powers of $\beta = \frac{v}{c}$:

$$e^{\frac{1}{4}\log(1-\frac{v}{c})}\ e^{-\frac{1}{4}\log(1+\frac{v}{c})} \simeq \exp -\frac{\beta}{2}\Big[\sum_{n=0}^{\infty}\big(\frac{\beta^{2n}}{2n+1}\big)\Big] \tag{34}$$

At first order in $\beta = (v/c)$ then:

$$\begin{cases} \psi_1^{'} = \phi_1(x,t)e^{\mu(t-\frac{v}{2\mu c})} \\ \\ \psi_2^{'} = \phi_2(x,t)e^{\mu(t+\frac{v}{2\mu c})} \end{cases} \tag{35}$$

We can look at the factor $-(v/2\mu c)$ at the exponential as a proxy of *difficulty* with the meaning of the factors used in the Rash model (see [30]), such parameter providing a way to *softmax* transform statistical data. The hyperbolic features are here reduced to some kind of generalized softmax transform. Such a parameter might be intuitively thought as a difficulty in adapting when changing between *(i)* the context of the measuring system frame's SubQuantum web and *(ii)* the context of the particle's SubQuantum web. Special Relativity can be then (re)stated as an adaptation formalism for linear changes of context. Which might be more appropriate for its discretization.

This seems to be providing an ingredient towards the formalisation of a part of the correct contextual form of emission theory, never considered to date for Special Relativity to the best of our knowledge, despite the numerous forms of emission theories unsuccessfully explored in the past. This is probably because the physics intuition is here opposite, in the sense that instead of a vibrational medium for the electromagnetic radiation, there is an enabling medium which does not transmit the vibrational modes at all.

It is also intriguing that a concept such as the *difficulty* can be introduced here, such concept arising in the study of psychometrics. As already argued, the strain modelled by the difficulty, is to be understood of similar nature to the strain of the zipping and re-zipping process, so that they can be composed. This could suggest that the intuition of those who see in Quantum Mechanics a contribution arising from some form of process involving the mind, although incorrect, might prove to be based on some sound analogies for completely different but somehow related reasons.

The relativistic Doppler coefficient is the ratio of two components, one related to light moving against the speed v and the other one related to light moving towards the speed v. We will then separate the two contributions. We will relate the *difficulty* $d_\pm$ of going against or together the speed v to the full components of the Doppler coefficient, rather than its square root, as it seems more natural to keep in line with the dimensionality of vectors rather than spinors. We define here $d_\pm$ as a percentage variation, the difficulty of the Rash model being then equivalent to the first order approximation, by setting:

$$1 + d_\pm = \sqrt{\frac{c \pm v}{c}} = e^{\frac{1}{2}\log\left(1\pm\frac{v}{c}\right)} \simeq e^{\pm\frac{v}{2c}} \tag{36}$$

Therefore $d_\pm = \sqrt{1 \pm \beta} - 1$. We think at this as measuring a difficulty of adaptation. The choice of $d_\pm$ not only well relates at first order to the difficulty of psychometric models, but it is also in line with the terminology of hyperbolic geometry, whereby the Poincaré distance defined on cross-ratios is here the term $\log\left[(1+\beta)/(1-\beta)\right]$ at the exponential. The approximation in the formula above links this interpretation to macroscopic quantum systems such as laser fields, which are quasi-$1D$ collective quantum condensates, of which the quasi-particle excitation is the laser "photon". In that context the corresponding coefficients are the squeezing and anti-squeezing factors. There is a common physical intuition behind these and other cases whereby the same hyperbolic structure appears, such as with the common use of the Bogolyubov transformation in the study of quantum condensates in the broader sense, such as the semi-classical treatments of quantum fields in curved space-time for the derivation of the formulas for Bekenstein-Hawking radiation or for the Unruh effect. For lasers, the back and forth reflection and the pick-up by stimulated emission which builds up the quantum condensate are also quite reminiscent of the $1D$ SubQuantum processes considered here.

For spinors, it will be the square root of $1 + d_\pm$ which appears in the Lorentz boost transformation:

$$\begin{cases} \psi_1^{'} = \sqrt{\frac{1+d_-}{1+d_+}}\ \psi_1(x(x',t'),t(x',t')) \simeq \phi_1(x,t)e^{\mu(t-\frac{v}{2\mu c})} \\ \\ \psi_2^{'} = \sqrt{\frac{1+d_+}{1+d_-}}\ \psi_2(x(x',t'),t(x',t')) \simeq \phi_2(x,t)e^{\mu(t+\frac{v}{2\mu c})} \end{cases} \tag{37}$$

One should then note again that the effect of the coefficients of the 2-spinors $1+1D$ Lorentz matrix in this case is to reduce ψ_1 and to increase ψ_2. In the development in β for the coefficients of the Lorentz boost matrix, in fact, only the odd powers of the rapidity are non-zero, whereby for ψ_1 all non-zero coefficients in the β development are negative, while for ψ_2 they are all positive. For the ϕ_i the effect of the boost turns out then to be equivalent to a delay or anticipation of the starting point of time for the relaxation process. If we look at the impact of the Lorentz matrix coefficients as a reset of reference time, at first order in β we would then define $\phi_i^{'} = \psi_i^{'} \exp\{-\mu[t-(v/2\mu c)]\}$. The numerical value of $\phi_i^{'}$ and ϕ_i are then the same. But they depend on (x',t') and (x,t) respectively.

If we were also to consider a simple case of initial values of ψ_1 as a Gaussian distribution $\exp\{-(x^2)/(2\sigma^2)\}$, we can then more easily explore explicitly the effect brought in by writing the transformed component of the bi-spinor under a Lorentz boost by also including the effect on the coordinates:

$$\frac{x^2}{2\sigma^2} = \frac{(vct'+cx')^2}{(c^2-v^2)2\sigma^2} = \frac{(x'+vt')^2}{2\sigma^2\left[1-\left(\frac{v}{c}\right)^2\right]} \tag{38}$$

Therefore the Gaussian in x with standard deviation σ has transformed into a Gaussian in $\tilde{x} = x' + vt'$ and standard deviation:

$$\tilde{\sigma} = \sigma\sqrt{1-\frac{v}{c}}\sqrt{1+\frac{v}{c}} = \sigma\ e^{\frac{1}{2}\log\left(1-\frac{v}{c}\right)}e^{\frac{1}{2}\log\left(1+\frac{v}{c}\right)} = \sigma\ (1+d_+)(1+d_-) \tag{39}$$

The same factors arising as a *difficulty* from the coefficients of the Lorentz matrix applied to the relativistic bi-spinor components, arise again as factors to the standard deviation, whereby the coordinates appear to be transforming separately according to Galilean transformations, as-if the hyperbolicity was not there. As the relative velocity seen from the system $(x^{'},t^{'})$ of the measuring and calibration system is $(-v)$, the Galilean transformation are a coherent change of mean for the Gaussian distribution. As we are looking at vectors rather than spinors, we get the factors $1+d_\pm$, rather than their square roots. The fact that the standard deviation's factor is the multiplication of the two difficulties factors rather than the ratio, might be understood by the difference of processes involved: *(i)* absorption and emission as separate and appropriate processes to detect the spinor from a relatively moving frame in the case of the ratio of the overall spinor component; to be compared to *(ii)* the back and forth combined, mixed and not separated composition of scattering in the case of the product for the diffusion constant. Therefore we are comparing the composition of two opposite effect processes versus the geometric average over the often repeated two way process. This in a way boils down to the observation that the inverse of the Lorentz factor γ and the Doppler coefficient are respectively the product and the ratio of the same factors, while providing an interpretation of these factors and relying them to the case of a Gaussian distribution, which is not general, but is quite meaningful within Quantum theory.

It would seem again that the SubQuantum web is globally standing still with respect to the reference system from which the measure is made (contextual-web), but the local part of the SubQuantum web contributing to the particle wave function is moving at a speed v along the single direction in $1D$ (local-web). At this stage, it seems natural if we take the simplest case allowing locally the web to contribute to the particle wave function, while the rest of the web is polarised by the context in which is immersed. The local web is charged, as in Figure 6. At the SubQuantum scale, the number of excess or deficit monomers in the web is finite and there is no infinite tail to infinity as for the quantum wave function. There is then an interface whereby the particle *ends* in the sense that the SubQuantum web has an interface between charged and uncharged areas. Just like the lipid barrier of a cell. Or the Anti de Sitter hyperbolicity barrier of the simplest non-quantum model for the interior of a black-hole. At this barrier the charged SubQuantum web must be transferring then the excess or deficit monomers through some form of autocorrecting combinatorics allowing the particle local web configuration to go through the rest of web with a relative speed v, therefore being locally unaffected. Such a mechanism enables the law of inertia for the particle, understood as the particle's resistance at the changing of its state of movement. The inertia mechanism must be combinatorial and dynamic, enabling a recomposition preserving the same structure, as the particle goes through the contextual web. In this sense it is autocorrecting. Its discussion takes us to a scale which seems to be even below the one at which we are exploring how to model at this stage. Because the law of inertia is to be derived from the underlying combinatorial dynamics, it is appropriate to say that SubQuantum Mechanics is pre-classical.

Before a photon is emitted or absorbed, it propagates while fitting coherently through the external SubQuantum web. It is then compressed at emission only if going against the web, and decompressed if going away from the web. At the emission and absorption there is then a strain. Because of the strain, the image of the net densities from the reference system of the particle appear distorted. It seems quite plausible that such strain could be modelled using spherical projection coordinates of some kind. This is because such coordinates arise in the cases where strain is self-recycling in mechanics and leads to integrable problems. Such is the basis of F.Klein's approach in the study of rotating bodies (see [31]) using the coordinates identified from his icosahedral solution of the quintic algebraic equation. Although published later, this class of mechanical systems and their features appear to be among the Classical Mechanics mathematical physics and symmetry motivations which led F.Klein to the formulation of the Erlangen program several years earlier. And which have provided the roots for spinor calculus and its further complexification into twistors theory. This kind of strain generates the elliptic functions based hyperbolic structure of the dynamics of numerous integrable mechanical problems. The first studied problems being the non-linear pendulum, the elastic horizontal bar (called the *lemniscate* for the shape of the orbits in phase space, or called the *lamina elastica*), the Euler buckling problem, the strained spinning top (rotating axis not going through the centre of gravity). In all these problems there are typically four configurations of the relative direction of two types of forces, which generate the strain circularity, enabling the system to be integrable and hyperbolic (see Appendix E).

From the relationship and forms of equations for the ψ_i and $\psi_i^{'}$ above, there is therefore a interlaced composite SubQuantum diffusion process for which the non-boosted and the boosted equation respectively are the Quantum limit. One would like to identify the relation between the processes underlying the first and the second equation and see what we can learn about the SubQuantum meaning of the Lorentz boost, with respect to the SubQuantum gas and the SubQuantum web. Because in $3+1D$ the Lorentz group is expressed by $SL(2,\mathbb{C})$, we can consider that in $1+1D$ there are no rotations and we get a simplified $SL(2,\mathbb{R})$ matrix. Furthermore, at SubQuantum modelling level we have the discrete nature of the web and we sample only at the web nodes to model. It would seem natural then to consider in general an $SL(2,\mathbb{Q})$ matrix, or possibly some subset of $SL(2,\bar{\mathbb{Q}}\cap\mathbb{R})$ matrix, whereby $\bar{\mathbb{Q}}$ is the usual notation for the algebraic numbers. For SubQuantum Mechanics in $3D$, one would expect $SL(2,\bar{\mathbb{Q}})$ to be a natural candidate for a discrete version Lorentz invariance, at least in the free particle case. By taking the Poincaré representation of the Lorentz group, its discretizations takes us straight to the domain of Kleinian, Fuchsian and Schotkky groups, as well as that of the subgroups of the modular group. A full physical translation of the mathematical context does not seem to be currently available in this sense. An example of discretisation which enables to write the basic formulas, can be explored by setting space and time-evolution steps equal to countable equipartitions of the respective units of measure (say the Ångström and the second):

$$\delta = \frac{1}{n}, \quad \text{and} \quad \epsilon = \frac{1}{r}, \quad n, r \in \mathbb{N}$$

Therefore:

$$\delta m = x \Longleftrightarrow x = \frac{m}{n}, \quad \text{and} \quad \epsilon s = t \Longleftrightarrow t = \frac{s}{r}$$

But $(\delta/\epsilon) = constant = c$. Therefore both n and r must scale with the same integer l:

$$n = lq, \quad \text{with } q, l \in \mathbb{N} \quad \text{and} \quad q \quad \text{constant}$$

$$r = lq', \quad \text{with } q', l \in \mathbb{N} \quad \text{and} \quad q' \quad \text{constant}$$

Then $c = (q'/q)$ and we can consider that q' is much larger than q. We can also take integer constants p and p' and scale with l also (m, s):

$$m = lp, \quad \text{and} \quad s = lp', \quad \text{with} \quad p, p' \in \mathbb{N} \quad \text{constants}$$

Then:

$$x = \frac{p}{q} \quad \text{and} \quad t = \frac{p'}{q'}$$

Similarly we can take:

$$v = \frac{j}{q}, \quad j < q', \quad \frac{v}{c} = \frac{j}{q'}$$

And we have:

$$\gamma = \frac{q'}{\sqrt{q'^2 - j^2}} \text{ and } \gamma\beta = \frac{j}{\sqrt{q'^2 - j^2}}$$

A Lorentz boost will deform then the (m, s) lattice in space and time through to a new lattice (m', s'). By looking at the form of coordinate transformation above, such transformation will be given by a matrix of the form:

$$\frac{1}{\sqrt{q'^2 - j^2}} \begin{pmatrix} q' & j \\ j & q' \end{pmatrix} \tag{40}$$

Similarly the 2-spinors would be transformed according to a discretised version of matrix L:

$$L_{2spinor}^{DiscreteBoost} = \begin{pmatrix} \sqrt[4]{\frac{q'-j}{q'+j}} & 0 \\ 0 & \sqrt[4]{\frac{q'+j}{q'-j}} \end{pmatrix} \tag{41}$$

In order to generalise this kind of discretisation paths to $3D$, the set of matrices to which the Lorentz boosts belongs will span part or all of $SL(2, \bar{\mathbb{Q}} \cap \mathbb{R})$ or of a similar related arithmetic group. In $3D$ one would then expect something like:

$$L_{4spinor}^{DiscreteXboost} = \frac{1}{\sqrt[4]{4(q'^2 - j^2)}} \begin{pmatrix} \sqrt{\sqrt{q'^2 - j^2} + q'} & 0 & 0 & \sqrt{\sqrt{q'^2 - j^2} - q'} \\ 0 & \sqrt{\sqrt{q'^2 - j^2} + q'} & \sqrt{\sqrt{q'^2 - j^2} - q'} & 0 \\ 0 & \sqrt{\sqrt{q'^2 - j^2} - q'} & \sqrt{\sqrt{q'^2 - j^2} + q'} & 0 \\ \sqrt{\sqrt{q'^2 - j^2} - q'} & 0 & 0 & \sqrt{\sqrt{q'^2 - j^2} + q'} \end{pmatrix} \tag{42}$$

If we take an (x, t) projection of the discretised 4-spinor Lorentz discretised boost matrix above, to single out the relevant boosts variables we get something different from the $1 + 1D$ matrix above:

$$\tilde{L} = \frac{1}{\sqrt[4]{4(q'^2 - j^2)}} \begin{pmatrix} \sqrt{\sqrt{q'^2 - j^2} + q'} & \sqrt{\sqrt{q'^2 - j^2} - q'} \\ \sqrt{\sqrt{q'^2 - j^2} - q'} & \sqrt{\sqrt{q'^2 - j^2} + q'} \end{pmatrix} \tag{43}$$

$\tilde{L}$ is the (x, t) sector of $L_{4spinor}^{DiscreteXboost}$ and is different from $L_{2spinor}^{DiscreteBoost}$. The $3D$ boost can be then considered as a lifting of $\tilde{L}$. The discrete Lorentz boost in the x direction is seen here as the action of an arithmetic group over the space-time lattice $(m, s) \in \mathbb{Z}^2$, whereby the hyperbolic features of the group provide a model of the strain at emission and absorption in a way which must be consistent with the heuristic for the single collapse discussed in Section V.

Observation a. The Einstein principle of Special Relativity, setting to a constant the speed of light detected in vacuum whatever the speed of the emitter with respect to the detector, is hereby realised by setting the speed of light post emission with respect to the contextual web and not to the web of the emitter. This implies that there is an additional differential strain at emission and absorption which is modelled by the velocity hyperbolic dependence of the discrete Lorentz linear transformations' coefficients. Such a strain is on the top of the strain discussed for emission and absorption, in the case of a particle at rest in the reference system of the detector and of its calibration system. Nevertheless, the two strains are of similar nature and it should be possible to compose them at some level. They seem both to be related to some form of modularity in the appropriate number theoretical setting. The total strain is the enabling feature of the un-zipping and re-zipping processes in Section V. The web is not a medium for the propagation of light, but it is an enabling medium, therefore generating a strain when there is a change of context. This kind of emission theory could not be conceivable in a framework whereby an ether had to be there first of all as a medium for the vibrations of the electromagnetic field, which is not the case here. This also clarify why those theories could recover only one of the hyperbolic coefficients of the Lorentz transformations but not the other, or vice-versa. A conundrum which was only resolved by Einstein introduction of the constant speed of light principle, from which it was straightforward to derive the correct form of hyperbolic geometry due to the courageous inclusion within such principle of the case of relative inertial motion of emitter and receiver. This did require the total denial of the possibility for a newtonian-like explanation. A mystical step, in the sense of "accepting the mystery" as not explicable, but only formalisable with mathematics. Which was the right practical choice at the time, but it required to restate causality within hyperbolic space, without giving a physical causal origin of hyperbolicity other than empirical or philosophical.

Observation b. It should be conceptually possible to distinguish between a SubQuantum constrained and discretised version of Lorentz-boost invariance and the full continuous Lorentz-boost invariance. If very large parts of the surrounding web can be kept contextually at rest with respect to the emitter rather than the detector, this physical intuition might lead to a difference with ordinary Special Relativity. Nevertheless, it seems to us that it is extremely difficult to identify an experimental system whereby the difference between the two could be observed. This could be the case if the contextual change is very far away from the emitter. An ultra-high vacuum linear and long environment for a very fast moving emitter would have to be built, whereby the emitter is rigidly attached to a rigid material support which can also move very fast (relative to the speed of light) within the ultra-high vacuum and in the direction of emission. Possibly a very long strong rigid arrow with a long cavity along the arrow axis. The emitter on the end of the cavity at the back extreme of the arrow, with its own shutter periodically opening. At the other end of the arrow, a hole to let the photon escape. There should then be a powerful rail cannon system within the ultra-high vacuum to shoot the arrow. One can then try to detect the time of flight of the photon at the extreme of the experiment opposite to the cannon and compare to Special Relativity. At this stage, it does not seem financially reasonable to deploy and modify a SLAC like infrastructure just to test this. But you never know what the future brings along.

Observation c. In the case of the ICARUS and OPERA Geneva to Gran Sasso neutrino experiments (see [32, 33]), it is interesting to note that the proton-on-target ratio in the second experiment has been decreased materially at the neutrino factory injection beam-line. The logic might have been to reduce noise of some sort. Nevertheless, from the perspective of this discussion, reducing the proton-on-target ratio in the second experiment, would probably reduce the chance of generation of any superluminal neutrino. The second experiment would then not seem to be providing solid evidence that the first measure was incorrect. Many have also noticed that any signal delay or extra reflexion on coaxial cables for time-of-flight measurements, which has been called upon to clarify the surprising values of the first experiment, would normally lead to slower neutrinos and not faster. Independently from these critical observations, if the framework here discussed does actually lead to superluminal signals, it seems difficult but not logically impossible that they could have been detected by the earlier of the above mentioned experiments, but not the later one. Furthermore, in our framework, any breach of Lorentz invariance would be extremely short lived and offset rapidly, more in line with the Cohen-Glashow effect discussion (see [34]), where Z boson are produced and decay rapidly to offset the excessive speed. To be able to detect anything with time-of-flight measurements one would then require to have neutrino detectors very very close to the neutrino factory, which is not the case in the existing settings around the world to date. Detection probability should increase with higher detectors proximity and not with more remote detectors, which is the assumption if the superluminal effect was to be long lived. Lorentz invariance breach here, has then to be thought as a very short lived and temporary feature. More like Brownian motion for an isolated particle could breach a little and for a very short time the second principle of thermodynamics locally. A Lorentz invariance breach would not be then an effect that could be detected on cosmic rays in principle, as the emission and reabsorption process on the path to earth would erase or dilute the impact of any very short lived Lorentz invariance breaching event. This is one of the reasons to consider Lorentz invariance as a second principle of thermodynamics at SubQuantum level.

Observation d. We can now revisit the Einstein thought experiment from the 1930 Solvay Conference, used by Einstein to try to show to Bohr that there was a case at least, whereby the Heisenberg principle for energy versus time was violated (see [35]). Such experiment is a simulation of a photon emission, by a source in a box, rather than by the atom itself. But because of the introduction of the box, the size of the emitter becomes macroscopic. It would seem that Einstein found such an example because he was deeply convinced that Heisenberg principle was purely empirical, worked only for the cases identified at atomic level and was not an universal principle. By introducing a macroscopical object emitting a photon as-if it was an atom, he thought that he had found where the relative scales were stretched to the point that they enabled to break the limit of applicability of the Heisenberg principle. The choice of how to stretch-test the Heisenberg principle was an act of profound physical intuition by Einstein. It was therefore even more so a triumph for Bohr to show that, provided the Heisenberg principle for position versus momentum of the box was assumed to be satisfied (being scale-comparable measured quantities), it was then Einstein who had not correctly taken into account all the first order experimental errors in the analysis of his own thought experiment. And that the first order error he had forgotten was arising from the gravitational Red-Shift of the emitted photon. Which showed that there was an impact on the microscopical photon by the macro-size of the box through gravity and because of Einstein theory of General Relativity. Or to be more precise, because of the equivalence principle and the extension of Special Relativity to uniformly accelerated systems, within first order approximation, from which the Red-Shift formula was first derived in 1907 by Einstein. And that by inserting such additional experimental error in the analysis, the Heisenberg principle for energy versus time was recovered. This convinced Einstein of the universality of the Heisenberg principle, even more strongly so, as Bohr counter-argument brought in a very macroscopic effect. Stretching within Heisenberg relations both the large macro scale (gravity) and the small micro scale (photon emission). In fact the analysis shows that in a world where Einstein gravitational Red-Shift does not exist, the Heisenberg principle would not work, at least for a case and for energy versus time, EVEN if the Heisenberg principle applicability was assumed for the respective position and momentum. Bohr showed therefore that Heisenberg principle incorporates somehow the gravitational Red-Shift effect. Therefore gravity and quantum mechanics are intimately and coherently interconnected at this level, a level where the very micro and the very macro coexist and cooperate neatly. As a reminder, Einstein analysis did not see any specific reason for which one could not make the uncertainty on the time of exit of the photon as small as needed, without impacting upon the value of the uncertainty of its energy in any way. Bohr on the opposite assumed that the Heisenberg principle was satisfied for the position and momentum of the box, as both are of the same scale and the mismatch argument between very different size scale would not apply. By using $E = \hbar\nu$, he then showed that this in turn implies that the frequency of the photon, using Einstein Red-Shift formula of 1907 (before the full formulation of General Relativity), had to have an uncertainty which recovered exactly the Heisenberg principle for energy versus time. In fact, using Bohr setting (see [35]), if ϕ_g is the gravitational potential, if Δm_g is the variation of gravitational charge (mass) needed to restore the box to its original position after the photon has gone out, if $\Delta m_g = \Delta m_I$ by the equivalence principle, then the Red-Shift formula gives:

$$\Delta\nu = \nu\frac{\Delta\phi_g}{c^2}$$

With $\nu = t^{-1}$ and $\Delta\nu = -(\Delta t/t^2)$ one then gets:

$$\Delta t \simeq t\frac{\Delta\phi_g}{c^2} = t\frac{g\Delta q}{c^2}$$

Then:

$$\Delta q \simeq \frac{c^2\Delta t}{gt}$$

Now, Δt is also the uncertainty of the time of the photon emission and t the time needed for the the impulse on the box to be rebalanced back to nil by the weight attached to the box. Therefore:

$$\Delta p < tg\Delta m_g$$

If the Heisenberg principle is valid for p and q, then $\hbar < \Delta p\Delta q$, $\Delta E = \Delta m_I c^2$ and

$$\hbar < (tg\Delta m_g)(\frac{c^2\Delta t}{gt}) = \Delta E\Delta t$$

If we keep Bohr analysis in mind, we should now consider that gravity can affect the average distance between SubQuantum web nodes. This is actually a rough description of what the gravitational potential term in the metric tensor would corresponds to. This in turn changes the mean free path of the SubQuantum scattering process, which causes the indeterminacy for the mass. The density of a gaussian distribution of net monomers will be affected with a related indeterminacy in momentum. The scattering frequency of the diffusion process will also be affected by a change of average distance between nodes. Therefore both *(i)* the Red-Shift which causes uncertainty in time and *(ii)* the uncertainty in gravitational energy, are the result of the same dynamical cause, affecting the position and momentum. The product among the uncertainty of each two canonically conjugated variables are therefore interlinked and have to remain within the same boundaries set by the Heisenberg principle assumed for the momentum and position. Conceptually this seems intuitive, as both the Heisenberg principle, and the law of inertia appear as the result of the same SubQuantum dynamical feature. At the SubQuantum level, gravity affects the SubQuantum structure with an inertia-equivalent dynamical impact. If gravitational waves can be thought as spin waves across the SubQuantum web, a change of gravitational potential might then possibly be seen as a change of density of SubQuantum web nodes. This is a pre-newtonian version of the spinon versus holon separation in strongly collective quasi-low-dimensional quantum condensates, the collective features arising here from the web condensation. If an isolated local holon-like SubQuantum web deformation acts coherently with a SubQuantum gas cloud, a particle forms: a conceptual SubQuantum equivalent of the Higgs mechanism.

Observation e. The discussion used for the Lorentz boost might be adaptable to the case of three reference systems, whereby the second is uniformly accelerated with respect to the first, and the third moves with constant speed with respect to the first, while the third also coincides with the second at a given time. This is the framework used by Einstein to derive the redshift formula in 1907, much before his formulation of a full theory of General Relativity (see [35]). This is the starting point to develop SubQuantum Mechanics towards the modelling of curvature-like effects, as it was the case for General Relativity.

Observation f. The language of GL_2 Galois representations also seems to be a complementary tool for the structuring of a discrete Lorentz invariance for cases more general than the free particle. *l-adic* analysis might be among the natural tools for the modelling of scaling renormalisation. Modularity theorems could be understood as statements about Lorentz-boost invariance compatibility with SubQuantum web admissible topologies. Fermat Last Theorem might be a statement about the arithmetic topology impossibility to use straight-hedge coordination in the structuring of discrete Lorentz invariance starting from $3D$, which should be otherwise compatible with a quadrupolar coordination, as in the tetrahedral configuration, being minimalistic in term of connectivity (the straight-hedge coordination in $3D$ would be sextupolar). It is temping to suggest that Fermat had some geometric intuition of the general arithmetic topology feature at hand as he stated FLT by saying that it is valid for $n = 3$, and then that it is valid for $n = 4$, and then that it is valid for all higher n. There might be then three incremental different reasons for each of his three sub-statements, not necessarily in their stated cardinal order. He might have not found a proof of his *last* theorem as it is believed today, but he might have identified an heuristic discrete topological reason for it to be valid for $n = 5$, which seemed permanent for $n > 4$. Surprisingly, an even tentative reason for Fermat statement of FLT has never been identified to the best of our knowledge, and it seems more than unlikely that he would have stated it, correctly or incorrectly, just out of the blue. We have mostly remembered Fermat for stressing the powerful formulation of number theory through more abstract algebra, so to reach results well beyond those coming from the mainly geometric intuition used at the time in the field by his contemporaries of the British school. We then forget how Fermat was far from overlooking geometrical intuition, as more recent studies in his contribution to the structuring of calculus have clarified, his stressing the algebraic point of view mostly a need to rebalance the excess of geometrization of his times. If there is a sensible reason for which Fermat wrote his note, the answer might possibly come from geometry and not from algebra. It is tempting therefore to see the arithmetic descent methods as reversed discrete renormalisation procedures, given a specific decomposition of space. The constraint set by asking for integer solutions is then a way to express that we are dealing with discrete geometry in the sense that there has to be a smallest possible finite scale which provides a cut-off to the reverse renormalisation procedure. The fact that the descent method is based on Pythagorean triples for $n = 4$ is then showing the role of the straight-edge coordination in the chosen deconstruction of space. The success of the descent method would then imply that the coordination is overabundant and leads to infinite reverse renormalisation steps. There is therefore no discrete fundamental underlying structure, therefore no cut-off is possible. The version for $n = 3$ is more elaborate, to reduce to a similar descent mechanism. S.Germain techniques, are a further highly sophisticated generalisation through auxiliary variables (see [36] tracking from Fermat to Wiles). The celebrated elliptic-curves-based general absence of solutions in the relevant discrete space by A.Wiles is then possibly a consequence of the strain compatibility requirement of the discrete structure behind the SubQuantum web features. Maybe it is possible to identify a reason for the tetrahedral coordination, being minimal, to enable the existence of solution for some form of corresponding Diophantine equations while retaining appropriate discrete modularity properties. If this can be shown in low dimensions and can be intuitively structural, this might

have been a basis for Fermat cryptic statement, who had found how to solve on his own the Pell equation and therefore plausibly knew a bit about modular transformations in their simplest practical context, which relates to continuous fraction arithmetics. The Pythagorean triples distribution provides also the possibly earliest known case of discrete hyperbolic geometry in the field of the rationals: $x^2 - z^2 = y^2$ and divide by y. We are then led to see Fermat statement in the context of the general study of Diophantine equation for low number of variables, whereby one needs to identify when: *(i)* a general formula holds, as for Pythagorean triples; *(ii)* isolated solutions occur, as shown in [37] for a case of generalisation of Fermat equation where the absence of solutions starts to breakdown only gradually; or *(iii)* no solutions occur at all, as in FLT. In the case of [37], there are 4 variables instead of the 3 of FLT. In addition, non-formula-based solutions persists at least for $n = 4$, rather than breaking down all at once for $n = 3$. It seems that Fermat did look at the broader space of Diophantine equations from a similar perspective, as in $D = 2$ with the polygonal number theorem. The fact that there is a sharp transition for three variables and straight-hedge coordination geometry is quite likely related to a meaningful arithmetic topological feature. It seems natural that Fermat, being a judge, was focused on the application of the law and not on its formulation. His statement needs to be put in the context of his studies. For example in $3D$ is easy to find relationships between 3 polyhedral numbers. As a simple example if T_n is the tetrahedral number of side n and P_n is the square basis pyramidal number of size n, $P_n = T_n + T_{n-1}$. The question is then what topological features make the FLT equation sharp transition from formula based ∞ solutions of the Pythagorean triples to the no solution at all of the $n \geq 3$ case. And what makes this persistent from $n = 5$. This should be implicitly embedded already in the low n proofs but not as a purely algebraic proof, and should involve modularity, understood in turn as an proxy of discrete Lorentz invariance, and therefore should be understood also from a physical perspective. In one single variable x, rather than the 3 variables x, y, z of FLT, and if we allow solutions to be on $\mathbb{C}$, the case of $n = 5$ is special and transitional towards hyperbolic geometry, as shown by F.Klein general solution using elliptic functions and the projective symmetries of the icosahedron.

Observation g. Complex hyperbolic transformations are also used to derive the bounded part of coherent states for the quantum hydrogen atom, obtained as deformations of the coherent (Schrödinger) states of the quantum oscillator. The hyperbolic boundary being provided by the separatrix at the ionisation threshold (see [38]). This feature should help to provide a mathematical description of the photon emission and absorption process in the specific case of the hydrogen atom. The wavelets basis used in these problems were introduced as a general technical tool realising the Riesz principle, of which the May 1925 (Thomas-Reiche)-Kuhn sum rules are a relevant predecessor (see [39]). Such sum rules, possibly unblocked W.Heisenberg path towards the quantum theory of anharmonic oscillators to model emission and absorption, published a couple of months later. By effectively learning that, to formulate a quantum theory of atomic spectra, there had to be what will be called later a Hilbert space, Heisenberg possibly realised that among all the variant calculations he had performed, there was a choice of variables which enabled such formalism. Such choice was not at all classical as it effectively SWAPPED the priority between which concept to identify first: vibrational modes rather than canonical coordinates. Bohr had already done the same SWAPPING of priorities when he took the proper physicist's choice to rely on the higher precision of measurement of spectroscopic data, rather than the less precise bremsstrahlung data for the charged particles, leading to the Bohr atom model and making largely obsolete the Thomson atom model formulated shortly before in the same laboratory (see [40]). In a way Heisenberg was moving further ahead ON THE SAME PATH. Both steps contributed to the structuring of what E.Cassirer called the *coordination principle*: by swapping priorities the correct way to coordinate photon energy and frequency is singled out. This also clarifies that the correspondence principle is a necessary *a posteriori* band-aid solution, keeping together the water under the ice (classical) and the skating over the ice (quantum) which Heisenberg had connected by breaking through a very narrow hole indeed. It seems difficult to do fully without such a band-aid solution unless possibly with a full SubQuantum theory. As Heisenberg had tried all combinations of calculations already, taking W.Kuhn work plus Bohr foundational approach, his swapping of priorities was in a way natural. Combining these considerations, the Heisenberg group naturally arises from the realisation of the Heisenberg principle in exponential form, which is closer to the sum rules which brought Heisenberg through his narrow path and which is the form used by H.Weyl. Such form provides the basis for the proof of the Stone-von-Neumann unicity of representation for Heisenberg principle. A.Weil's discrete form of the same theorem is unknowingly a SubQuantum proxy: he formulated it after being hosted by G.W.Mackey. The Heisenberg group arises naturally in this context, an is related to hyperbolic geometry properties. We hope that the general approach of this course does shed some light on why and how indeterminacy and hyperbolicity are naturally and intrinsically connected, and not just at the formal level. Since the beginning of his interest in atomic physics, E.Schrödinger was searching for a bridge between: *(i)* de Broglie coherent matter waves along the electron orbits of Bohr atom (de Broglie started from relativity and gravitation, see [41]) and *(ii)* Sommerfeld fascination with the fine structure constant, intuitively believed at the time to lead to the ultimate bridge between electro-magnetism and General Relativity, through Quantum theory. Schrödinger initial motivations resurfaced when he worked on Einstein's theory of the affine field (see [42]), but he seemed to have overlooked that Special Relativity can be found within Heisenberg rules, whereby hyperbolicity arises by complex extension of the Weyl form of the uncertainty principle (see [18]). Which can also be derived from Schrödinger equation.

VII. AN HEURISTIC FOR THE BORN RULE

In order to collect the data sample to get a given statistics for a specific quantum measurement, the un-zipping and re-zipping processes are repeated over a large sample of reasonable identical systems represented by reasonable identical wave functions. In terms of relative timing of each experimental measure, the limiting cases are: *(i)* at the same time, or *(ii)* in a well separated sequential succession. There is therefore a parallel or sequential repeated non-linear process over a multitude of systems each evolving linearly before each non-linear process is imposed. The linear evolution is provided by the combinatorial dynamics in Figure 4. The non-linear process is provided by the combination of un-zipping and re-zipping processes in Figure 6. It is therefore quadratically non-linear in $|\psi| = \sqrt{\psi^* \psi}$. It is bilinear in ψ and ψ^*.

The sampling process is therefore reminiscent of a machine learning technique, whereby the objects involved *learn* the Born rule. In this sense one can see that there is no in-principle inconsistency between the Qbism approach (see [43]) and early interpretational views. In fact, it is the learning process which generates the Born distribution of measuring outcomes. Such a population of outcomes does not exist before the sampling has been completed, not in the sense of a statistics of post un-zipping and re-zipping process collapsed states. It is created by the sampling process through a learning-like mechanism. But the numerical values of the statistics of such a resulting sample must be equal to the numerical values derived from the renormalised distribution of the net SubQuantum gas densities before the un-zipping and re-zipping process. In this sense each one of the reasonable comparable states before the respective un-zipping and re-zipping processes, already holds the information determining the numerical values of the statistics, which later emerges from the sampling process on several reasonable identical systems. Among the subtleties of this framework, one should take into account the fact that the natural nomalizations required in order for $|\psi|$ and for $|\psi|^2$ to be treated as probability distributions are different. But the normalization of $|\psi|$ is never used at the Quantum level. That is why the p_i were not normalized and the density approach was used to derive ψ.

In order for the Born rule to be the outcome of the sampling whatever the learning path, it is also necessary that, if the sampling deviates from the Born rule statistics corresponding to the wave function of the system, then there is a mechanism auto-correcting it back. Such mechanism would then play a similar role to the gradients or other functional inputs used in machine learning to enable the learning process. The persistency of the calibration of the local macroscopic measuring system is the natural candidate as an enforcing agent of such an auto-correcting non-dissipative strain. The intensity of such effect is to be measured by some statistical distance between the actual sampling and the Born statistics. In fact in this framework, if the Born rule is respected, the net exchange with the measuring system of the physical variable which is canonically conjugated (in the Hamiltonian sense) to the one being measured, must be nil. Else the measuring system shifts out of calibration. If a non-zero statistical distance builds up in time, in order to avoid shifting out of calibration, the calibration system returns any excess or defect accumulated to the next sampling processes, possibly through heat photons, which anticipate the next collapse to an appropriate steady state. In this sense Born rule is some kind of first principle of thermodynamics for SubQuantum Mechanics: it encapsulates the enforcement of conservation laws in a quite specific way (see also Appendix D). If we consider for the sampling the case with highest possible time resolution, i.e. a sequential sampling enabling to look at the process stroboscopically, a schematic representation the learning auto-balancing process is sketched in Figure 7.

At the beginning of the sampling, the measurement instrument plays the role of Wigner's friend and causes the collapse process. If there is no distance between the Born rule distribution and the sample collected, Wigner never plays a role. But if the sample deviates, then the calibration system causes the sampling to align to the Born distribution calculated from the starting wave function, playing a Wigner-like role. If we use the statistical language of causal inference (see *randomisation* in [44]) we should consider that there is randomisation of the un-sampled remaining population, as long as there is no distance from the Born distribution calculated from the equal initial state for all particle-like systems sampled. If on the opposite there is a non-zero statistical distance, then there is a process of partial de-randomisation of the residual non-collapsed sample which is proportional to the statistical distance. It is not a generic de-randomisation. It is specifically structured so to reset to zero the statistical distance from the Born rule of the sampled population as the sampling accumulates further. We should then probably talk of **conditional controlled de-randomisation**, as a temporary source of de-markovisation, enforced by the persistency of calibration. Whereby calibration should be considered in the broader sense, i.e. both calibration of the measuring probe locally and calibration of the relative global calibration between different measuring probes in different places.

It is also relevant to clarify that the randomisation and de-randomisation hereby discussed has nothing to do with the critics to possible lack of randomisation in the choices of Alice and Bob polarisers alignments for Bell-like experiments. These seems hardly to be questionable with this framework. It is instead the persistency of the randomisation of the un-sampled part of the population of each of Bob or Alice, as their respective samplings build up separately, which are here at risk. But they do not change at all the fact that Bell inequality are violated. On

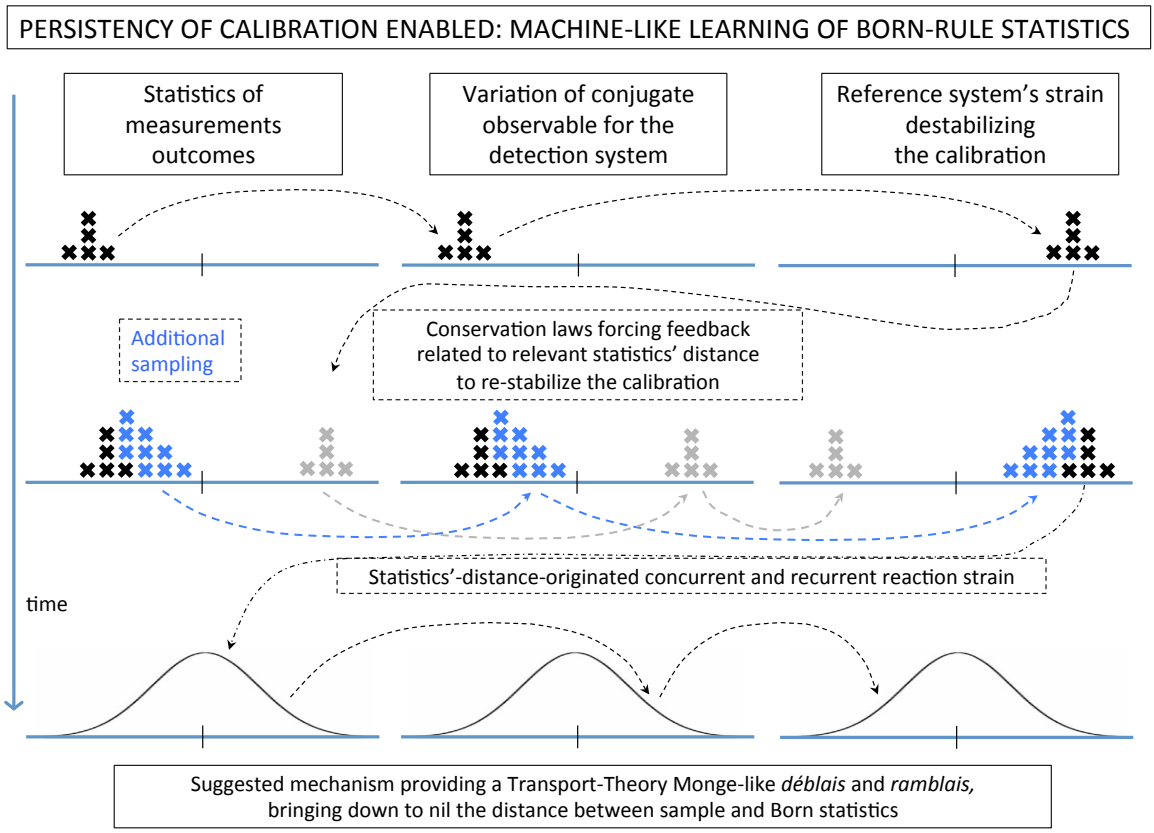

FIG. 7. Sketch of the circular feedback enforcing the Born rule. By analogy to Transport Theory and Machine Learning. The system providing the rigidity which keeps persistent the calibration of the detectors does enable a cross-statistics transfer process. As the sampling evolves, if its likelihood moves away from what is expected by the Born-rule statistics, such feedback prevents the sample set from building up a distance from the Born statistics. The higher the precision which the calibration has to insure, the sooner the reaction strain kicks in. The calibration reference system plays the role of Wigner, who is here taking part in the stabilisation of the Born rule statistics. It is therefore Wigner's friend who causes the single collapse of the wave function. But if the sampling drifts away from the Born rule statistics calculated from the wave function (net SubQuantum densities), it is Wigner who intervenes to assure that the residual sample is de-randomised exactly what it takes to counterbalance the effect and recover the Born rule. If Wigner falls asleep the calibration is lost.

the opposite: such de-randomisation contributes towards the coherent violation of Bell's inequalities. In order for the initial randomisation to be temporarily and partially lifted, there has to be a class of processes which involve the calibration system and through which the remaining part of the population to be sampled is affected. This could be quantum of heat transfers, not necessarily only in one direction.

In [45] for example, the randomisation of Bob and Alice choices of polarisers orientations has been assured to an extreme. But an analysis of the randomisation of residual sampling data does not seem to have attracted any attention of the teams writing the paper. To clarify, we can discuss for example what reported by the team number 9 (Farrera-Heinze-Riedmatten), who seemed to provide a good transparency about the structure of the experimental data collected. They started from approximately 365 millions of events. They selected by coincidence diagnostics about 1100 events from which they grouped the sets giving the 12 averages of Bell parameter all in excess of the classical level shown in their chart. It would be interesting for example here to see if there is any information within the 1100 events retained before they are grouped to calculate the averages, in particular by taking into account their order of recording, to see a trace of some mechanism of this kind at play. Similarly it would be interesting to look into the other 365 millions events where a time mismatch in the coincidence selection can be caused by a feedback-like process which results in the exclusion of meaningful events for the study of this kind of features. The aim of this type of analysis would not be to disprove Bell violations. But to study if the data provides information in line with this framework, highlighting how the violation comes about. Similar consideration might apply to the work of other teams in [45] .

Bell-like theorems exclude local non-contextual hidden variable models. And the only non-local, contextual hidden variable model at the time of the formulation of such theorems was Bohm theory ([46]), which can reproduce much of non-relativistic Quantum Mechanics, but which appears to be undistinguishable from it and does not seem to provide a tool for structured exploration. According to [46] in fact, J.S.Bell was not in search of a way to exclude hidden variable models, but to narrow as much as possible their scope. So that Bohm theory could be supported as the right hidden variable theory. From our framework for SubQuantum Mechanics it would seem that the non-local contextual way to look at the geometric frustration in the colouring arguments of impossibility, which are behind the no-go theorems, is to say that each observable is multicoloured in this kind of contextual setting. There is then no geometrical frustration and all nodes are coloured in the same multicoloured way.

As seen in this course, there are hidden variables at the interlaced diffusion process level, both by the variables which do not contribute in the Quantum Limit, and by the reciprocal variable in the SubQuantum web. These also contribute in a different way to the un-zipping and re-zipping processes. But there are also latent variables (very short-lived hidden variables), describing the reciprocal temporary causal inference which de-randomises the residual samples, if the sampling drifts away from the Born distribution. By taking as a reference the diagrammatic methods used in [47], we can describe the causal structure arising from the autocorrection imposing the Born rule in the simplest case as depicted in Figure 8. The red and green arrows are virtual events, which might be or might be not detectable, micro calorimetry being far from such challenging tasks to the best of our knowledge. Except that the fragility of entanglement in the simplest versions of quantum thermal machines might provide a route to enable these kind of measurements in the near future, by detecting the breaking down of entanglement.

We can then consider that variables describing these types of events can be seen as auxiliary variables, similarly to what used for virtual photons in Quantum-Electro-Dynamics, or Faddeev-Popov ghosts in other gauge theories. They are auxiliary variables which disappear at the end of a calculation, but they are key to bridge the modelling formally and highlight how the outcomes might be actually come about in term of virtual fields. They are short-lived virtual variables in the sense of causal inference theory. It is instructive to note that virtual variables where introduced in the 1930s in the study of statistics and causal inference for medical treatments, not so long before the EPR paper. Ideas appear to drift horizontally among fields of knowledge almost silently, just like the concept of *contextuality* is now important across all the fields of knowledge, probably because we can finally model it conceptually and at times also mathematically. By comparing to the statistical mathematical framework originated in the 1930s for the statistical study of medical treatments, the un-zipping and re-zipping process on each individual of the sampled population should be considered independent events and are our equivalent of the medical treatment.

As for medical treatments, we should then consider that there can be events which are fully independent, but which do not satisfy the Stable Unit Treatment Value Assumption (SUTVA violations). SUTVA being the assumption that the observation on one unit should be unaffected by the particular assignment of *treatments* to the other units (see [44]). In our case *treatments* is the choice of measure. The typical SUTVA violation example in medical treatments is the case whereby a couple of individuals in the sample treated do live under the same roof and always the first of the two individuals cooks. The treatment has an independent effect on the first individual, effect which causes in turn the cooking habits of the first individual to change. Such change of habits then affects the second individual leaving under the same roof. Although the impact of the treatment is independent on the second individual, there is a virtual variable effect by the differential of food. If the violation is mediated by a physical identifiable agent, one talks about hidden variables, rather than virtual variables. For the case of Figure 8, the cross-feedback has to be in all possible directions and the total net effect has to be zero. Even if the physical agent might eventually turn out to be detectable, it seems then more appropriate at this stage to consider these kind of features as virtual. Form the point of view of decision-making-theory causality analysis, it is as being in a case of cross manipulation of the decision making process, whereby the manipulation can not be in principle seen or retraced at the end. But it is real (irreversible and material) in the way it affects the final decision.

Observation 1. In order to avoid confusion it should also be noted that in the case of Quantum Metrology and Quantum Open Systems, the considerations in this Section would require a much more structured discussion. In such cases in fact, there is an intermediate quantum collective field which mediates the probing process, such as a laser or maser field. Decoherence models then realise the study of the interaction between the quantum system and the quantum collective environment composed by a collective quantum state. Decoherence theory finds its initial formalisation out of the study of L.D.Landau theory for quantum liquids. The ideas leading to the Gorini-Kossakowski-Sudarshan-Lindblad equation (Lindbladian) are in fact already mostly contained within the formulation of Relaxation Theory by L.D.Landau's school (see [48]), whereby Relaxation was intended in the sense of close to equilibrium quantum liquids thermodynamics. Within such theoretical frameworks, the interaction by the quantum system with the quantum liquid in which is immersed (such interaction being for example through the exchange of photon-like excitations of the ground state of a laser field), is modelled typically through spontaneous emission, spontaneous absorption and

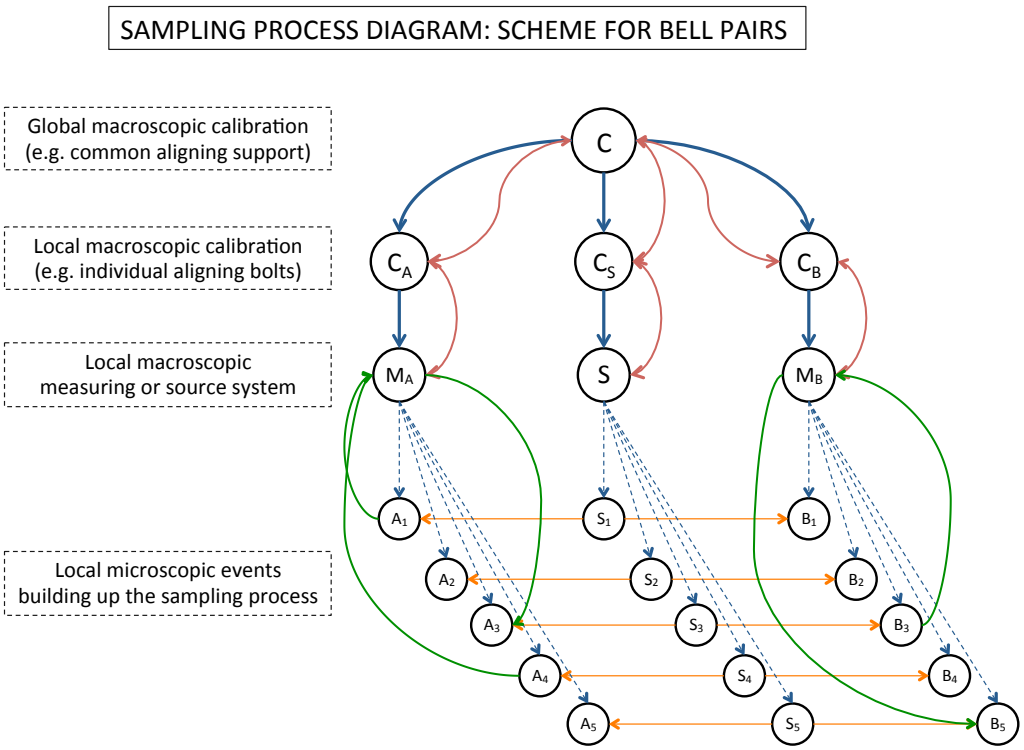

FIG. 8. Sketch of the causal structural modelling for the sampling scheme in the case of Bell-pairs statistics, showing the structure of multiple level contextuality and cross-inference, even in a relatively base case, whereby each part inter-relationship needs to be analysed and modelled. C_S is responsible for the persistency of calibration which enables the persistency of the entanglement of each pair emitted, with an overall nil momentum exchange between the source S and its calibration system C_S. C_A and C_B are respectively the local calibration systems for Alice and for Bob. M_A and M_B are respectively the measuring apparatus for Alice and for Bob. A_i are the single measures performed by Alice to collect her sampling leading to a given quantum average. Similarly are the B_i for Bob. The green and red arrows generate the learning process, i.e. correct the sample when the resulting average exchange does not net to nil. The global calibration system provides the rigidity forcing each of the C_i to be co-calibrated. The red colouring hints to the possibility that heat wavelengths might be involved, although not necessarily with overall dissipation. The green colouring hints to the fact that conservation laws are the enabling balancing feature, which make any hidden effect of red and green arrows to net to zero when one looks at the quantum averages. Red and green arrows are then causal inference effects which overall net to zero in order for all causal inference to disappear at quantum averages level. From this scheme it should be intuitive to see that more complex experiments, or real world analysis, would rapidly lead to causal scheme structures similar to those used for deep learning algorithms.

stimulated-absorption operators of the photon-like excitations, taking into quantum field theory Einstein theory of absorption and emission coefficients and following the direction sketched by L.D.Landau at the end of the 1920s, whereby Kraus operators provide the base for the formal bridge. These systems provide nevertheless quantum macroscopic phenomena proxies for the SubQuantum framework here discussed, therefore contributing useful elements to structure further SubQuantum Mechanics. At this stage, we will therefore not get into such complex systems where the quantum object is in turn immersed into a collective quantum macroscopical state. As an example, contemporary realisations of Qubits-like devices seem to fall in this category, being close enough to the Quantum Computing definition of Qubits, but likely to be uneasy to be controlled into a fully stable calibration, as more of them are combined, because of such additional complexity. For these multiple quasi-Qubits systems it is most likely to be the calibration procedures data, and the machine learning methodologies used for the calibration, which carry meaningful information about the physics and the different ways a modular Quantum Computer should be engineered for each given technology.

Observation 2. Wigner's friend is clearly the one causing the collapse of the wave function here. But Wigner's friend can not enforce or guarantee the Born rule statistics to form, without the help of the calibration system, therefore clarifying the policing active role of Wigner in this sense.

Observation 3. A learning process for the sampling to converge to the Born rule introduces effectively a non-symmetric version of retro-causality, or partial retro-causality. This is different from asking for full simple symmetry

of causality over the arrow of time as discussed for example by O.Costa de Beau Regard (see [49]). Such a partial retro-causality is enforced by an action for example imposed by the bolts of the calibration system jointly with the larger reference systems providing a super-calibration to the calibration system (think at the Jura mountains for the LHC tunnel). Such action re-qualifies a posteriori the statistical relevance of a previous event. It is more similar to what we observe in real life, when a future decision (*action*) changes the cognitive understanding by others of previous events, and therefore their meaning. This is extremely similar to the concept discussed in philosophy of beliefs, from the well known etymology of the biblical Tetragram as an inter-capsulated superposition of the past, present and future of the verb *to be*. In the Bible story of the exit from Egypt, the Pharaoh's heart is hardened because he has used his free will to accumulate too many terrible deeds at his count. Therefore his free will is lifted, clouding his judgement, so that he is forced into a position which will cause an opposite outcome with respect to what he think his choice will cause. And this fact is understood to be the righteous (rebalanced) outcome. According to the Exodus narrative, such outcome is achieved by the suspension of the free will of the Pharaoh by the Lord. According to this Bible teaching therefore, free will is not given indefinitely. It is preserved only if the right choices are made. This feature is understood to be observable over a long enough time and to effectively enable an indirect proof, specific to each individual and ideally before we pass away, that we are not living in a predefined video-game like world. There would be an administrator, who takes away free will and gives it back according to quite complex rules, identifiable only much much later in the game, thanks to the late appearance of partial-retro-causality features. Just as a loving father corrects the child from making a big mistake, so this suspension of free will is enforced. The strongest is the love, the most frequent and specific is the suspension. This is a quite different notion of the free will when compared to other notions, as the one used in the Conway-Kochen Free-Will-Theorem which is static (see [50]). In the same way, if the un-zipping and re-zipping processes do not accumulate so to lead to the appropriate conservation-laws outcome, in order to preserve the calibration of the measuring instrument, the calibration systems imposes a specific form of de-randomisation of the remaining sample which leads back to the Born rule. Free will is temporarily suspended. If the conservation laws are restored before the strain towards de-calibration becomes permanent, free will is automatically restored. The transient is extremely difficult to detect. Partial retro-causality features can also be found within option pricing theory, whereby the agent explores the macro-space from a micro perspective as time goes by. The arrow of time is therefore opposite. The decision making at the end. The partial-retro-causality is by giving meaning to the diffusion process through the decision at the end. The Born rule equivalent is possibly the payout in this case. Although it is unclear if the mathematics of option pricing could be adapted to formalise this part of the theory, such parallel should be leveraged (see [51]). Also to note on this matter, that even without such a structured biblical notion of Free-Will with partial retro-causality, a softening of the Lorentz invariance can also lead to a different conclusion from the one of the Free-Will-Theorem, even without changing its definition of Free Will.

Observation 4. Bell and other similar no-go theorems' are fully correct and even more so from this perspective. All called upon loopholes non applicable. But this is only ruling out hidden variables in the Bell-like theorems assumptions sense. Hidden variables of other nature and effect being present here, both at the sampling level, at the un-zipping and re-zipping level and at the linear dynamics level. But all of them are not strictly necessary to describe the Quantum Mechanics scale. In this sense Quantum Mechanics is *complete*. But there is a wider SubQuantum Mechanics allowing to provide a more detailed description at lower scales, which are not accessible to date. But which can be inferred as a necessity, including for synthesis and coherence.

Observation 5. At a macroscopic scale, these ideas might help in the ongoing work for the development of auto-calibration auto-controlled technology, by resolving the time series of the build up of the Born statistics during the calibration processes and using it to auto-correct. A bit like the Van der Meer technique used for the high focusing of accelerator beams at CERN in the 1980s but applied here to the sampling (un)likelihood to generate a given statistical distance. Including in the search for additional mechanisms for auto-stabilisation of physical Qubits to improve the technology accuracy or to reduce quantum computing errors by the newborn branch of Quantum Engineering.

Observation 6. Quantum teleportation here, can not be achieved as for Captain Kirk in Star Trek unfortunately. In fact one needs to have full co-calibration of the emitter and receiver stations. No teleportation to the surface of an unexplored planet could ever make sense, sorry. Teleportation to a well known station could be imagined in this framework, but if a strong relative calibration is lost, your left arm might turn out at the place of your right foot, which would seem unfortunate. Even if there is nothing else mixed up in the transmission, as in The Fly movie.

Observation 7. A-causality concepts, in the sense identified by the Norton Dome example (see [52]), should be discarded. The Norton Dome model is using a projection direction of the force which is not physically compatible with the mechanics. If the correct projection direction is introduced, the a-causality features disappear.

Observation 8. Each of the red and green arrow of Figure 8 could be possibly modelled as a credit and debit accounting record. There are then two (double) bookkeeping of causal inference events, one for the lender and one for the borrower, such that each role can be reversed and the total lending position averages to zero within an approximation related to the size of the minimal event capable to de-calibrate C. Including for example an event able to de-calibrate C_A without affecting a opposite and reversible de-calibration on C_B. An accounting register would then be required to keep track of the latent variables, while an additional balancing condition would guarantee that the variable are only latent and that there are no hidden variable for the averages. This might be the right way to pin point the kind of temporary non-markovian action involved.

VIII. SEMIQUANTUM LIMIT OF CLASSICAL MECHANICS

At this point, we are naturally led to explore the question if one can identify any classical system which can simulate SubQuantum Mechanics processes and therefore to observe quantum-like phenomena at the non-quantum macroscopic level. Such quantum behaviour would then be in addition to that arising from collective macroscopic quantum liquid behaviour, such as laser, superfluidity, superconductivity, charge or spin density waves states, quantum Hall effects states. R.Feynman effectively asked a similar question (see [53]), coming from a mathematical point of view, motivated also by the discretisation of his path-integral formulation of quantum mechanics, which is the basis for calculation of path integrals and their practical computational definition. This led him to the chessboard model and to the idea of building a quantum simulator, rather than by using quantum information bits, initially more with the intention to find a computational non-quantum way to simulate quantum mechanics. Feynman therefore also compared such approach for a classical simulation of quantum mechanics with the alternative of leveraging the full computational resources of quantum objects. This in turn led to the formulation of Quantum Computing in the contemporary sense (see [27]). At the same time, the discretisation of the Feynman path integral for the quantum oscillator (a quadratic form Hamiltonian) leads straight to the Fourier Transform proof of quadratic reciprocity (see [54]).

Any system enabling SubQuantum-like processes with a mathematical model leading to quantum evolution equations would describe what seems more appropriate to call the SemiQuantum limit of Classical Mechanics, or similarly the QuasiQuantum limit of Classical Mechanics, by analogy to its quantum to classical counterpart. It seems obvious that it is extremely difficult to imagine that we can find macroscopic classical mechanical objects which behave exactly as the SubQuantum entities in this course, because such specific properties have never been observed exactly at the macroscopic scale, to the best of our knowledge. Nevertheless it should be possible to find cases whereby, within specific values of given control parameters, the behaviour could be engineered to be similar. Micro-mechanics, micro-fluid dynamics and small-scale soft-matter physics or biochemistry is where it seems natural to look, as some kind of analogue to mesoscopic devices. What has been realised by [55] and the subsequent research work (see [56, 57]) appears to be micro-physics of this kind. Although this type of physics has been denoted as emerging quantum mechanics, it would seem risky to use the word emerging, which implicitly indicates that the full features of quantum mechanics could be simulated. This appears quite incorrect in the systems identified to date and could mislead future research towards impossible goals, although it would seem reasonable to expect other physical systems to be able to get closer to the SemiQuantum limit of Classical Mechanics. The term SemiQuantum limit of Classical Mechanics seems therefore more clear in its mathematical and reverse-engineering meaning. Such terminology also clarifies the relevant mirror role with respect to the semi-classical limit of Quantum Mechanics.

The physical SemiQuantum system used in [55] and related work, does build on the physics of Faraday-waves self-propelling lubricant drops. These experiments seem key to identify selected features relevant for SubQuantum dynamics modelling which should not be overlooked. To extract such type of information it is necessary to identify the physical correspondence between Faraday-waves self-propelling drops and the dynamical framework discussed in this course. We first note that this class of systems is quite close to be a SemiQuantum system but only for what concerns the quantum evolution and not for what concerns the quantum wave function collapse or Born statistics formation. This in turn seems to make Y.Couder team's achievement more enlightening in our view, because it allows to physically isolate the analysis relevant for the linear evolution, a feature which can not be isolated in principle in any quantum system, except possibly at very high probe coupling regimes, where the quantum physics can become semi-classical.

To prepare such experiments, the French team filled a tank with silicon oil. Silicone oils are good electrical insulators, non-flammable and temperature-stable with good heat-transfer characteristics and can be used as lubricants. Silicone oils with low surface tension are potent anti-foaming agents. Therefore they provide overall a good stable and smooth support for Faraday waves' generation. Although the publications seem not to identify which silicon oil has been used, it is probably of the low surface tension type and experiments appear to be performed at room temperature. Therefore the silicon oil molecules are probably Si oxides and hydroxide compounds polymeric chains of limited length.

Possibly providing some kind of coherently decomposed SemiQuantum version of the SubQuantum web. The micro-fluid dynamics is here taking place at a low Reynolds number regime whereby, for SemiQuantum limit comparison purpose, the Reynolds number seems best compared to the ratio between the Compton length and a typical length of the compared quantum system. The silicon oil used has viscosity typically of 20 times water, or say a fourth of the viscosity of olive oil, with very low surface tension. The tank is placed on a plate with a mechanical oscillator underneath performing typically 80 oscillations per second providing a sinusoidal acceleration to the silicon oil of amplitude which can be varied between the value of gravity acceleration at sea level and the Faraday wave instability threshold, which is close to four times gravity, i.e. at the last integer ratio Feigenbaum bifurcation route to chaos (see also figures in [58]).

Such mechanism is not too dissimilar from the four phases delay of motion anchor oscillation of the mechanical clock, which actually has more dyadic structure, as quite well known from the regulation options for the spiral release at the clock shell (see [15]). This comparison actually hints to the fact that the Feigenbaum number might be a period, or some kind of period extension, connected to these kind of combinatorics, where by period we mean in the sense of Kontsevitch-Zagier in number theory (see [59]), which we should denote by $\mathfrak{O}$. Their special features related to physics position these numbers as quasi-trascendental.

Within such a parameters settings, the silicon oil movement becomes stationary as stable standing waves. Faraday waves of wavelength $4.75mm$ are selected for the experiment. This appear to provide the empirical optimisation of the molecular to drop size ratio, which allows good stability of the drop while keeping it as small as possible. Faraday waves typically oscillate at half the driving frequency and there is then an alternate phase opposition and phase coherence with the driving mechanical oscillator, whereby the polymeric structure of the silicon oil must find its equilibrium to stabilise the standing wave.

The French experimental teams leveraged on work done in the 1970s and the 1980s by other research teams about drops standing on the surface of a lubricant or detergent, thanks to the formation of a thin film of air between the liquid surface and the drop. Combining these lubricant properties with a fine tuned optimisation against coalescence, as obtained by the choice of lubricant and other parameters, together with the Faraday wave stability, they experimented bouncing of drops on the Faraday waves and period doubling route to chaos, which turns out to be in line with the Feigenbaum model, as to be expected. The Paris teams soon realised that both at bouncing in phase with the oscillation of the surface (on the top of the wave) and at period doubling, it is possible to maintain a stable and persistent bouncing. If the amplitude and frequency of the Faraday wave are then appropriately modulated versus the size and weight of the drop, then the relative phase with which the drop falls on the wave is such that the drop is pushed sideways and it is said to "walk". The drop in fact does not fall on the top of the wave anymore, but for a limited time tends to fall always with the same partial phase of the wave resulting in a consistent sideways force. This typically happens at (1/4) of the wave, or half way as the phase goes down and the slope is more appropriate to push the drop sideways.

Depending on the weight of the drop and its size, below the instability threshold, there is a range of acceleration amplitudes of the mechanical oscillator under the plate for which the drop becomes itself the source of a different set of damped Faraday waves: as soon as the drop hits hard enough the lubricant surface. The damped Faraday waves originated by the drop provide phased feedback to the drop, which then reaches a stable velocity (the equivalent of the speed of light). Therefore the drop continues to move at constant velocity following the shape of the Faraday wave, which depends also on the shape of the tank and on any additional object that could be added in the tank, such as a double slit barrier (contextuality features). This causes the drop self propulsion, whereby the Faraday wave brings in an effect comparable to a ciliate cell wavy movement. It is recommended to watch the YouTube videos posted by Y.Couder's team.

These features are possibly mimicking the local part of spermatozoid and similar ciliate cells electro-mechanical with-the-flow self-propulsion mechanisms. The ciliate cells self-propulsion mechanism is an oscillating movement, often with rotational (in the sense of polarisation) stabilisation features, which enables the ciliate cells to move in a straight line, with the direction of the flow. A longer ciliates' structure might enable stronger propulsion power. But, if the flow deviates from a straight line, the length of the ciliate cell enhances the non-local features and the ciliate cell will eventually follow the flow. Therefore important barriers of intimacy can be passed only by directing strongly the flow. To overcome a biological form of *difficulty*.

It is then relevant to remark that a photon straight-line movement **enabled** by the SubQuantum web has to be understood in a similar way, whereby the sources of deviation from a straight line initiated by some flow can be various and notably include the isolated action of the shape of the underlying SubQuantum web. This can then be suggested for the modelling of light curvature by the gravitational field, which in turn would arise only from a selected part of the degrees of freedom of the SubQuantum web, being the full or partial source of different effective fields at once.

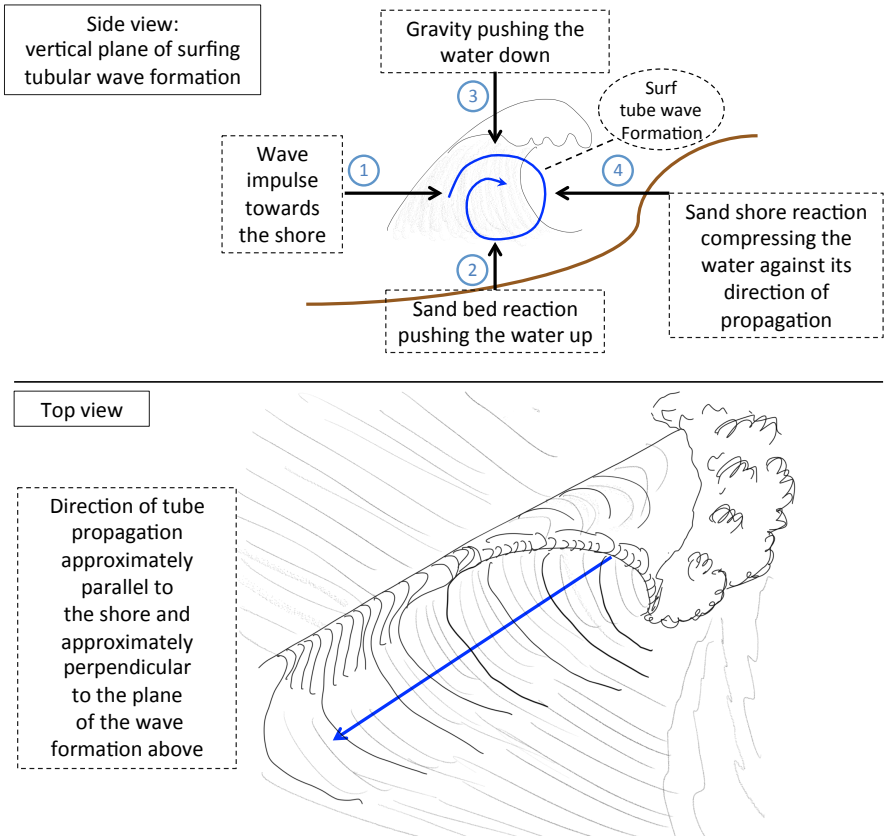

FIG. 9. Schematic representation of the forces enabling the formation of the wave rotation dynamics in the vertical plane almost perpendicular to the shore and the sea bed. The tubular surf wave propagates in a direction approximately perpendicular to such plane. None of the physical mediums surrounding the tubular surf wave vibrate, rotate, alternate or move along the arrow direction with the wave: neither the air, nor the shore, nor the sand bed, nor the water pushing from the side opposite to the shore. But they enable its formation and propagation along the arrow direction. Einstein is quoted to have asked: *light quantum is a wave until is detected and absorbed?* If understood in the right way, the answer to his question would seem to be in the affirmative. Drawings by the author using free online tutorials by B.Penuelas, creator of the surfers' comics Wilbur Kookmeyer.

That is also why the light is not transmitted by the SubQuantum web, and therefore why there is not an ether for electromagnetic waves propagation.

Another way to think about this is by analogy with the formation of a surf tubular wave. In this case there are four forces shaping the tube and the shape is characteristic. As shown in Figure 9, the forces are: the up-vertical reaction of the shore sand bed; the down-vertical force of gravity; the impulse towards the shore of the wave; and the horizontal back-reaction by the shore. These four forces confine into rotational motion the tubular surf wave which then propagate in the direction of the shore line, which has a relevant component perpendicular to the plane of such four forces. The quadrupolar features of the SubQuantum web might possibly be replicating a similar balance at the time of emission or absorption to form the photon. These considerations support the idea that emission and absorption of light might require a modelling approach inspired by similar biological processes involving ciliate cells, and in connection to the interpretation of the discrete Lorentz invariance discussed in Section VI. Lorentz invariance appears again to be seen as a result of some form of overlooked contextual version of discarded emission theories, whereby the speed of light is set by the SubQuantum web even if it is "only" an enabling agent and not a propagating medium. Not too dissimilar from how the Faraday waves feedback stabilises the speed of the bouncing drop.

The Faraday waves regime used by the French team is called the *walking* regime (see [60]). In several of the experiments mentioned, the walking regime speeds realisable with the given choice of setting were in the range of 10 mm per second (say half a meter every minute). This allows very good quality stroboscopic observation of the details of paths and dynamics in multiple settings. Therefore this seems in line with a fully optimised experimental

setting. Using the right kind of magnetising and anticorrosive alloy nano-particles and with the right solvent, the drop was also made sensitive to magnetic fields. A large variety of experiments have then been performed to study such a SemiQuantum micro-mechanics classical regime. These include diffraction by a slit, by multiple slits, equivalent versions of the now celebrated Merli-Missiroli-Pozzi electron diffraction experiment (see [61]), equivalent versions to Landau level quantisation, study of the structure of the composition of all passed originated waves and many others. Each of these experiments, performed over more then ten years, deserves in principle a detailed discussion within the framework of this course. This is quite involved and does not seem useful at this stage. For our purpose, a limited number of observations seem to be relevant:

1. There is a quasi-hidden linearity of the surface waves, which results in the same linear wave equation of the vector potential for free Hertzian waves (see [58]), which is also invariant under Lorentz transformation. This is because the combination of oscillator and bouncing simulate the diffusion process introduced by Ord, but without multiple components and by using the transversal dimension as an internal additional dimension, a bit like extra dimensions in Kaluza-Klein theories, but at a classical physics level. This is possible because the system is bi-dimensional, and the third dimension is used as an internal dimension. Einstein's physical intuition of the extra dimension in Kaluza-Klein theory was surprisingly similar to this physical realisation (see [35]). The same setting cannot then reproduce a $3D$ system featuring the same quasi-quantum properties. Completely different ideas need to be introduced at experimental level if a $3D$ quasi-quantum analogue has to be explored.

2. The constant speed and high level of localisation of the drop indicates that we are locally looking at a classical SemiQuantum simulation of a semi-classical free particle. Therefore we appear to be there where classical and quantum mechanics can touch more closely. The speed can also be varied by changing other parameters and the shape or size of the tank: due to the contextuality of the system, it is a bit like changing the de Broglie wavelength of a free electron.

3. The phase diagram for the drop behaviour in function of size and oscillator acceleration shows that the walker regime appears mainly: *(i)* by changing the acceleration, between period doubling and Faraday instability and *(ii)* when changing size, between Feigenbaum route to chaos and a rolling type of bouncing behaviour which is unstable. It does stabilise then at the balancing of two competing instabilities, reproducing an alternate configuration equilibrium, therefore using an alternative but similar feature of the multiple components feature of the Ord-process (see [55] and references therein).

4. In the single diffraction experiment (see [62]), the measured deviations of successive individual particles passing through the slit is then compared with the formula for the "amplitude diffraction pattern of a wave passing through a slit". The formula shown by the authors, which successfully fits the experimental data, appears to be the formula for the amplitude of the wave. It is not the square module of the amplitude as in optics or as in the Merli-Missiroli-Pozzi experiment. This seems to be the first experimental evidence that, at least in the SemiQuantum limit of Classical Mechanics, the class of processes which appears to model the Quantum limit of SubQuantum Mechanics, also do show that the physical density which follows the evolution equation **is the absolute value of the amplitude and not its modulo squared**. This would be in line with the SubQuantum Mechanics formulation hereby discussed. It seems in line with the understanding that there should be something else in the probing process, which is at the basis of the wave function collapse and, separately, of the modulo-square-probability of the Born rule. These SemiQuantum limit experiments lack a fully equivalent physical process corresponding to a wave function collapse. Therefore, and quite remarkably, these experiments appear to be able to separate the effect of a SemiQuantum evolution dynamics from the physics of the wave function collapse and the Born rule. This seems impossible to do for quantum systems. It would appear therefore that these micro-mechanics experiments play the crucial role of enabling the isolation of one of the key different Sub-Quantum-like features. In this sense these experiments seem to us to be a fundamental discovery.

R.Brady and R.Anderson have highlighted some of the mathematical physics reasons for these systems to show some features of Quantum Mechanics (see [58]). But they obtain a real version of the non-relativistic wave equation. In order to get a proxy of the Schrödinger equation they need to artificially analytically continue their wave function into the complex plane. But one can not see any reason from the physics principles used to do so. It might rather be the consideration under point (3) above and the knowledge of the Ord-process, which possibly justify *a posteriori* to do so. Furthermore they seem to have overlooked what we deem to be the most important point, under (4) above.

Another group of systems whereby some features of quantum mechanics might be reproduced at the micro-mechanical scale level is possibly provided by quasi-low-dimensional low-Reynolds-number two-liquid systems, whereby the oil type liquid almost satisfies the Burgers equation. Just like the type of exploration within micro-fluid-mechanics which led to the Faraday-waves self-propelling drops, these systems are important for engineering applications, such

as lubrication for chemical industrial production and for oil exploration technology, or at the boundaries with soft matter physics, and will continue to be extensively studied. In [63], for example, it was observed that even in $2D$ the flowing droplets of the oily fluid move in a regular wave form with wave vector aligned with the direction of the flow. Although some of the dynamical features are caused by the low-Reynolds number implications at the boundaries, as for Faraday-waves self propelling drops, the way in which the plane wave stabilise in the bulk in such case might again produce a form of underlying oscillations enabling physics at the SemiQuantum limit of Classical Mechanics.

Recent work on self-gravitating discs in astrophysics seems to fall within this same class of problems (see [64]). Typically one would expect SemiQuantum limit of Classical Mechanics features to appear in other areas, including outside physics, whereby the combinatorial dynamics might be close to the ones in SubQuantum Mechanics. And to be found retrospectively in other ares. For example, Heaviside transatlantic cable model (see [20]) is a precursor of the Ord-process, case I or Figure 5. This might clarify the balancing mechanism which enabled telegraphic transmission at long distances with limited signal loss over a century ago. P.A.M.Dirac had well learned Heaviside theory as an electrical engineering undergraduate in Bristol. Heaviside theory having been developed in Bristol where it was best taught, including for its first definition of the square root of a differential operator, as well as its iterative discrete models leading to partial differential and integral equations. Although P.A.M.Dirac did not seem to have made the full connection, he seems to have leveraged upon the mathematics by Heaviside somehow.

If we allow now macroscopic phenomena to be of quantum type, we are exiting the SemiQuantum discussion. Nevertheless, numerous systems in quantum control theory feature some analogies to these physical systems. In such an area of active research, it seems most notable the experiment by M.Devoret's Yale's group, whereby it is the density matrix which seems to clearly have a tangible and real physical meaning (see [65]).

IX. STRUCTURING SUBQUANTUM MECHANICS

Starting from this introductory course and in order to further structure the Quantum limit for the linear evolution equations of SubQuantum Mechanics, the following roadmap is suggested:

1. Complete the $1D$ evolution framework following the lead of [66], [67], and within the physical intuition hereby provided which suggests that there are a number of models which are related to such work and provide relevant input, as discussed below.
2. Fully formalise the $1D$ SubQuantum web dynamics for the free particle. This might require the appropriate credit and debit, double booking, two agents bookkeeping. Then generalise to two particles, whereby the web is shared.
3. Generalise to the $3D$ free particle case. This requires to use the full combinatorial dynamics in Figure 4.
4. Generalise to $3D$ the SubQuantum web dynamics. This also requires to use the full combinatorial dynamics proposed in Figure 4 and to formalise the $3D$ SubQuantum web structure proposed.
5. Analyse the discretizations of the Lorentz group in view of the steps above to single out the meaningful options for SubQuantum Mechanics.
6. Build the harmonic oscillator case, starting from $1D$. This is likely to require elliptic curves and quadratic reciprocity.
7. Build the SubQuantum hydrogen atom model. This requires to generalise the web to a centre-symmetric version of the diamond and to map the harmonic oscillator using the techniques mentioned in Observation *(g)* above.
8. Use the free particle, harmonic oscillator and hydrogen atom as base tools for more general problems. Including higher spins and multiple particles.

This course further provides the core elements required to formalise the un-zipping and re-zipping processes, as well as the Born rule conditional controlled de-randomisation features. In addition to the observations already made, this might require modelling tools not too dissimilar from those used for non-markovian processes in open quantum systems, which provide a quantum condensate proxy. This part of the analysis should take into account the fact that there are two relative scales involved and that there is conditional controlled de-randomisation inbuilt in the process which effectively realises the asymmetric form of partial retro-causality discussed in Observation (3). Although possibly unrelated, an area of modelling whereby these two features appear in a similar and coordinated way is in the study of strike price and term dependent option pricing theory (see [51]). Furthermore, the probability distributions functional spaces involved in the description of decomposition and recomposition combinatorics for the absorption and

emission processes, should be able to include extremal distributions like the Gumbel distribution (see [68]), because the statistics of an extremal over time of a given distribution (respectively of an extremal of extremals) tend to naturally involve two scales (respectively more scales). The double (multiple) logarithm would be the scale(s) change enabling function.

In parallel to the study of the Quantum limit of SubQuantum Mechanics, one should explore the rest of the Combinatorial Mechanics which is not immediately relevant in the Quantum limit. This should clarify the use of the two proposed names for the theory, depending on the context. In order to engage on such roadmap, we list a number of observations which we deem relevant.

Observation α**.** In [66] G.N.Ord explored the case where instead of modifying the starting process with $\mu\epsilon$, the average scattering per unit time is made to vary with position with a function:

$$a(x) = \frac{e^{-\epsilon v(x)}}{(e^{-\epsilon v(x)} + e^{\epsilon v(x)})} = \frac{1}{2}\frac{e^{-\epsilon v(x)}}{\cosh \epsilon v(x)} = \frac{1}{2} - \frac{1}{2}\tanh\big[\epsilon v(x)\big]$$

Which brings to the non-relativistic case a potential $V(x) = \hbar v(x)$ when taking the continuum limit. The choice of the denominator allows then to recover the $(1/2)$ coefficient for zero potential. If $a(x)$ is the weight for not scattering, then the weight for scattering is:

$$(1 - a(x)) = \frac{e^{\epsilon v(x)}}{(e^{-\epsilon v(x)} + e^{\epsilon v(x)})} = \frac{1}{2}\frac{e^{\epsilon v(x)}}{\cosh \epsilon v(x)} = \frac{1}{2} + \frac{1}{2}\tanh\big[\epsilon v(x)\big]$$

The weight difference between scattering and not scattering is therefore $\tanh\big[\epsilon v(x)\big]$. The potential induces then an hyperbolic deformation in the scattering pattern, which could prove useful in the search for particle boundary modelling. For small ϵ we can take:

$$a(x) \simeq \frac{1}{2}\big[1 - \frac{\epsilon}{\hbar}V(x)\big]$$

Therefore the potential decreases the likelihood of particles not scattering. Similarly it does increase the one of scattering, as:

$$\big(1 - a(x)\big) \simeq \frac{1}{2}\big[1 + \frac{\epsilon}{\hbar}V(x)\big]$$

There is here an implicit interpretation of the action of the potential at SubQuantum level: the energy of the field is stored by modulating the web or the gas with an exponential related weight. It is coherent with the physical description of the action of the pure potential term of the gravitational field discussed previously and must have a matching process at the SubQuantum web level. If we then take the linearised pendulum potential, M the pendulum mass, l its length and g the gravity acceleration, the coefficient for not scattering becomes:

$$\frac{1}{2}\big[1 - \frac{\epsilon}{\hbar}\frac{Mg}{l}x^2\big]$$

And the coefficient for scattering becomes:

$$\frac{1}{2}\big[1 + \frac{\epsilon}{\hbar}\frac{Mg}{l}x^2\big]$$

Therefore the gas scatters a lot more than usual where the potential is large, while it scatters much less where the potential is small. There is then an oscillation generated by the alternating concentration between regions whereby the potential is large and is small. The oscillator alternating motion is superposed on the SubQuantum circular dynamics. There is then also a double periodicity where one is unconstrained and fast, while the second is related to the linearised strain generated by gravity and slower. This suggest that it might be beneficial to introduce elliptic curves mathematics in order to model SubQuantum oscillators of different kinds.

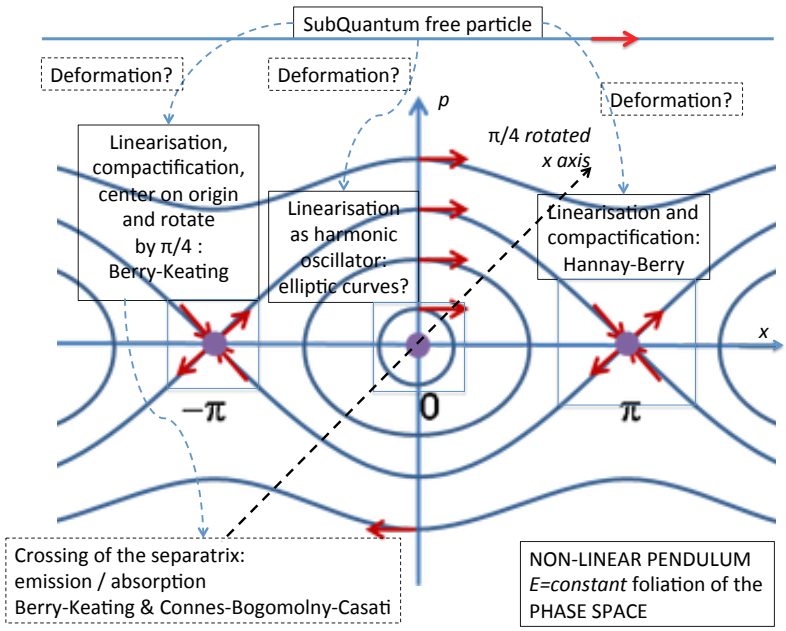

FIG. 10. Schematic suggested relationships between SubQuantum-like models which seem to be related by different local forms of the non-linear pendulum phase space. It seems natural that deformations among them could be identified. At the Quantum limit of SubQuantum Mechanics, they should relate to different local expansions of the Mathieu equation's transcendental solution of the quantum non-linear pendulum.

Observation β**.** Quadratic reciprocity should be a tool to reproduce a double covering structure at combinatorial dynamical level. Because the discretisation of the Feynman propagator for the quantum harmonic oscillator is closely related to the Fourier analytic proof of quadratic reciprocity (see [54]), such combinatorial dynamics is likely to be the one of SubQuantum harmonic oscillators. The relationship between quadratic reciprocity and the metaplectic group is natural in this framework, because quadratic reciprocity arises from the equal split of integers as quadratic residues and non quadratic residues, given a module for a given modular arithmetics. There should be a discrete combinatorial dynamical description of this number theoretical split. The persistency of the structure of arithmetic reciprocity for higher powers or algebraic number fields should then be related to the structuring of the same class of combinatorics for higher complexity structures (say spin $n/2$). The generalised feature of arithmetic reciprocity laws would then become as a necessity *a posteriori*. It would also seem natural if, given such a spectacular, general and fundamental property of numbers, second possibly only to Pythagorean triples, the universe is using it to structure itself. Which would shed light on the tentacular nature of the arithmetic reciprocity laws within contemporary mathematics, a feature which had so much fascinated C.F.Gauss and all those who followed his footsteps on the topic.

Observation γ**.** The local compactification of the phase space around the unstable fixed point in Figure 10 identifies a reduced dynamical system, whereby its Poincaré-map is an hyperbolic area preserving automorphisms of the torus. Taking the Poincaré-map sections and compactifying in (x, p) causes space, momentum and time to be discrete. We get therefore a dynamics reminiscent of the Ord-process. Furthermore, also the configuration space for the Hall effect can be represented as an unstable fixed point. This is because the Landau levels, which arise in a planar configuration for an electron in a plane perpendicular to a magnetic field, have momentum which is indexed by the length in the direction of the Lorentz force. Such direction provides then a effective momentum direction, while the electric field direction provides the ordinary space direction along which the transport takes place. The crossing features of the forces in the Hall effect reproduce then an unstable fixed point configuration in a $1D$ phase space. The quantisation for the Quantum Hall Effect and for maps arising from a linearisation around an unstable fixed point, is therefore essentially the same. Just as the resistivity turns out to be quantised for the QHE, in the case of quantisation of the hyperbolic area preserving torus automorphism there are similarly numerable representation which are indexed by the admissible values of $\hbar = (1/N)$ with N any integer. Such values need to be thought based on dimensional analysis with respect to the compactification length L as $(\hbar/mc) = (L/N)$. Therefore each case correspond to a different length in terms of size, or $L = (\hbar/mc)N$, where N counts the number of units included within the length L. The smallest the N, the smallest is L and the more accurate the compactification. The largest is N, the more the size approaches a size for which the linearisation is not accurate. This issue is moderated by the periodicity imposed to compactify around the unstable fixed point. We can then bring SubQuantum physical intuition to these models to see what we

can learn about SubQuantum Mechanics. And to identify a deformation or another form of analytical relation with the processes discussed in this course. The typical model to consider is the Hannay-Berry model where we can use the intuition coming from its physical context, which is better known. This toy model was in fact formulated to reproduce the space periodicity of transversal grids in high energy electron microscopes, where a periodic modulation of the impulse can arise in the transmission direction of the electron beam, perpendicular to the grids. The torus phase space iterative formulation derives from this double periodicity. Because of the high energies, the semi-classical limit is very important in high-energy electron microscopy, whereby the two big enemies to image resolution are the caustics (Lagrangian singularities) and the vibrations (noise), any good experimentalist knowing the empirical equivalence in many observed cases. Which in turn is mathematically connected to the Montgomery pair correlation conjecture, relating the pairs of Riemann ζ function zeros (encoding arithmetic chaos concentrating around Lagrangian caustics) to the correlation function of random Hermitian matrices (energy conserving quantum noise). As the noise can be often moderated by colossal shock absorbers chambers below the 10 meters high microscope chamber, the study of chaos around caustics becomes the most important technical improvement route.

Observation δ**.** It should be possible to provide a physical interpretation of the Berry-Keating model and of its mirroring Bogomolny-Casati inspired formulation by A.Connes (see [69]), within the framework of SubQuantum Mechanics. With a view of trying to connect a crossing of the separatrix at Classical Mechanics level with the modelling of the un-zipping and re-zipping process. Some of the ingredients for this exploration have already been sketched under Observation (iv), (v) and (vi) above. If we look at the foliation in equal energy levels of the non-linear pendulum as shown in Figure 10, the Berry-Keating Hamiltonian is the rotation by an eighth of turn of the unstable fixed point linearised Hamiltonian, after a translation of the origin. All these models should turn out to be deformations of each other, when embedding them into the right number theoretical language. In Figure 10, the question is also raised about elliptic curves for the modelling of harmonic oscillators, as one is here naturally facing two frequencies: one is the oscillator frequency, the other is the diffusion scattering frequency, whereby a strain is generated by the coexistence of the two. By taking the transversal dimensions into play, one can see a discrete solution of an elliptic curves Diophantine problem as a decomposition from a pyramidal-like configuration with the axis along the oscillation direction into a planar-like configuration. This might correspond to a diffusion process whereby, during the oscillation, the SubQuantum gas penetrates with a point into the bulk, while at the extreme of the oscillation the SubQuantum gas occupies a surface perpendicular to the oscillation direction and parallel to the pyramid basis. Torsion points trajectories might then describe transient paths toward a stable oscillation. Tangent points to infinity could correspond to the symmetric oscillation. The torsion group would become a dynamical modelling tool, possibly at some level of discrete Fourier Transform. The group law composition of elliptic curves with its inversion features could then be related to the interlacing of the dynamics.

Observation ϵ**.** The use of cubic lattices in $D > 1$ seems to lead to excessive spurious variables (see [70]). It is unclear therefore how to balance correctly *(i)* the geometric diffusion process on the discretised space provided by the nodes, with *(ii)* the circular dynamics. Which in turn has to be purely combinatorial as in Figure 4 and not using directions as an internal variable anymore, as in Figure 5. The diamond network is isotropic at large distances. Although the diamond network is not a lattice, its nodes sit on a $3D$ projection of the $4D$ hypercube, which is a lattice. Therefore 4 excessive coordinates can be used to represent the nodes position of the undeformed web in a natural way (see [71]). This might allow to match the combinatorial dynamics of Figures 4 and recover the coarse graining principles used in $D = 1$. There could be then an embedding of both $3D$ web and gas combinatorics into the $E8$ lattice. The quasi-crystal sections of $E8$ (see [72]) might provide some approximation of a simplified mechanisms related to the the formation of the photon. Which might give a very very rough explanation of fine structure constant from the geometry of the $E8$ lattice. This would demystify some of the almost esoteric arguments called upon, starting from purely empirical numerical algebraic formulas approximations, about the quasi-integer nature of the inverse of the fine structure constant, when measured in the appropriate system of units. P.Cartier quite abstract vision of a cosmic Galois group (see [73]), might be related in the case of no gravitational curvature. The *mod* 8 structure of the Schrödinger case might be related to the structure of an ultra-simple motif (see also Appendix A). In case of gravitational curvature, this framework suggests that periods Ω number theory would likely be required.

Observation ζ**.** For central forces in $3D$ we would consider centre-symmetric equivalents to the diamond network. Typically caged fullerenes webs, where the double bonds are replaced with single links plus a radial links to the next or previous cage in term of size. $K4$ crystals topologies (see [74]) are also likely to be relevant to model chirality. In fact one does expect the SubQuantum web excitations to carry some form of right-handedness (gravity) while the SubQuantum gas and web unbalance degrees of freedom contributing to the wave functions should carry some form of left-handedness (Standard Model) in line with current implications of established physical theories (see [75] for a comment about the left-right specialisation between Standard Model and gravitation). Notably, even the Biblical tradition identifies the right hand of the Lord as supporting the universe, whereby the left hand would be giving to the universe.

Observation η. To identify the relevant discretisations of the Lorentz group in $3D$ for SubQuantum Mechanics, we need to leverage on the highly structure field of Kleinian group theory, most likely also in relation to the Mandelbrot set and its generalisation. For the interested and more patient reader we sketch the context in Appendix E.

Observation θ. When looking at two particles, the SubQuantum web is common. The interlaced diffusion processes of each particle cloud has to cross balance in its exchange with the SubQuantum web, which provides a basis for quantum interference. When coexisting within the same bounded states areas, primes combinatorics or some related number theory feature has to be used to enable a coherent coexistence of each process among the others. Prime numbers are a key tool for the modelling of the preservation of intimacy, as cryptography largely shows. Prime numbers at this level might enable a description of quantum entanglement as a kind of common intimacy, and the change of quantum state as a change of state of intimacy.

X. CONCLUSIONS

The framework presented in this course is just a Jurassic Park of SubQuantum Mechanics. We are to a certain extent wandering in no man's land, whereby heuristics are useful guides, but are well able to evolve. We will then need to continue to bring in more contemporary ideas for seasoned questions, as well as very old ideas, in order to provide further structure to such a program. Nevertheless, this framework does show that it is conceptually possible to explain Quantum Mechanics in a NeoClassical way, but that the path is very hard indeed, possibly requiring a large amount of advanced techniques and modelling work. We hope therefore that this introductory course has convinced that highly structured realistic theories which elude Bell-like assumptions can be built. And that there are natural options which involve hidden variables, virtual variables and processes at different levels, more in line with the contemporary higher formalisation by Computer Scientists of Aetiology, the study of causality. In Machine Learning there is a strong parallel (see [76]) between: *(i)* closed-systems statistical mechanics and supervised-learning; *(ii)* open-systems statistical mechanics and unsupervised-learning; and *(iii)* specific microscopic base of statistical models and reinforcement-learning techniques. Many of the most advanced machine learning process tend to be produced by the wise mix-and-match combination of techniques coming from all these three general methods. Similarly, in statistical mechanics the three techniques need often to be combined to achieve new results. In the same way, the approach here presented is seeking a similar mix-and-match optimisation in order to achieve as much of a reverse engineering of Quantum Mechanics, reverse engineering being a form of learning process. As D.Mermin noticed in [46], it is not constructive to use imagination wildly. But if it leads to a conceptual coherent structure, it does provide a base for the observation which D.Mermin quotes from J.S.Bell, about Bell's own theorems, that *what is proven by impossibility proofs, is lack of imagination.*

Because of the effective lower scale solid-state-like modelling approach, the discretisation and the potential effective use of regular geometry to provide a first level generalisation of these models, it seems that algebraic numbers play a prominent role and that higher arithmetics and its geometrisation language can be key tools for SubQuantum Mechanics. Its symmetries more likely to be found within number theory and its language. In order to reverse engineer further into the baryon structure and into the three particles families, so to link into the structure of high-energy physics, the very large amount of information within the various extensions of the Standard Model, Quantum String Theory, Loop Quantum Gravity and Conformal Field Theory is likely to be compatible to this framework. They might require to be re-explored from a different angle, which could also prove useful for their development. As a possible example, when compared to experiment, Lattice QCD can show higher accuracy than analytical formulas, suggesting that the discretisation scheme might encapsulate information about the SubQuantum structure of matter. As another possible example, neutrino oscillations could be arising as a signature of effective mass, due to the scattering of the neutrino's SubQuantum gas along the lateral directions of propagation of the neutrino: a specific and somehow different kind of mass, clarifying further the physical reasons of its weakness.

SubQuantum Mechanics might also have a cognitive follow-on implication for the organisation of mathematics. There should be a larger class of combinatorial dynamics which provide a basis for the (re)structuring of a very large part of mathematics from arithmetic topology in the broader sense. This would allow to reclassify much of the interconnections among different areas of pure mathematics using SubQuantum physics and models, as well as their broader combinatorial generalisations. There might be a non-abstract way to restate the Bourbaki program starting from the assumption that there is a *quasi-animistic principle* in how nature uses mathematics. A non-abstract *animistic* version of neo-Bourbakism. By this we mean that, by trying in a furious way so many mathematical structures, nature has already solved all the problems we are currently studying, used the solutions to structure itself, and can therefore complete calculations, at each atto-second, with speeds well beyond those of near future Quantum Computers.

XI. ACKNOWLEDGMENTS

The initial seeds leading to the physical framework hereby discussed find their roots out of the tentative analysis of a question made by C.Viterbo to the author in 1992 with respect to an envisaged unification of all symplectic singularities regularisation procedures (see [77]): many thanks to Claude for leaving the unpublished preprint online after so many years. In such a context, this framework suggests that the ADE correspondence and quasi-crystals symmetries appearing in the classification of Lagrangian singularities, which obsessed V.I.Arnold so much (see [78]) since after he became famous for KAM theory, has a geometrical basis in the solid-state-like structure of matter at SubQuantum level, which affects the nature and symmetry of the symplectic singularity from a topological classification point of view. The fact that the ADE classification for Lagrangian singularities appears more clearly by looking at the evolvements' symmetries becomes related to the fact that at the evolvements level it is easier to single out any hidden hyperobolicity and set it apart (see Figure 11). With hindsight it seems indeed possible to formalise a single approach unifying all procedures for the regularisation of symplectic singularities, across fields whereby the classical Hamiltonian formalism arises. Including the semi-classical limit of Quantum Mechanics. This seemed an heroic task then: how could one question Quantum Mechanics and Special Relativity at once? As a physicists, I could not allow myself. To achieve Claude's goal now, it seems appropriate to explore a metaplectic extension of the approach using symplectic capacities topological invariants, from which the method exposed in [77] does arise. At the time, no such concept could be identified, while it becomes natural today by looking at the semi-classical limit directly from SubQuantum Mechanics, skipping all together the Quantum Mechanical level of description. This in itself seems quite remarkable.

In 1993, P.Favia at EPFL allowed the author to be her assistant for one day of high energy electron microscopy measures, providing physical intuition towards the understanding of the Montgomery's pair correlation conjecture, by observing the equivalent imaging distortion effect of chaos generated around electron beams caustics and the imaging distortion caused by random vibrations. Also at the experimental physics level, some of the structuring of the concept of a SubQuantum web has been made possible through the study of well-above-room-temperature in-bulk Charge-Density-Wave-like macroscopic quantum phases in MonoPhosphate Tunsgsten Bronzes with Pentagonal Tunnels, with J.P.Pouget, in the first half of the '90s (see [79]). These phases appear starting from the stoichiometric parameter value $m = 8$, which is 2 electrons for each group of 8 WO_3 octahedra.

Since those days, a selection of discussions with many talented people contributed at reorganising the concepts here presented. More recently, M.Benedetti at UCL was key to improve clarity of exposition, allowing me to give a first series of lectures out of this course and suggesting specific features of this paper, such as the content of Figure 4 or the graphic approach for the content of Figure 8. Without M.Benedetti, the quality of this paper would be significantly below the current one, because of his role both as a supervisor and as a professional student. A special thanks goes to University College London for having enabled this course and to the Institut Henri Poincaré in Paris for hosting me for the couple of months needed to finalise this document.

Appendix A: Schrödinger Combinatorial Dynamics

1. Comparison of 1D Combinatorical Dynamics

If we use the same notation of Case I, the diffusion process of Case II in Figures 5 can then be written as:

$$\begin{cases} p_1(m,s+1) = \frac{1}{2}p_1(m-1,s) + \frac{1}{2}p_2(m+1,s) \\ p_2(m,s+1) = \frac{1}{2}p_2(m+1,s) + \frac{1}{2}p_3(m-1,s) \\ p_3(m,s+1) = \frac{1}{2}p_3(m-1,s) + \frac{1}{2}p_4(m+1,s) \\ p_4(m,s+1) = \frac{1}{2}p_4(m+1,s) + \frac{1}{2}p_1(m-1,s) \end{cases} \tag{A1}$$

One can observe immediately that, just like in Case I, on the right hand side there are always both one term of space argument equal to $(m-1)$ and one term with space argument equal $(m+1)$. These appear to be matched if we take cross differences. One can then change variables to $\phi_1 = p_1 - p_3$ and $\phi_2 = p_2 - p_4$ and the process will depend on the same net density again. This is because there are no vertical arrows for Case I and II in Figure 5. If we look for example at Case III instead, we will get:

$$\begin{cases} p_1(m,s+1) = \frac{1}{2}p_1(m-1,s) + \frac{1}{2}p_3(m-1,s) \\ p_2(m,s+1) = \frac{1}{2}p_2(m+1,s) + \frac{1}{2}p_1(m-1,s) \\ p_3(m,s+1) = \frac{1}{2}p_3(m-1,s) + \frac{1}{2}p_4(m+1,s) \\ p_4(m,s+1) = \frac{1}{2}p_4(m+1,s) + \frac{1}{2}p_2(m+1,s) \end{cases} \tag{A2}$$

Because of the vertical arrows, on the right hand side there are cases where both terms have the same space dependence. When taking the cross differences there are then differences on the right hand side which do not depend on the same space value. We can not change variables to a smaller set of variables such as ϕ_1 and ϕ_2. There can not be reduced variables for which a double interlaced process can be identified.

2. 8-steps Time Evolution in Position Space

For simplicity of notation we will calculate without the renormalisation parameter $\tilde{\alpha}$ and reinsert it at the end. We will keep the calculation as detailed and explicit as possible to allow the observation of the structure of the combinatorical dynamics. We start from the 1-step time evolution for the $\tilde{\phi}_i$ in Case I:

$$\begin{cases} \tilde{\phi}_1(m,s+1) = \frac{1}{2}\tilde{\phi}_1(m-1,s) - \frac{1}{2}\tilde{\phi}_2(m+1,s) \\ \tilde{\phi}_2(m,s+1) = \frac{1}{2}\tilde{\phi}_1(m-1,s) + \frac{1}{2}\tilde{\phi}_2(m+1,s) \end{cases} \tag{A3}$$

Then for two time steps the $m-1$ and $m+1$ terms disappear and only even multiples of spacing to the left and right of m remain:

$$\begin{cases} \tilde{\phi}_1(m,s+2) = \dfrac{1}{2}\tilde{\phi}_1(m-1,s+1) - \dfrac{1}{2}\tilde{\phi}_2(m+1,s+1) \\ \qquad\qquad = \dfrac{1}{2}\Big[\dfrac{1}{2}\tilde{\phi}_1(m-2,s) - \dfrac{1}{2}\tilde{\phi}_2(m,s)\Big] - \dfrac{1}{2}\Big[\dfrac{1}{2}\tilde{\phi}_1(m,s) + \dfrac{1}{2}\tilde{\phi}_2(m+2,s)\Big] \\ \tilde{\phi}_2(m,s+2) = \dfrac{1}{2}\tilde{\phi}_1(m-1,s+1) + \dfrac{1}{2}\tilde{\phi}_2(m+1,s+1) \\ \qquad\qquad = \dfrac{1}{2}\Big[\dfrac{1}{2}\tilde{\phi}_1(m-2,s) - \dfrac{1}{2}\tilde{\phi}_2(m,s)\Big] + \dfrac{1}{2}\Big[\dfrac{1}{2}\tilde{\phi}_1(m,s) + \dfrac{1}{2}\tilde{\phi}_2(m+2,s)\Big] \end{cases} \tag{A4}$$

Therefore:

$$\begin{cases} \tilde{\phi}_1(m,s+2) = \frac{1}{4}\tilde{\phi}_1(m-2,s) - \frac{1}{4}\Big[\tilde{\phi}_1(m,s) + \tilde{\phi}_2(m,s)\Big] - \frac{1}{4}\tilde{\phi}_2(m+2,s) \\ \tilde{\phi}_2(m,s+2) = \frac{1}{4}\tilde{\phi}_1(m-2,s) - \frac{1}{4}\Big[\tilde{\phi}_1(m,s) - \tilde{\phi}_2(m,s)\Big] + \frac{1}{4}\tilde{\phi}_2(m+2,s) \end{cases} \tag{A5}$$

We can then calculate $\phi_i(m,s+4)$ as $\phi_i\big(m,(s+2)+2\big)$ using the formulas above, which leads to:

$$\begin{cases} \tilde{\phi}_1(m,s+4) = \dfrac{1}{16}\Big\{\tilde{\phi}_1(m-4,s) \\ \qquad - \Big[3\tilde{\phi}_1(m-2,s) + \tilde{\phi}_2(m-2,s)\Big] + \Big[\tilde{\phi}_2(m,s) - \tilde{\phi}_1(m,s)\Big] \\ \qquad - \Big[\tilde{\phi}_1(m+2,s) - \tilde{\phi}_2(m+2,s)\Big] - \tilde{\phi}_2(m+4,s)\Big\} \\ \tilde{\phi}_2(m,s+4) = \dfrac{1}{16}\Big\{\tilde{\phi}_1(m-4,s) \\ \qquad - \Big[\tilde{\phi}_1(m-2,s) + \tilde{\phi}_2(m-2,s)\Big] - \Big[\tilde{\phi}_1(m,s) + \tilde{\phi}_2(m,s)\Big] \\ \qquad - \Big[\tilde{\phi}_1(m+2,s) - 3\tilde{\phi}_2(m+2,s)\Big] + \tilde{\phi}_2(m+4,s)\Big\} \end{cases} \tag{A6}$$

If we separate each contribution of factors 1, 2 and 2^2 in the 4-steps calculation above in order to keep each power of 2 contribution separate, we can then more easily calculate $\phi_i(m, s+8)$ as $\phi_i\big(m, (s+4)+4\big)$ in the form:

$$
\begin{cases}
\tilde{\phi}_1(m,s+8) = \dfrac{1}{\big((2^2)^2\big)^2}\Big\{\Big[\tilde{\phi}_1(m-8,s) - \tilde{\phi}_2(m+8,s)\Big] \\
\qquad + \Big[-8\tilde{\phi}_1(m-6,s) + 4\tilde{\phi}_2(m+6,s)\Big] + \Big[\tilde{\phi}_2(m-6,s) + \tilde{\phi}_1(m-6,s)\Big] + \Big[\tilde{\phi}_1(m+6,s) - \tilde{\phi}_2(m+6,s)\Big] \\
\qquad + \Big[4\tilde{\phi}_2(m-4,s) + 8\tilde{\phi}_2(m+4,s)\Big] - 4\tilde{\phi}_1(m+4,s) + \Big[\tilde{\phi}_1(m-4,s) - \tilde{\phi}_2(m-4,s)\Big] \\
\qquad\qquad - \Big[\tilde{\phi}_2(m+4,s) - \tilde{\phi}_1(m+4,s)\Big] \\
\qquad + \Big[4\tilde{\phi}_1(m-2,s) + 4\tilde{\phi}_2(m-2,s) + 4\tilde{\phi}_2(m+2,s)\Big] - \Big[\tilde{\phi}_1(m-2,s) + \tilde{\phi}_2(m-2,s)\Big] \\
\qquad\qquad + \Big[\tilde{\phi}_1(m+2,s) + \tilde{\phi}_2(m+2,s)\Big] \\
\qquad + \Big[4\tilde{\phi}_1(m,s) + 4\tilde{\phi}_2(m,s)\Big] - \Big[\tilde{\phi}_1(m,s) + \tilde{\phi}_2(m,s)\Big] \\
\tilde{\phi}_2(m,s+8) = \dfrac{1}{\big((2^2)^2\big)^2}\Big\{\Big[\tilde{\phi}_1(m-8,s) + \tilde{\phi}_2(m+8,s)\Big] \\
\qquad + \Big[-4\tilde{\phi}_1(m-6,s) - 8\tilde{\phi}_2(m+6,s)\Big] - \Big[\tilde{\phi}_1(m-6,s) + \tilde{\phi}_2(m-6,s)\Big] + \Big[\tilde{\phi}_2(m+6,s) - \tilde{\phi}_1(m+6,s)\Big] \\
\qquad + \Big[8\tilde{\phi}_1(m-4,s) + 4\tilde{\phi}_2(m-4,s)\Big] + 4\tilde{\phi}_1(m+4,s) + \Big[\tilde{\phi}_1(m-4,s) + \tilde{\phi}_2(m-4,s)\Big] \\
\qquad\qquad - \Big[\tilde{\phi}_1(m+4,s) + \tilde{\phi}_2(m+4,s)\Big] \\
\qquad + \Big[4\tilde{\phi}_1(m-2,s) + 4\tilde{\phi}_1(m+2,s) - 4\tilde{\phi}_2(m+2,s)\Big] + \Big[\tilde{\phi}_1(m-2,s) - \tilde{\phi}_2(m-2,s)\Big] \\
\qquad\qquad + \Big[\tilde{\phi}_1(m+2,s) - \tilde{\phi}_2(m+2,s)\Big] \\
\qquad + \Big[4\tilde{\phi}_1(m,s) - 4\tilde{\phi}_2(m,s)\Big] + \Big[\tilde{\phi}_2(m,s) - \tilde{\phi}_1(m,s)\Big]
\end{cases}
\tag{A7}
$$

Form the $8-$ *steps* time evolution above, we can see how the interlaced composition of different multiples of 1, 2, 2^2 and $(2^2)^2$ generates formulas which look asymmetrical at first sight, but which at a closer look do show some form of regularity.

In fact we then get:

$$\left\{\begin{array}{l}
\tilde{\phi}_1(m,s+8) = \frac{1}{(16)^2}\Big\{\tilde{\phi}_1(m-8,s) - \Big[7\tilde{\phi}_1(m-6,s)+\tilde{\phi}_2(m-6,s)\Big] + \Big[9\tilde{\phi}_1(m-4,s)+5\tilde{\phi}_2(m-4,s)\Big] \\
\qquad + \Big[5\tilde{\phi}_1(m-2,s)-\tilde{\phi}_2(m-2,s)\Big] + \Big[3\tilde{\phi}_1(m,s)-3\tilde{\phi}_2(m,s)\Big] + \Big[3\tilde{\phi}_1(m+2,s)-3\tilde{\phi}_2(m+2,s)\Big] \\
\qquad + \Big[3\tilde{\phi}_1(m+4,s)-\tilde{\phi}_2(m+4,s)\Big] + \Big[5\tilde{\phi}_2(m+6,s)-\tilde{\phi}_1(m+6,s)\Big] - \tilde{\phi}_2(m+8,s)\Big\} \\
\tilde{\phi}_2(m,s+8) = \frac{1}{(16)^2}\Big\{\tilde{\phi}_1(m-8,s) - \Big[5\tilde{\phi}_1(m-6,s)+\tilde{\phi}_2(m-6,s)\Big] + \Big[\tilde{\phi}_1(m-4,s)+3\tilde{\phi}_2(m-4,s)\Big] \\
\qquad + \Big[3\tilde{\phi}_1(m-2,s)+3\tilde{\phi}_2(m-2,s)\Big] + \Big[3\tilde{\phi}_1(m,s)+3\tilde{\phi}_2(m,s)\Big] + \Big[\tilde{\phi}_1(m+2,s)+5\tilde{\phi}_2(m+2,s)\Big] \\
\qquad + \Big[9\tilde{\phi}_2(m+4,s)-5\tilde{\phi}_1(m+4,s)\Big] + \Big[\tilde{\phi}_1(m+6,s)-7\tilde{\phi}_2(m+6,s)\Big] + \tilde{\phi}_2(m+8,s)\Big\}
\end{array}\right. \tag{A8}$$

We can obtain the renormalised version by multiplying the right hand sides by $(\sqrt{2})^8 = 16$ above, replacing the $\tilde{\phi}_i$ by the ϕ_i and taking s to be a multiple of 8 ($s \bmod 8 = 0$), $8\hat{s} = s$. Furthermore, in the continuum limit we can then develop in powers of δ, with $(x = m\delta, t = 8\hat{s}\epsilon)$, and get:

$$\left\{\begin{array}{l}
\phi_1(m,s+8) \simeq \frac{1}{16}\Big\{(1-7+9+5+3+3+3-1)\phi_1(m,s) \\
\qquad + \big[(-8)+(-7)(-6)+9(-4)+5(-2)+3(0)+3(2)+3(4)-(6)\big]\ \delta\ \frac{\partial\phi_1}{\partial x}(m,s) \\
\qquad + \big[(-8)^2-7(-6)^2+9(-4)^2+5(-2)^2+3(0)^2+3(2)^2+3(4)^2-(6)^2\big]\frac{\delta^2}{2}\frac{\partial^2\phi_1}{\partial x^2}(m,s) \\
\qquad + (-1+5-1-3-3-1+5-1)\phi_2(m,s) \\
\qquad + \big[(-1)(-6)+5(-4)+(-1)(-2)-3(0)-3(2)-4+5(6)-8\big]\delta\frac{\partial\phi_2}{\partial x}(m,s) \\
\qquad + \big[-(-6)^2+5(-4)^2-(-2)^2-3(0)^2-3(2)^2-(4)^2+5(6)^2-8^2\big]\frac{\delta^2}{2}\frac{\partial^2\phi_2}{\partial x^2}(m,s)+\ldots \\
\phi_2(m,s+8) \simeq \frac{1}{16}\Big\{(1-5+1+3+3+1-5+1)\phi_1(m,s) \\
\qquad + \big[(-8)+(-5)(-6)+(-4)+3(-2)+3(0)+(2)+(-5)(4)+(6)\big]\ \delta\ \frac{\partial\phi_1}{\partial x}(m,s) \\
\qquad + \big[(-8)^2-5(-6)^2+(-4)^2+3(-2)^2+3(0)^2+(2)^2-5(4)^2+(6)^2\big]\frac{\delta^2}{2}\frac{\partial^2\phi_1}{\partial x^2}(m,s) \\
\qquad + (-1+3+3+3+5+9-7+1)\phi_2(m,s) \\
\qquad + \big[-(-6)+3(-4)+3(-2)+3(0)+5(2)+9(4)+(-7)(6)+(8)\big]\delta\frac{\partial\phi_2}{\partial x}(m,s) \\
\qquad + \big[-(-6)^2+3(-4)^2+3(-2)^2+3(0)^2-5(2)^2+9(4)^2-7(6)^2+8^2\big]\frac{\delta^2}{2}\frac{\partial^2\phi_2}{\partial x^2}(m,s)+\ldots
\end{array}\right. \tag{A9}$$

Only the first and the last sums for the first equation in the previous formulas are not zero, and they are equal respectively to 16 and 128. Only the third and the fourth sums for the second equation are not zero, and they are equal respectively to (-128) and 16.

The values of the sums above do reveal that there is a high level of symmetry in the combinatorics of the 8-steps evolution, arising from the interlacing of the diffusion processes, but not immediately visible from the numerical coefficients.

We have provided all the detail above also to show that there is some form of group structure here. It seems somehow reminiscent of something possibly close to a flattened version of a Selmer group, as seen in the theory of elliptic curves. There should be some deformation from this flattened version linking to a different local discrete dynamic, including one modelled by elliptic curves arithmetics, as sketched in Figure 10.

Up to quadratic terms the power series above therefore simplify to:

$$\begin{cases} \phi_1(m, s+8) \simeq \phi_1(m,s) + 8\frac{\delta^2}{2}\frac{\partial^2\phi_2}{\partial x^2}(m,s) + \dots \\ \\ \phi_2(m, s+8) \simeq \phi_2(m,s) - 8\frac{\delta^2}{2}\frac{\partial^2\phi_1}{\partial x^2}(m,s) + \dots \end{cases} \tag{A10}$$

By taking the ϕ_i terms on the right to the left and dividing by 8ϵ:

$$\begin{cases} \dfrac{\phi_1(m, 8(\hat{s}+1)) - \phi_1(m,s)}{8\epsilon} \simeq \dfrac{\delta^2}{2\epsilon}\dfrac{\partial^2\phi_2}{\partial x^2}(m, 8\hat{s}) + \dots \\ \\ \dfrac{\phi_2(m, 8(\hat{s}+1)) - \phi_2(m,s)}{8\epsilon} \simeq -\dfrac{\delta^2}{2\epsilon}\dfrac{\partial^2\phi_1}{\partial x^2}(m, 8\hat{s}) + \dots \end{cases} \tag{A11}$$

We take the limit for $8\epsilon \to 0$, $\delta \to 0$, with $(\delta^2/2\epsilon) = (\hbar/2m_I)$ constant, $m\delta = x$ constant and $8\epsilon\hat{s} = t$ also constant

$$\begin{cases} \dfrac{\partial\phi_1(x,t)}{\partial t} = \dfrac{\hbar}{2m_I}\dfrac{\partial^2\phi_2}{\partial x^2}(x,t) \\ \\ \dfrac{\partial\phi_2(x,t)}{\partial t} = -\dfrac{\hbar}{2m_I}\dfrac{\partial^2\phi_1}{\partial x^2}(x,t) \end{cases} \tag{A12}$$

We can therefore consider to take the limit also by introducing the constant c for dimensional analysis coherence, and by using in the limit a single variable $\eta \to 0$, whereby $\epsilon = (\hbar/m_I c^2)\sqrt{\eta}$ and $\delta = (\hbar/m_I c)\eta$.

3. 8-steps Time Evolution in Momentum Space

The one time step transfer matrix for Case I, before any renormalisation is:

$$T_\epsilon = \frac{1}{2}\begin{pmatrix} e^{-ip\delta} & -e^{ip\delta} \\ e^{-ip\delta} & e^{ip\delta} \end{pmatrix} \tag{A13}$$

By algebraic calculation by hand or using automatic algebra calculators such as Wolfram, the 8 time steps evolution matrix is:

$$T_\epsilon^8 = \frac{e^{-6i\delta p}}{256}\begin{pmatrix} e^{-2ip\delta}(1-7e^{2ip\delta}+9e^{4ip\delta}+5e^{6ip\delta}+3e^{8ip\delta} & (-1+5e^{2ip\delta}-e^{4ip\delta}-3e^{6ip\delta}-3e^{8ip\delta} \\ \quad +3e^{10ip\delta}+3e^{12ip\delta}-e^{14ip\delta}) & \quad -e^{10ip\delta}+5e^{12ip\delta}-e^{14ip\delta}) \\ e^{-2ip\delta}(1-5e^{2ip\delta}+e^{4ip\delta}+3e^{6ip\delta}+3e^{8ip\delta} & (-1+3e^{2ip\delta}+3e^{4ip\delta}+3e^{6ip\delta}+5e^{8ip\delta} \\ \quad +e^{10ip\delta}-5e^{12ip\delta}+e^{14ip\delta}) & \quad +9e^{10ip\delta}-7e^{12ip\delta}+e^{14ip\delta}) \end{pmatrix}$$

$$= \frac{1}{256}\begin{pmatrix} (e^{-8ip\delta}-7e^{-6ip\delta}+9e^{-4ip\delta}+5e^{-2ip\delta}+3 & (-e^{-6ip\delta}+5e^{-4ip\delta}-e^{-2ip\delta}-3-3e^{2ip\delta} \\ \quad +3e^{2ip\delta}+3e^{4ip\delta}-e^{6ip\delta}) & \quad -e^{4ip\delta}+5e^{6ip\delta}-e^{8ip\delta}) \\ (e^{-8ip\delta}-5e^{-6ip\delta}+e^{-4ip\delta}+3e^{-2ip\delta}+3 & (-e^{-6ip\delta}+3e^{-4ip\delta}+3e^{-2ip\delta}+3+5e^{2ip\delta} \\ \quad +e^{2ip\delta}-5e^{4ip\delta}+e^{6ip\delta}) & \quad +9e^{4ip\delta}-7e^{6ip\delta}+e^{8ip\delta}) \end{pmatrix} \tag{A14}$$

By rearranging by wave vector:

$$T_\epsilon^8 = \frac{1}{256}\begin{pmatrix} e^{-8ip\delta} & -e^{8ip\delta} \\ e^{-8ip\delta} & e^{8ip\delta} \end{pmatrix} + \frac{1}{256}\begin{pmatrix} (-7e^{-6ip\delta}-e^{i6p\delta}) & (-e^{-6ip\delta}+5e^{6ip\delta}) \\ (-5e^{-6ip\delta}+e^{6ip\delta}) & (-e^{-6ip\delta}-7e^{6ip\delta}) \end{pmatrix} + \frac{1}{256}\begin{pmatrix} 3 & -3 \\ 3 & 3 \end{pmatrix}$$

$$+\frac{1}{256}\begin{pmatrix} (9e^{-4ip\delta}+3e^{4ip\delta}) & (5e^{-4ip\delta}-e^{4ip\delta}) \\ (e^{-4ip\delta}-5e^{4ip\delta}) & (3e^{-4ip\delta}+9e^{4ip\delta}) \end{pmatrix} + \frac{1}{256}\begin{pmatrix} (5e^{-2ip\delta}+3e^{2ip\delta}) & (-e^{2ip\delta}-3e^{2ip\delta}) \\ (3e^{-2ip\delta}+e^{2ip\delta}) & (3e^{-2ip\delta}+5e^{2ip\delta}) \end{pmatrix} \tag{A15}$$

By taking apart symmetric contributions at each wave vector number:

$$T_\epsilon^8 = \frac{1}{256}\begin{pmatrix} e^{-8ip\delta} & -e^{8ip\delta} \\ e^{-8ip\delta} & e^{8ip\delta} \end{pmatrix} + \frac{1}{256}\Big[\begin{pmatrix} -2\cos(6p\delta) & -2\cos(6p\delta) \\ 2\cos(6p\delta) & -2\cos(6p\delta) \end{pmatrix} + \begin{pmatrix} -6e^{-6ip\delta} & 6e^{6p\delta} \\ -6e^{-6p\delta} & -6e^{-6ip\delta} \end{pmatrix}\Big]$$

$$+\frac{1}{256}\Big[\begin{pmatrix} 3\times 2\cos(4p\delta) & -2\cos(4p\delta) \\ 2\cos(4p\delta) & 3\times 2\cos(4p\delta) \end{pmatrix} + \begin{pmatrix} 6e^{-4ip\delta} & 6e^{-4p\delta} \\ -6e^{4p\delta} & -6e^{4ip\delta} \end{pmatrix}\Big] \tag{A16}$$

$$+\frac{1}{256}\Big[\begin{pmatrix} 3\times 2\cos(2p\delta) & -2\cos(2p\delta) \\ 2\cos(2p\delta) & 3\times 2\cos(2p\delta) \end{pmatrix} + \begin{pmatrix} 2e^{-2ip\delta} & -2e^{2p\delta} \\ 2e^{-2p\delta} & 2e^{2ip\delta} \end{pmatrix}\Big] + \frac{1}{256}\begin{pmatrix} 3 & -3 \\ 3 & 3 \end{pmatrix}$$

Rather than having $2^8 = 256$ components, as it would have been for the initial process for the p_i, the derived coarse graining process implies a formula grouped into 8 terms:

$$T_\epsilon^8 = \tfrac{1}{256}\begin{pmatrix} e^{-8ip\delta} & -e^{8ip\delta} \\ e^{-8ip\delta} & e^{8ip\delta} \end{pmatrix} - \tfrac{6}{256}\begin{pmatrix} e^{-6ip\delta} & -e^{6ip\delta} \\ e^{-6ip\delta} & e^{6ip\delta} \end{pmatrix} + \tfrac{6}{256}\begin{pmatrix} e^{-4ip\delta} & -e^{-4ip\delta} \\ e^{4ip\delta} & e^{4ip\delta} \end{pmatrix} + \tfrac{2}{256}\begin{pmatrix} e^{-2ip\delta} & -e^{2ip\delta} \\ e^{-2ip\delta} & e^{2ip\delta} \end{pmatrix}$$

$$-\tfrac{2}{256}\begin{pmatrix} 1 & 1 \\ -1 & 1 \end{pmatrix}\cos 6p\delta + \tfrac{2}{256}\begin{pmatrix} 3 & -1 \\ 1 & 3 \end{pmatrix}\cos 4p\delta + \tfrac{2}{256}\begin{pmatrix} 3 & -1 \\ 1 & 3 \end{pmatrix}\cos 2p\delta + \tfrac{3}{256}\begin{pmatrix} 1 & -1 \\ 1 & 1 \end{pmatrix} \tag{A17}$$

There are therefore 8 classes of diffusion paths at the p_i interlaced double diffusion process level, each path in a group giving rise to the same phase-shift structure for the net densities after 8 steps. At the modulo 8 level, it is as-if there were 8 paths, each with the respective weighting factor.

The same calculations for Case II, reversed-Ord process, are similar and give:

$$T_\epsilon^8 = \tfrac{1}{256}\begin{pmatrix} e^{-8ip\delta} & e^{8ip\delta} \\ -e^{-8ip\delta} & e^{8ip\delta} \end{pmatrix} - \tfrac{6}{256}\begin{pmatrix} e^{-6ip\delta} & e^{6ip\delta} \\ -e^{-6ip\delta} & e^{6ip\delta} \end{pmatrix} + \tfrac{6}{256}\begin{pmatrix} e^{-4ip\delta} & -e^{-4ip\delta} \\ e^{4ip\delta} & e^{4ip\delta} \end{pmatrix} + \tfrac{2}{256}\begin{pmatrix} e^{-2ip\delta} & e^{2ip\delta} \\ -e^{-2ip\delta} & e^{2ip\delta} \end{pmatrix}$$

$$-\tfrac{2}{256}\begin{pmatrix} 1 & -1 \\ 1 & 1 \end{pmatrix}\cos 6p\delta + \tfrac{2}{256}\begin{pmatrix} 3 & 1 \\ -1 & 3 \end{pmatrix}\cos 4p\delta + \tfrac{2}{256}\begin{pmatrix} 3 & 1 \\ -1 & 3 \end{pmatrix}\cos 2p\delta + \tfrac{3}{256}\begin{pmatrix} 1 & 1 \\ -1 & 1 \end{pmatrix} \tag{A18}$$

It should be noted the swapping of minus sign across the diagonal for all matrices but for the 4th harmonics wave vector term.

If we develop in powers of δ, at the zeroth order we get, for Case I:

$$T_\epsilon^8 \simeq -\tfrac{1}{256}\begin{pmatrix} 1 & -1 \\ 1 & 1 \end{pmatrix} - \tfrac{6}{256}\begin{pmatrix} 1 & -1 \\ 1 & 1 \end{pmatrix} + \tfrac{6}{256}\begin{pmatrix} 1 & 1 \\ -1 & 1 \end{pmatrix} + \tfrac{2}{256}\begin{pmatrix} 1 & -1 \\ 1 & 1 \end{pmatrix}$$

$$-\tfrac{2}{256}\begin{pmatrix} 1 & 1 \\ -1 & 1 \end{pmatrix} + \tfrac{2}{256}\begin{pmatrix} 3 & -1 \\ 1 & 3 \end{pmatrix} + \tfrac{2}{256}\begin{pmatrix} 3 & -1 \\ 1 & 3 \end{pmatrix} + \tfrac{3}{256}\begin{pmatrix} 1 & -1 \\ 1 & 1 \end{pmatrix} = \tfrac{1}{16}\mathbb{I}_2 \tag{A19}$$

After renormalisation this gives the identity matrix $\mathbb{I}_2$. We did the calculations before renormalisation to avoid the reading nuisance generated by the appearance of the constant α in each part of the calculation. For Case II it is notable that one gets exactly the same result, both for the sum and for each single term.

Both Case I and II give nil at first order of δ. The second order is provided in Section III.

Appendix B: Dirac Combinatorial Dynamics

We recall the derivation of the Dirac equation by development in power series and taking the continuum limit. We start from equation (21) whereby we keep again for simplicity the notation (m, s) as a shortened form of $(m\delta, s\epsilon)$ for the argument of the functions involved:

$$\begin{cases} \phi_1(m, s+1) = (1 - \mu\epsilon)\ \phi_1(m-1, s) - (\mu\epsilon)\ \phi_2(m+1, s) \\ \phi_2(m, s+1) = (1 - \mu\epsilon)\ \phi_2(m+1, s) + (\mu\epsilon)\ \phi_1(m-1, s) \end{cases} \tag{B1}$$

Then:

$$\begin{cases} \phi_1(m, s+1) = (1 - \mu\epsilon)\Big[\phi_1(m, s) - \delta\frac{\partial\phi_1}{\partial x}(m, s) + \dots\Big] - \mu\epsilon\Big[\phi_2(m, s) + \delta\frac{\partial\phi_2}{\partial x}(m, s) + \dots\Big] \\ \phi_2(m, s+1) = (1 - \mu\epsilon)\Big[\phi_2(m, s) + \delta\frac{\partial\phi_2}{\partial x}(m, s) + \dots\Big] + \mu\epsilon\Big[\phi_1(m, s) - \delta\frac{\partial\phi_1}{\partial x}(m, s) + \dots\Big] \end{cases} \tag{B2}$$

By grouping at each order in δ and ϵ:

$$\begin{cases} \phi_1(m, s+1) - \phi_1(m, s) = -\mu\epsilon\Big[\phi_1(m, s) + \phi_2(m, s)\Big] - \delta\frac{\partial\phi_1}{\partial x}(m, s) + \mu\epsilon\delta\Big[\frac{\partial\phi_1}{\partial x}(m, s) - \frac{\partial\phi_2}{\partial x}(m, s)\Big] + \dots \\ \phi_2(m, s+1) - \phi_2(m, s) = -\mu\epsilon\Big[\phi_2(m, s) - \phi_1(m, s)\Big] + \delta\frac{\partial\phi_2}{\partial x}(m, s) - \mu\epsilon\delta\Big[\frac{\partial\phi_2}{\partial x}(m, s) + \frac{\partial\phi_1}{\partial x}(m, s)\Big] + \dots \end{cases} \tag{B3}$$

Dividing by ϵ we can see the terms relevant in the limit:

$$\begin{cases} \dfrac{\phi_1(m, s+1) - \phi_1(m, s)}{\epsilon} = -\mu\Big[\phi_1(m, s) + \phi_2(m, s)\Big] - \dfrac{\delta}{\epsilon}\dfrac{\partial\phi_1}{\partial x}(m, s) + \mu\delta\Big[\dfrac{\partial\phi_1}{\partial x}(m, s) - \dfrac{\partial\phi_2}{\partial x}(m, s)\Big] + \dots \\ \dfrac{\phi_2(m, s+1) - \phi_2(m, s)}{\epsilon} = -\mu\Big[\phi_2(m, s) - \phi_1(m, s)\Big] + \dfrac{\delta}{\epsilon}\dfrac{\partial\phi_2}{\partial x}(m, s) - \mu\delta\Big[\dfrac{\partial\phi_2}{\partial x}(m, s) + \dfrac{\partial\phi_1}{\partial x}(m, s)\Big] + \dots \end{cases} \tag{B4}$$

As $\epsilon \to 0$ and $s \to \infty$ with the product $s\epsilon = t$ fixed, and as $\delta \to 0$ and $m \to \infty$ with the product $m\delta = x$ fixed, while the ratio $(\delta/\epsilon) = c$ is also fixed, we get:

$$\begin{cases} \frac{\partial\phi_1}{\partial t}(x, t) = -\mu\Big[\phi_1(x, t) + \phi_2(x, t)\Big] - c\frac{\partial\phi_1}{\partial x}(x, t) \\ \frac{\partial\phi_2}{\partial t}(x, t) = -\mu\Big[\phi_2(x, t) - \phi_1(x, t)\Big] + c\frac{\partial\phi_2}{\partial x}(x, t) \end{cases} \tag{B5}$$

To highlight the transients and the interlaced wave equations at the same time, we can write:

$$\begin{cases} \frac{1}{c}\Big[\frac{\partial}{\partial t} + \mu\Big]\phi_1(x, t) + \frac{\partial\phi_1}{\partial x}(x, t) = -\frac{\mu}{c}\phi_2(x, t) \\ \frac{1}{c}\Big[\frac{\partial}{\partial t} + \mu\Big]\phi_2(x, t) - \frac{\partial\phi_2}{\partial x}(x, t) = \frac{\mu}{c}\phi_1(x, t) \end{cases} \tag{B6}$$

Appendix C: Lorentz Boost for D=1+1 Spinors

We show first that in D=1 the Lorentz transformation of a relativistic bi-spinor is diagonal. Although we take a more naive approach to be closer to the reverse engineering discussion, we effectively follow the more formally and complete paper [28].

The Lorentz transformations for a system of coordinates are given by the customary linear matrix with hyperbolic coefficients, whereby $\beta = (v/c)$, $\gamma = (1/\sqrt{1-\beta^2})$ and $\tanh\phi_r = (v/c)$:

$$\begin{pmatrix} ct \\ x \end{pmatrix} = \begin{pmatrix} \gamma(ct^{'}) & \beta\gamma(x^{'}) \\ \beta\gamma(ct^{'}) & \gamma(x^{'}) \end{pmatrix} = \begin{pmatrix} \frac{1}{\sqrt{1-\beta^2}} & \frac{\beta}{\sqrt{1-\beta^2}} \\ \frac{\beta}{\sqrt{1-\beta^2}} & \frac{1}{\sqrt{1-\beta^2}}) \end{pmatrix} \begin{pmatrix} ct^{'} \\ x^{'} \end{pmatrix} = \begin{pmatrix} \cosh\phi_r & \sinh\phi_r \\ \sinh\phi_r & \cosh\phi_r \end{pmatrix} \begin{pmatrix} ct^{'} \\ x^{'} \end{pmatrix} \tag{C1}$$

And the differential operators transform as:

$$\begin{cases} \partial_{ct} = (\cosh\phi_r)\ \partial_{ct'} + (\sinh\phi_r)\ \partial_{x'} \\ \\ \partial_{x} = (\sinh\phi_r)\ \partial_{ct'} + (\cosh\phi_r)\ \partial_{x'} \end{cases} \tag{C2}$$

Therefore:

$$\begin{cases} \partial_{ct} + \partial_{x} = (\cosh\phi_r + \sinh\phi_r)\big[\partial_{ct'} + \partial_{x'}\big] \\ \\ \partial_{ct} - \partial_{x} = (\cosh\phi_r - \sinh\phi_r)\big[\partial_{ct'} - \partial_{x'}\big] \end{cases} \tag{C3}$$

A very important feature of the Lorentz transformations is that they are linear. It is the coefficients of the linear transformation which have in turn a hyperbolic dependence from the velocity. If a vector transforms with a linear transformation, also a spinor field, which is a square root of a vector filed, will transform linearly but not with the same linear coefficients. Upon change of reference system a generic transformation for a $(1+1)D$ spinor (ψ_1, ψ_2) will be given by:

$$\begin{pmatrix} \psi_1 \\ \psi_2 \end{pmatrix} = \begin{pmatrix} A & B \\ C & D \end{pmatrix} \begin{pmatrix} \psi_1^{'} \\ \psi_2^{'} \end{pmatrix} = \begin{pmatrix} A\psi_1^{'} + B\psi_2^{'} \\ C\psi_1^{'} + D\psi_2^{'} \end{pmatrix} \tag{C4}$$

Where $AD - BC \neq 0$. To identify the form of the linear transformation matrix for the spinors, we need then to insert the formulas for the (ψ_1, ψ_2) and (ct, x) as functions of $(\psi_1^{'}, \psi_2^{'})$ and $(ct^{'}, x^{'})$ into the Dirac 1D equation. If $k_C = (m_I c/\hbar)$ is the Compton wave vector:

$$\begin{cases} \Big[\frac{1}{c}\frac{\partial}{\partial t} + \frac{\partial}{\partial x}\Big]\psi_1 = -k_C\ \psi_2 \\ \\ \Big[\frac{1}{c}\frac{\partial}{\partial t} - \frac{\partial}{\partial x}\Big]\psi_2 = k_C\ \hbar\psi_1 \end{cases} \tag{C5}$$

Which gives:

$$\begin{cases} (\cosh\phi_r + \sinh\phi_r)\ \big[\partial_{ct'} + \partial_{x'}\big](A\psi_1^{'} + B\psi_2^{'}) = -k_C\ (C\psi_1^{'} + D\psi_2^{'}) \\ \\ (\cosh\phi_r - \sinh\phi_r)\big[\partial_{ct'} - \partial_{x'}\big](C\psi_1^{'} + D\psi_2^{'}) = k_C\ (A\psi_1^{'} + B\psi_2^{'}) \end{cases} \tag{C6}$$

This has to be true for all $(\psi_1^{'}, \psi_2^{'})$ and has to give the same form of Dirac equation in order for the Lorentz invariance to be preserved. We therefore need to find A, B, C, D such that $\forall\ \psi_1^{'}, \psi_2^{'}$:

$$\begin{cases} \Big[\frac{1}{c}\frac{\partial}{\partial t'} + \frac{\partial}{\partial x'}\Big]\psi_1^{'} = -k_C\ \psi_2^{'} \\ \\ \Big[\frac{1}{c}\frac{\partial}{\partial t'} - \frac{\partial}{\partial x'}\Big]\psi_2^{'} = k_C\ \psi_1^{'} \end{cases} \tag{C7}$$

By multiplying by A the first equation in (C6) and by C the second equation in (C6), then the sum of the two products has on the right hand-side only the term $-k_C\ \psi_2^{'}(AD - BC)$. This in turn, a part for the factor of the determinant of the linear spinor transformation, is the functional form on the right hand side in the first equation of (C7) above. We can then divide such sum of products by $(AD - BC)$ to get the right terms on the right hand side. By requiring that all coefficients on the left match the functional form of the Dirac equation, what ever the spinor, we get:

$$\begin{cases} (\cosh\phi_r)[A^2 + C^2] + (\sinh\phi_r)[A^2 - C^2] = 1 \\ \\ (\cosh\phi_r)[A^2 - C^2] + (\sinh\phi_r)[A^2 + C^2] = 1 \\ \\ (\cosh\phi_r)[AB + CD] + (\sinh\phi_r)[AB - CD] = 0 \\ \\ (\cosh\phi_r)[AB - CD] + (\sinh\phi_r)[AB + CD] = 0 \end{cases} \tag{C8}$$

Therefore $ABCD = 0$. Say $B = 0$, then $AD = 1$ and $C = 0$. $D = A^{-1}$, i.e. the Lorentz boost in $1 + 1D$ is a loxodromic matrix in $PSL(2, \mathbb{C})$ in canonical form. Then:

$$A^2[\cosh\phi_r + \sinh\phi_r] = 1 \tag{C9}$$

Or also:

$$A = \sqrt[4]{\frac{c - v}{c + v}} = \sqrt{\sqrt{\frac{1 - \beta}{1 + \beta}}} \tag{C10}$$

The factor multiplying or dividing ψ_i to get $\psi_i^{'}$ is therefore the square root of the relativistic Doppler coefficient:

$$\begin{cases} \psi_1^{'}(x^{'}, t^{'}) = \sqrt[4]{\frac{c - v}{c + v}}\ \psi_1\Big(x(x^{'}, t^{'}), t(x^{'}, t^{'})\Big) \\ \\ \psi_2^{'}(x^{'}, t^{'}) = \sqrt[4]{\frac{c + v}{c - v}}\ \psi_2\Big(x(x^{'}, t^{'}), t(x^{'}, t^{'})\Big) \end{cases} \tag{C11}$$

Appendix D: Born Rule

Take a SubQuantum gas and its net densities in the Quantum limit (i.e. a Quantum particle). Take a very large number of substantially equal systems. Take one of the observables, say the energy. Consider the case that each of such particles are initially in a given state ψ and that the initial state can be decomposed over a base of countable stationary states ψ_n, each with given energy E_n, as in the case of bound states:

$$\psi = \sum_{n=0}^{\infty} c_n \psi_n \tag{D1}$$

From a SubQuantum point of view, before the measure is made there is an energy $E(\psi)$ which can be associated to the particle as an *extractable* energy. The un-zipping and re-zipping processes freeze then each particle into a stationary state that has given energy. For one of them indicate then by E_f the final state energy. The difference between the energy before and after the zipping and un-zipping for this specific particle is:

$$\Delta E_{particle} = E(\psi) - E_f \tag{D2}$$

Therefore the difference between final and initial energy can be either positive or negative depending on the relative size of $E(\psi)$ and E_f. If E_f is larger than $E(\psi)$, where is the excess energy coming from? If E_f is smaller than $E(\psi)$, where has the missing energy gone? By conservation laws it has been either released or absorbed (*extracted*) by the measuring instrument; and through the measuring instrument possibly released into (absorbed from) the calibration system. We can write:

$$\Delta E_{instrument} + \Delta E_{particle} = 0 \tag{D3}$$

Once all the sampling is completed then:

$$Cumulated\{\Delta E_{instrument}\} + \sum_{All\ particles} \Delta E_{particle} = 0 \tag{D4}$$

But because of the quadratic nature of the zipping and un-zipping process the probability of each final state being ψ_f is $|c_f|^2$. Therefore:

$$Cumulated\{\Delta E_{instrument}\} + \sum_{All\ particles} (E(\psi) - E_f)|c_f|^2 = 0 \tag{D5}$$

Absence of de-calibration is realised by setting:

$$Cumulated\{\Delta E_{instrument}\} = 0 \tag{D6}$$

Therefore:

$$\sum_{All\ particles} (E(\psi) - E_f)|c_f|^2 = 0 \tag{D7}$$

But $\sum_f |c_f|^2 = 1$. Therefore:

$$E(\psi) = \sum_{All\ particles} E_f |c_f|^2 \tag{D8}$$

Born rule for energy. This seems to confirm that the energy exchanged (extracted) through the collapse is carried by the SubQuantum gas and the SubQuantum web. While we can think of an energy carried by the SubQuantum gas alone before the collapse as equal to $\sum_f |c_f| E_f$, i.e. without the squaring. $E(\psi)$ provides then the total extracted energy through the sampling process, and therefore is to be considered a total extractable energy. Extractable from SubQuantum gas and web through un-zipping and re-zipping.

Appendix E: Lorentz Group Discretisations

The deep connection between the theory of complex variable functions and hyperbolic geometry finds its roots in ideas which go way back to before the beginning of mechanics. The mathematical formulation of the *lamina elastica* problem, initiated probably by the mathematician J.Nemorarius in the 13th Century, started to find its proper form with Galileo in the 17th Century. This and similar problems, as the non-linear pendulum, were much studied by all best mathematicians in the following couple of centuries, including J.L.Lagrange, N.H.Abel, C.G.Jacobi, K.Weierstrass and many others. And generated a blooming of mathematics much in Central Europe. Until F.Klein, L.Fuchs and H.Poincaré provided the resolving force for the full building of the bridge between complex function theory, Kleinian groups and hyperbolic geometry. Kleinian groups, being the discrete subgroups of the $PSL(2,\mathbb{C})$, provide a representation of the set of possible discretisations of the Lorentz transformations. Such formal and conceptual bridge has evolved into a highly structured translation dictionary in the second half of the 20th Century and never stops to provide surprises to our days (see [81]). It is instructive here to retrace the intellectual path, not chronologically, but in view of the ideas taught in this course. In order to see how they can help in the choice of discretisation of the Lorentz group. It will also prove useful to provide elements of the context in which these ideas have emerged.

As a young man, H.Poincaré seemed to be intrigued by sizeable holes, as a mining inspector and as a mathematician studying lacunary functions (functions with a large hole). H.Poincaré was a pupil of C.Hermite, who in turn was a late pupil of the French nobleman A.L.Cauchy one of the leading figures of the French intellectual elite. Hermite had found a path back to his social peers, accepting after years his permanent handicap which had made it impossible for him to finish the academic program by École Polytechnique. Under Hermite's supervision, Poincaré mathematical task was to develop the theory of functions of a complex variable with lacunary singularities. This task was meant to extend to singularities of $2D$ non-zero measure in the plane (lacunas) the already extremely successful theory initiated by Cauchy for singularities with point-like zero measure (poles) and $1D$-like singularities (logarithmic type). In the projective complex plane, these lacunary singularities are the external part of what is now called the Poincaré disk, whereby - by inverting the radial coordinate - all of the space outside the Poincaré disk becomes the lacunary singularity of the complex value function. In order to have a lacunary singularity one requires a mechanism which makes it harder to reach the lacunary boundary the more you get close to it. This mechanism is what today we call hyperbolicity. But hyperbolicity arises in different forms. One which turned out to be effectively equivalent to the one looked at by Poincaré had already been well studied outside of Cauchy's theory. At the time it had become quite sophisticated within the German school, from Gauss and Riemann to Klein and Fuchs, whose work adopted by Penrose then inspired later part of the famous Escher artwork. Escher gave it beauty, but unfortunately took it out of context, making us forget that the key source which had lead to such mathematical research by the German school, was actually classical mechanics.

Possibly out of fascination by the German science he had studied, Poincaré seemed to have suggested indirectly that the way other beliefs seemed to manage the relationship between Science and Religion might have been more effective than the approach adopted by those within his mainstream belief. For a Frenchman coming form the core of his country's conservative society, Poincaré was also being too close to the German mathematical elite, with no excuse whatsoever. He was close to the point of Poincaré honouring L.Fuchs, a disciple of F.Klein, by giving Fuchs' name to the discrete subgroups of $SL(2,\mathbb{R})$, a specific part of the Kleinian groups. To get away with a not so popular approach within his social group, Poincaré possibly had to prove his allegiance by challenging a bit aggressively the competitors in the German camp. Maybe this might give a context to the fact that Klein had an exhaustion while competing with Poincaré; and Hilbert had to face a difficult environment at the Paris mathematical congress where he stated his famous problems. Poincaré also seems to have called back those in the latin world who dared exploring other German intellectual ways too much, typically Peano in Italy, who was leading the latin élite into the path of German-British formal logic, a domain daring to seek to define from mathematics *what is truth*. VERITAS validation being under the only authority of the religious institutions under Canonical Law in the latin countries. The last one who had dared in Italy had been Galileo and, despite his fame and rehabilitation, to our days and even in his home town of Pisa, nobody seems to know where is Galileo's house. Peano got away better than Galileo, so that those who live in Cuneo seem to know today where his house is, but he got no fame, except among the specialists. Although these kind of non-stated and possible unconscious factors might have contributed towards the French school focus on areas as complex function theory, it was also possibly one of the factors which caused formal logic to be effectively banned and separated as much as possible to the area of philosophy in France. To our days in fact, the Anglo-Saxon concept of *Computer Science* seems totally absent in contemporary French culture, whereby *Computer Science* in the Anglo-Saxon cultural sense, is a field with very structured cognitive bridges with all the areas of knowledge, be it technology or science, economics or behavioural sciences, medicine or psychology, art and philosophy, and so on. Computer Science, in fact, is not just a technical tool, but is a highly sophisticated theoretical formalisation of cognitive sciences. It seems then ironic if some of the sophisticated French mathematics coming from those days became so important for reasons arising within

Computer Science, while the *Poincaré-Klein dictionary* with its extensions and their relevance to physics might have been partially lost. We will then try to recover it a bit in this Appendix, trying to start to repair the possible negative effect of a cognitive blocking barrier in the past.

To remind how classical mechanics can be the source of hyperbolic geometry, it is useful to step back and to recall the basic physics of Galileo's *lamina elastica*. This is a system that today would be considered in civil engineering for the simple case of an horizontal bar fixed on one side to a column and with the opposite side free to move. On the free side a weight is temporarily imposed and the stability of the vibrations is studied. The free side of the horizontal bar vibrates then up and down. When the bar is moving **back** towards its horizontal position, the elastic force is acting **together** with the force of gravity if the bar is **above** the horizontal position, while is acting **against** the force of gravity when the bar is **below** the horizontal position. On the opposite, when the bar is moving **away** from the horizontal position, the elastic force is acting **against** the force of gravity if the bar is **above** the horizontal position, while it is acting **together** with the force of gravity when the bar is **below** the horizontal position. There are then four different combinations of the two forces which alternate in a rotating way, a bit like the alternating of the Ord process, Case I in Figures 5. This generates a strain which alternates on the bar. But if the vibration are not too large, there is a stable vibrational regime which can be easily observed and measured. This corresponds to the fact that in the linear approximation whereby the recalling elastic force is treated as a harmonic oscillator and gravity is a constant acceleration, the equations of mechanics are integrable, there is no dissipation (despite the strain!) and the phase space trajectories have the well known shape of an horizontal number 8, each quadrant corresponding to one of the four configurations explained, as summarised in Figure 11. If we explore further the analogy with Case I in Figure 5, then the two modes in the bottom of Figure 11 would correspond to the two option of scattering or not scattering.

This surprising integrability is caused by the fact that the strain is in a form which recycles energy among vibrational (elastic) modes and modes which are damping or amplifying (against or with the gravity acceleration). This is what today we describe with an elliptic curve and provide parametric description with elliptic functions, as it is equivalent to the movement of a particle on a constrained spherical surface (see [82–84]). A large number of classical mechanics phenomena fall into this class of mathematical formalisation. Many of these phenomena were known well before Galileo, but what changed then is that they were put within the context of the high formalisation and conceptualisation of mechanics, whereby all details could be formalised and calculated (starting with the Bernoullis and Euler in Bern, leveraging on the Italian school). The key problems which fell in the same group were the non-linear pendulum (solved fully only later by Jacobi), the vertical version of the elastic bar called the buckling problem (solved by Euler), and the strained spinning top where the axis of rotation does not necessary go through the centre of gravity (many important works, including Poincelet, whereby the more contemporary solution is given by Klein [31]). The Kepler problem is also in this class (conservative strain between gravitational and inertial forces), but the feature is hidden by the double degeneracy of the problem (a shy emergence of the equivalence principle), which simplifies it significantly, and arises only when the time dependence of the planet trajectory needs to be calculated. In selected symmetrical cases, the three body problem falls in the same group. The source of number fields and modern number theory is found here in these non-linear integrable problems of classical mechanics, and Gauss saw it early on and so clearly that he could formalise higher arithmetics as-if it was a separate field. But even if artificially separated from her beloved sources, the queen of mathematics finds the way back to them, all the times, leaving an Ariadne's thread for us to see.

The theory of elliptic functions is at the core of the mathematical solution of these problems, as well as for the understanding of their physics. As a matter of fact they also provide the analytical tool fully solving the geometry for the general solution of the single-unknown algebraic equation of the 5th degree, being at a transitional order between the lower degrees which are solvable by quadrature and the higher degrees which are solvable by hyper-elliptic functions - such geometry change possibly to provide an ingredient for the understanding of the context of the yet unmotivated Fermat Last Theorem statement. Being a judge, Fermat was little concerned about writing down the Law: he was concerned about applying the Law and on which principles, therefore unlikely that such a statement was written without an heuristic at all, even if tentative, even if not really correct.

Also thanks to Weierstrass function theory, elliptic curves formalism provides now a mapping into an algebraic form whereby the physics seems hidden, but the high level of structure with its symmetries is highlighted. The mapping into the Poincaré models of hyperbolic geometry becomes then a lexicographic tool enabling to use the complex function theory evolved from Cauchy's theory. This is so powerful, that Poincaré was able to obtain results at a speed that made Klein fall into exhaustion. We can actually thank Poincaré for having caused Klein an exhaustion, as this was followed by an amazing period of productivity in mathematical physics by Klein, highlighting among other things the direct link between Klein's Erlangen program and these problems of classical mechanics, which in turn do provide a clear foundational motivation for Klein's program (see [31]). Poincaré became then so acquainted with hyperbolic geometry that he was the first to clearly recognise that Lorentz transformations where really just a form of hyperbolic geometry. Lorentz at least intuitively understood the classical mechanics connection to elliptic functions

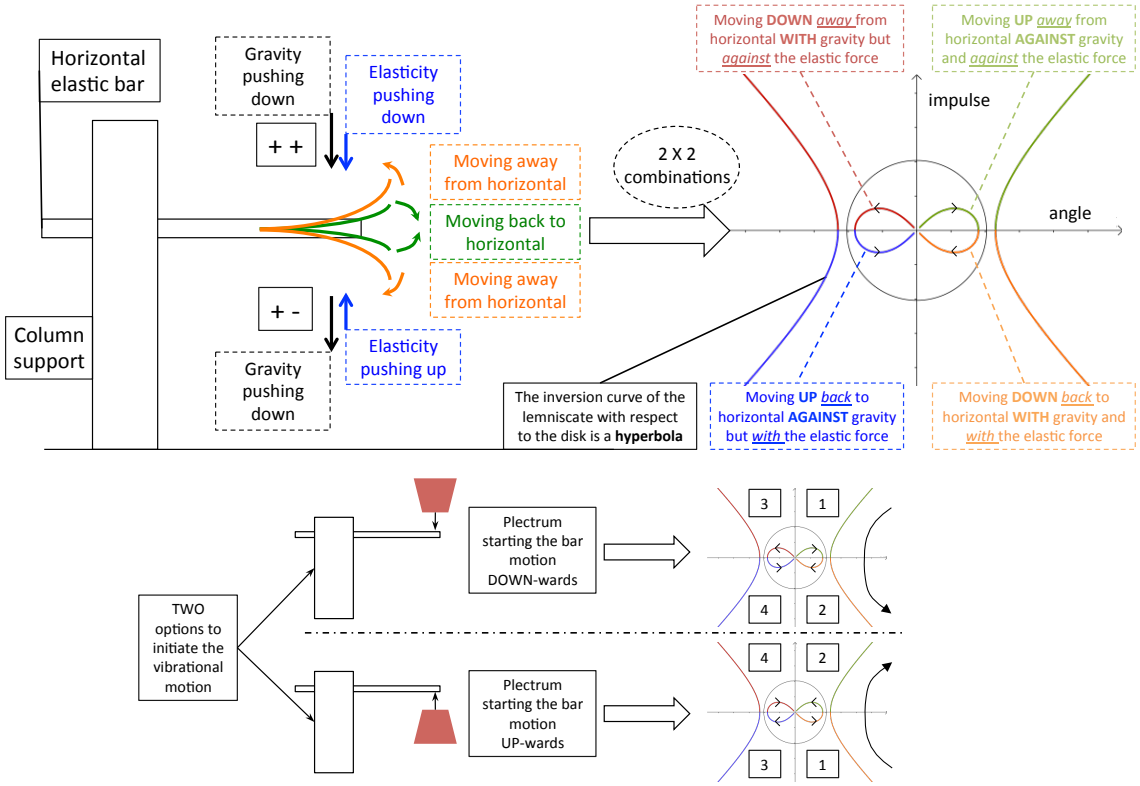

FIG. 11. Top of the figure: classical linearised mouth harp in a gravitational field. Showing the four combinations of motion with respect to the alignment of the two forces: gravity and elasticity. The infinity shaped curve on the right is the lemniscate, describing the (double) periodic motion. The inverse curve with respect to the drawn disk, by the function $1/z$ if the phase space is represented as an Argand plane, is a hyperbola: a graphical way to highlight the hyperbolic character of the lemniscate. Such hyperbolic features are also visible in other ways by drawing the evolute or the involute (evolvement) curve of the lemniscate. Bottom of the figure: for a given action, the oscillations are given by the combination of two main modes, differentiated by the vertical direction towards which the mouth harp is pushed to initiate the sound. The two modes are not equivalent: one starts with two forces acting together (pick and gravity pushing down) and one against (elasticity pulling back), while the other starts with one force acting to initiate the motion (from the action of the pick) and two forces acting against (gravity and elasticity). The oscillations have to remain within the bounds of these two modes. At given action and under noise, the probability of a given oscillation mode can be modelled by a Bernoulli process, with a probability of being in one of the modes related to the logistic function $x(1-x)$.

and the physical relationship to strain. He was therefore encouraged to look for a microscopical theory explaining what kind of strain was behind the formal structure of his transformations. This led to emission theories, but with the fundamental mistake that the pervading substance in the universe to be seen as enabling the strain was also believed to be a medium for the propagation of electro-magneto-mechanical waves. This constrained the models so they could justify only one component of the hyperbolicity or the other, but never the full geometry.

When the hypothetical medium role in the propagation of electromagnetic waves was shown to be incorrect even in the more limited case where the light emitting source and the detector are not moving with respect to each other, as in the Michelson-Morley experiment, the role of a pervading medium as an enabling agent for strain was dropped at the same time. The framework in this course allows us to clarify that, by a contextual version of the original emission theories, it is possible to separate the two matters and to model the strain even if there is no medium for the propagation of electromagnetic waves. The matter might have been overlooked because it did not seem that the two features could be analysed separately, which on the opposite is natural within this re-formulation of SubQuantum Mechanics.

In parallel to the complex-function-theory to hyperbolic-geometry correspondence, through the 19th Century, the imaginary unit rotation representation in the complex plane enabled to represent incompressible two dimensional

flows of hydrodynamics and electrostatics through conformal invariance. $2D$ potential theory became related to complex dynamics, whereby the iteration of complex functions generalised the Poincaré map approach to the paths of the lines of force. The simple centre-symmetric smooth case in $2D$ could then be mapped to increasingly more complex problems. G.Julia price-winning memoire of 1918 and P.Fatou work clarified the extent of the power of such techniques, by identifying highly complex generalisations of the Poincaré disk which are now known as Julia-sets (the interior) and Fatou-sets (the exterior). Because of the mapping of the Poincaré disk to most of the Julia sets, this was also showing that hyperbolic geometry survives in very unusual and in principle unfriendly environments. It was then time to complete the building work of the bridge started by Klein and Poincaré, by walking through it in the opposite direction and then back and forth many times, realising an extended *Poincaré-Klein dictionary*. L.Alfhors and L.Bers explored then how to test such methods limits, identifying and developing the theory of quasi-conformal mappings (see [85]). This in turn led D.Sullivan towards the formulation of a quasi-conformal mapping extension of the original dictionary, which translated results and conjectures between the dynamics of holomorphic functions and the study of Kleinian groups. Which enabled a speed-up in the understanding of one topic from the other and vice-versa. And took us to recent times, where J.C.Yoccoz on the complex function side versus W.P.Thurston on the Kleinian groups and Riemann surfaces side have unravelled and clarified old problems and new structures. But the full dictionary seems to have become overly complex and its multiple links to the original physics, at least partially, lost. As-if another one of Ariadne's threads had been swiped away at some stage.

In fact, as this dictionaries were only starting to find their contemporary form, on the side something happened which might have unintentionally highjacked the cognitive path: M.J.Feigenbaum studied the route to chaos numerically using the iteration of a deformation of the logistic map (see [86]). He was coming from the study of turbulence, whereby Navier-Stokes equations are projected over a discrete subspace of periodicities' modes, in order to make the reduced equations treatable from a computational point of view. The huge importance of these works relate not only to the understanding of a relevant subset of dynamical systems' complexity from a computational point of view, but also and very much to the fact that such numerical systems provide quite efficient and simple ways to produce random numbers generators of good quality, a fact of paramount importance for Computer Science in the 1970s and to our days. Feigenbaum made indeed his own company out of improved Monte Carlo techniques for option pricing algorithms. Empirical observations in the study of turbulence had strongly identified its randomness-like features. Therefore the study of turbulence and random numbers generators were seen as closely equivalent. With hindsight such connection was too optimistic to fully explain turbulence, but it turned out to be successful for Computer Science random number generators. In fact, one of the two key features of turbulence was indeed treatable as deterministic chaos, arising from a draconian reduction of the degrees of freedom involved in the relevant fluid dynamics. The logistic map is the simplest of these discrete reductions as it effectively describes only the two main competing modes. As a matter of fact, the logistic function appears in general any time we encounter a smooth concave function close to a maximum, whereby the immediate values of the function on the two sides of the maximum correspond to a constrained area of variations of a control parameter for a given dynamical system. The two extreme points of such constrained area of variation represent then the extremal configurations. Within the theory of convection as a path to turbulence, this configuration arises in the description of the splitting of convection eddies. At the same time, in Computer Science, the logistic map is based on the logistic function used by Boole at the beginning of the 19th Century to schematically represent a decision-making process: a finalised decision being modelled by the zeros of the function, i.e. $(0, 1)$, while the intermediate values being retained to model all possible interpolating undecided preferences. It was also introduced possibly by analogy to the use of the logistic function in competing population and similar dynamics. In case of absence of decision, such as through the iteration of the logistic map away from $(0, 1)$, it was not surprising in decision-making theory that it could lead to decision-making unpredictability. As it is ancient wisdom that no decision-making leads to social chaos, which was incorrectly used to justify dictatorship, at least for emergency situations, since ancient times. The fact that the complex analytic extension of the logistic map (see [87]), by simple change of variable, linked directly into Julia-set theory, was then seen as quite promising and encouraged further search for a next generation complex numbers version of similar random numbers generators. It was then very relevant to understand what happened when complexifying Feigenbaum approach. This also required to reverse the analytical approach of Julia-Fatou by studying the variation of the parameter in the complex polynomial dynamics, rather than studying the variation of the complex variable in the plane at a given parameter. Considering the parallel study of complex function theory and Kleinian groups, it does not seem surprising that on the group theoretical side the Mandelbrot set had also been identified, without noticing that there was a level of mathematical complexity looking promising for a next generation random number generator (see [88]). From a Computer Science point of view, the study of complex iterations of the logistic map also provided a way to complexify Boole's approach to logic, well before the more recent complexification of decision making theory whereby it was preferred to follow a semi-empirical approach in order to connect to the use of Quantum formalism (see [80]). Unknowingly, the underlying forces providing the foundations for the abstract research had been hijacked. From the bridge between hyperbolic geometry and integrable strained systems of nonlinear Classical Mechanics or Special Relativity, towards the practical

imperatives of Computer Science. We will then try to reconnect them back starting from the analysis which first identified the relevance of the Mandelbrot set in the study of Kleinian groups.

In the study of discrete hyperbolic symmetries, the modular group represents the base model and environment. The modular group $\Gamma = PSL(2,\mathbb{Z})$ is just $SL(2,\mathbb{Z})$ with its action on the Argand plane through Möbius transformations (see [17]) with integer coefficients. The variable in the Argand plane can be seen then as the ratio of the two components of a three dimensional complex bi-spinor as done to build spinor calculus and its complexification to twistor theory (see [89]). The modular group is a two-generators discrete subgroup of $PSL(2,\mathbb{C})$ where the generators are the inversion S (but for a sign, the symplectic matrix, a square root of minus the identity) and the translation T:

$$S = \begin{pmatrix} 0 & -1 \\ 1 & 0 \end{pmatrix} \qquad\qquad T = \begin{pmatrix} 1 & 1 \\ 0 & 1 \end{pmatrix} \tag{E1}$$

$Sz = -1/z$ corresponds to the swap and change of one sign for ψ_1 and ψ_2 (a Dirac-like inversion), with z being the ratio between the two components of the bi-spinor. T corresponds to the replacement of ψ_1 by the sum of the two components of the bi-spinor, while the second component remains unchanged. Therefore T is the basic building block to build changes of variables providing different integer combinations of SubQuantum densities. In this case the two-generators subgroup of $PSL(2,\mathbb{C})$ is generated by a parabolic transformation T, or a null-rotation in the language of spinors, and a rotation transformation S.

Discrete subgroups of $PSL(2,\mathbb{C})$ are called Kleinian groups (although in some literature this is extended to subgroups of $PGL(2,\mathbb{C})$ whereby one can relate one to the other with the appropriate scaling factors from the value of the determinant). If $\mathbb{C}$ is limited to $\mathbb{R}$ then the discrete subgroups of $PSL(2,\mathbb{R})$ are called Fuchsian groups. We see here that their classifications seems to be closely related to the options at SubQuantum level to discretise the Lorentz transformations all together in $3+1D$ or to discretise a given $1+1D$ restriction. When T is kept and the other generator is varied one can still obtain a discrete 2-generator subgroup of $PSL(2,\mathbb{C})$. To generalise the modular group, following [88], we call then the two generators:

$$X = \begin{pmatrix} 1 & 1 \\ 0 & 1 \end{pmatrix} \qquad\qquad Y = \begin{pmatrix} a & b \\ c & d \end{pmatrix} \tag{E2}$$

It is then a classical result by Shimizu and Leutbecher that if X and Y generate a discrete subgroup of $PSL(2,\mathbb{C})$, then $|c| \geq 1$ or $c = 0$ (see [88] and references therein). Although these conditions can be made more general, to study in general the 2-generators subgroups of $PSL(2,\mathbb{C})$, which are the simplest full generalisation of the modular group, one really needs an implication in the other direction, i.e. a criteria to say if X and Y are generators of a discrete subgroup of $PSL(2,\mathbb{C})$. Brooks and Matelski found at the end of the 1970s a criterion which applies to X and Y, when X is loxodromic, therefore with $(Trace\ X)^2 \neq [0,4]$. As this corresponds to Lorentz boosts along rotated axis, this just means that we are looking at 2-generators discretisation of Lorentz transformations which seems relevant for SubQuantum Mechanics. In such case one then defines the Brooks and Matelski sequence as in [88]:

$$Y_1 = YXY^{-1} \qquad Y_2 = Y_1 X Y_1^{-1} = YXY^{-1}X(YXY^{-1})^{-1} \qquad Y_{i+1} = Y_i X Y_i^{-1} \tag{E3}$$

To state the Brooks-Matelski condition one needs to rewrite the sequence using two complex variables from hyperbolic geometry. The first one is the complex translation length τ of X, i.e. the complex hyperbolic distance between: *(i)* a geodesics perpendicular to the axis of X going through its fixed points; and *(ii)* the geodesic obtained by applying the transformation X to the first geodesic. The real part of τ gives the Lorentz boost and the imaginary part provides the rotation.

Such angle only depends on X and identifies it in full:

$$X = \begin{pmatrix} \cosh\frac{\tau}{2} & \sinh\frac{\tau}{2} \\ \sinh\frac{\tau}{2} & \cosh\frac{\tau}{2} \end{pmatrix} \tag{E4}$$

The second hyperbolic complex parameter is the complex hyperbolic distance β_i between the axis of X and the axis of Y_i. This second parameter allows to write the action of Y_i as:

$$Y_i X Y_i^{-1} = \begin{pmatrix} \cosh\frac{\tau}{2} & e^{\beta_i}\sinh\frac{\tau}{2} \\ e^{-\beta_i}\sinh\frac{\tau}{2} & \cosh\frac{\tau}{2} \end{pmatrix} \tag{E5}$$

Using these two complex hyperbolic variables, the Brooks-Matelski sequence is rewritten as (note that the factors (1/2) for τ do not appear anymore):

$$\cosh \beta_{i+1} = (1 - \cosh \tau) \cosh^2 \beta_i + \cosh \tau \tag{E6}$$

If we multiply both sides by $(1 - \cosh \tau)$, this can be simplified by introducing the non-hyperbolic variables, back to the ordinary coordinates for the complex plane:

$$C(\tau) = (1 - \cosh \tau) \cosh \tau \qquad z_i = z(\tau, \beta_i) = (1 - \cosh \tau) \cosh \beta_i \tag{E7}$$

Starting from $i = 1$, the Brooks-Matelski sequence can then be written as:

$$z_{i+1} = z_i^2 + C \tag{E8}$$

The Brooks-Matelski condition for the group generated by X and Y to be a 2-generator discrete subgroup of $PSL(2, \mathbb{C})$ is then that the previous sequence is bounded in the complex plane. Note that the variable $C(\tau)$ is the complex logistic function $x(1 - x)$, where $x \in \mathbb{C}$ (we use x to avoid confusion with the z above) is represented with a complex hyperbolic parametrisation. Note that the formula for z_1 provide a two-variable version of the complex logistic map iterations $(1 - x)w$, each variable with its complex hyperbolic parametrisation. We can further extend the sequence back to $i = 0$ by setting $z_0 = 0$. In the specific case of $\beta = \tau$ we then get the definition of the Mandelbrot set. Which arises from the iteration of the complex logistic function except for a linear change of variables. Figure 12 provides a graphical synthesis of the cross relationships among these widely studied problems. Non-discrete (continuous) 2-parameters sub-groups of the Lorentz group are the continuum limit of these discrete 2-parameters sub-groups, the continuum version being discussed also in [34] with respect to Special Relativity.

Each part of the Mandelbrot set corresponds to a given number of iterations required in order to observe the periodicity or quasi-periodicity of the complex dynamics arising from the iteration of the complex logistic map, rewritten on variables which relate to the Brooks-Matelski analysis. Being in the complex plane and the M-set being simply connected, quasi-conformal mapping theory allows to study the quasi-potential around the set and its spectacular features. Quasi-conformal mappings can here stretch the deformation of the standard $2D$ static potential from potential theory to a maximum, enabling the transformation between the Poincaré disk and the boundary of the fractal set to preserve hyperbolic-geometrical structures. Quasi-conformal mappings, in fact, can be locally defined by only three points ratios, therefore adapting locally to the highly structured boundary, insinuating in-between its local details (see [90]). The overabundant four point geometry definition is more popular, but it tends to hide this toolkit property of the quasi-conformal mappings, which clarifies the reason of their relevance for these problems.

From this perspective, the Mandelbrot set should probably be looked at as a complex plane stereographic projection of a $3D$ four-pointed tetrahedral-like version of the Feigenbaum doubling route to chaos. The cardioid-like central generating lobe would reflect then the side-ways $3D$ to $2D$ projection of a $3D$ object. The Buddhabrot structure for the internal of the M-set provides then projective information about the $3D$ shape and orientation in space. The nose of the Mandelbrot set would be related to one of the pointing axes. The four points minimal coordination in $3D$ of a tetrahedron can then be recovered by identifying two axis on the sides and by adding the vertical projection direction. In each dimension n in fact, the minimalistic coordination is $n+1$ (this is also the basis of V.I.Arnold's proof of Hilbert 13th Problem in 1957), which is also connected to the already mentioned fact that a straight-hedge coordination is $n > 2$ is not minimal and likely to cause combinatorics inefficiencies for a discrete decomposition of space ($n = 2$ is special because of the star-triangle relation: the triangle coordination is 6, more than the corresponding straight-hedge coordination of 4, but the star coordination is 3, less than straight-hedge; in $n = 1$ there is only one option anyways).

We can now reverse the Brooks-Matelski change of variable, using the variables:

$$\cosh \tau = \frac{1 + \sqrt{1 - 4C}}{2} = \tilde{\gamma} \tag{E9}$$

$$\cosh \frac{\tau}{2} = \sqrt{\frac{\tilde{\gamma} + 1}{2}} \tag{E10}$$

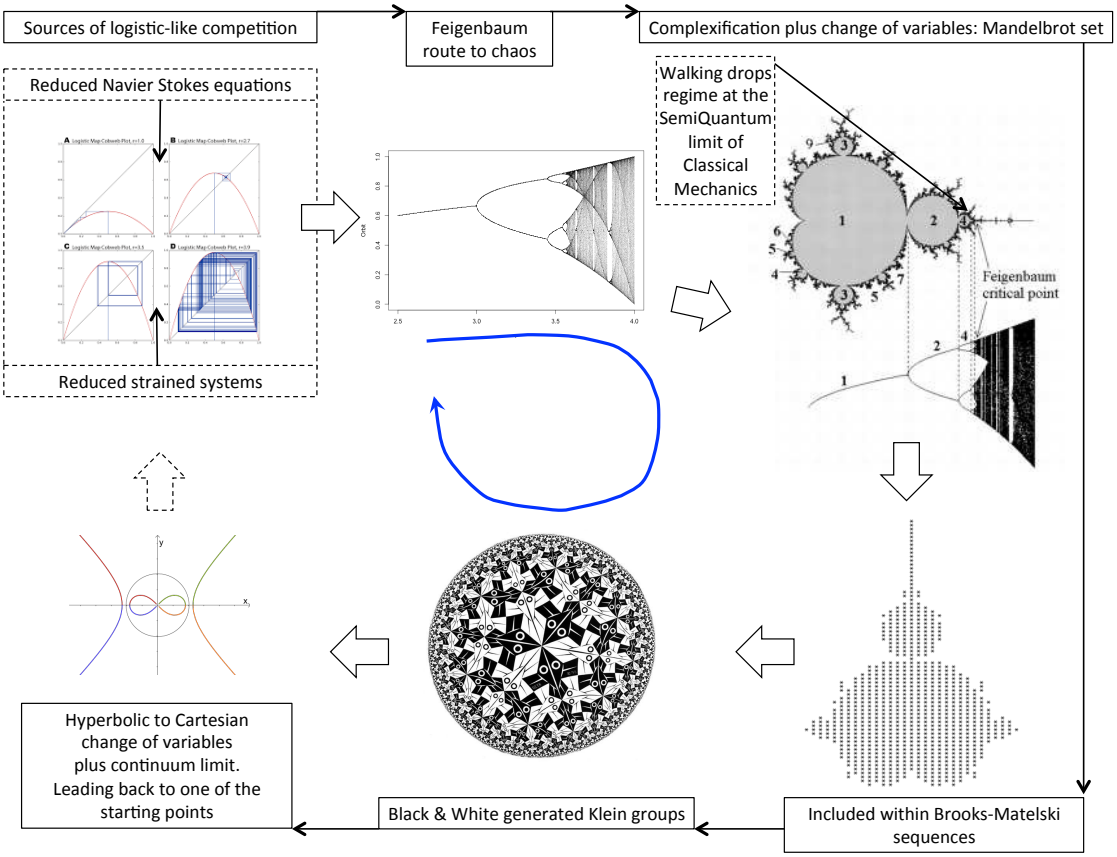

FIG. 12. Graphical summary of well known areas of study, linking specific forms of non-linearity to complex variable function theory and hyperbolic geometry. The logistic map arising in a wide range of non-linear problems is a model to the universal Feigenbaum route to chaos. After a change of variables, its complex version leads to the study of the Mandelbrot set in the complex plane. Which in turn is a specific case of the iterative study of 2-generators discrete subgroups of $PSL(2,\mathbb{C})$, here represented by the Esher two colourings of the hyperbolic plane in its unit disk representation. At the continuous limit this leads back to lemniscate-like classical mechanical systems or to the dissipation-induced dimensional-reduction of selected dissipative systems. Graphics taken from the internet under open source policy, allowing free use for didactical purposes, as here.

$$\begin{aligned} e^{\beta_i} &= \cosh\beta_i + \sinh\beta_i \\ &= \cosh\beta_i + \sqrt{1+\cosh{\beta_i}^2} \\ &= \frac{z_i}{\tilde{\gamma}} + \sqrt{1+\left(\frac{z_i}{\tilde{\gamma}}\right)^2} \end{aligned} \tag{E11}$$

Given a point C in the Mandelbrot set, there is then z_1 with $\beta_1 = \tau$, defining an X and Y, which generate an iteration of Y_i, which in turn are discrete and form a 2-generators discretisation of the Lorentz group in the $PSL(2,\mathbb{C})$ representation. These are a generalisation of the modular group for which we have focused the simplified discretisation discussion in the paragraph on the Lorentz boost, in the sense that they are 2-generators discrete subgroups. Many are trivial, with just a few items. Others are more structured, particularly as we move toward the pointy nose of the Mandelbrot set. Higher order polynomial generalisations of the Mandelbrot set should contribute towards the study of the n-generators discrete subgroups of the Lorentz group. The iterations of the Mandelbrot sequences become trivial if a change of variable can be made to a base whereby the polynomial to iterate becomes linear (renormalisation). Through a change of variables this linearisation problem can be restated in term of linearisation of germs of analytic diffeomorphisms, for which the solution is exactly known (see [91] and references therein). When the constants involved are complex, the linearisability depends on the phase. The linearisation condition on the phase

α, measured in multiples of 2π, is the now celebrated Brujno condition. If the continuous fraction approximating $\alpha \in \mathbb{R}\backslash\mathbb{Q}$ is (P_n/Q_n), the condition is a constraint on the denominators of the successive approximations. Each integer denominator $Q_{n+1} > Q_n$ sets the scale refinement with respect to the previous Q_n and their dependence on n implicitly defines the scaling law arising by the successive approximations refinements:

$$\sum_{n=1}^{\infty} \frac{\log Q_{n+1}}{Q_n} < \infty \tag{E12}$$

For $\alpha \in \mathbb{R}\backslash\mathbb{Q}$ the sum above with $\log Q_n$ instead of $\log Q_{n+1}$ always converges. The Brujno condition is therefore equivalent to the request that the scaling of Q_n at the denominator of the continuous fraction development follows at most a power law $Q_{n+1} \simeq Q_n^a$ with $a > 1$ constant. A.D.Brujno introduced this set of numbers in the 1960s, being dense on the real line, dense in the transcendental numbers, as a key tool to build his power geometry arising from the optimal description of selected non-linear classical mechanical problems like the restricted three body problem (therefore one expects to have a translation of the Brujno condition to elliptic functions theory, which would also be useful). It seems therefore appealing to seek a relationship between the non-renormalisable winding numbers, i.e. the lack of Brujno condition, and the possible breach of discrete Lorentz invariance by investigating the sequence of change of variables involved and their physical meaning in this context. This approach linking discretisation of Lorentz invariance, hyperbolicity and fractal geometry should further encourage to explore the idea that the Feigenbaum constants are possibly periods $\mathbb{\Omega}$ in the sense of [59], or at the boundary between $\mathbb{\Omega}$ and the set of fully transcendental numbers, because of their physical generative nature. This might provide a physical reason for the difficulty to prove if the Feigenbaum numbers are transcendental or not. Furthermore the Yoccoz para-puzzle techniques might encrypt physical relevant information for the purpose of Lorentz invariance discretisation analysis and in particular for the area immediately outside of the Mandelbrot set, where technical information about the breach of discrete Lorentz invariance might be found. Schottky groups might prove useful to study higher spins and multiple particle entangled configurations.

---

[1] R. Bellman and R. Kalaba, *Selected Papers on Mathematical Trends in Control Theory* (Dover Publ., New York, 1964).
[2] H.F.Judson, *The Eighth Day of Creation: Makers of the Revolution in Biology*, expanded 2013 commemorative ed. (Cold Spring Harbor Laboratory Press, Cold Spring Harbor, New York, 1979).
[3] J.J. Fleming, "Sub-Quantum Entities," Philosophy of Science **31**, 271–274 (1964).
[4] J. Grea, "Remarques Concernant les Relations Pouvant Exister entre la Mécanique Quantique et une Théorie Subquantique Possible," Annales de l'IHP, Physique Théorique **8**, 275–286 (1968).
[5] N. Seiberg and E. Witten, "Electric-Magnetic Duality, Monopole Condensation, and Confinement in N=2 Supersymmetric Yang-Mills Theory," arXiv: hep-th/9407087v1, (July 1994).
[6] C. Mao, "The Emergence of Complexity: Lessons from DNA," Public Library of Science (PLOS) Biology **2**, e431 (2004).
[7] H.M. Haggard and C. Rovelli, "Black Hole Fireworks: Quantum-gravity Effects Outside the Horizon Spark Black to White Hole Tunneling," arXiv: gr-qc/1407.0989, (July 2014).
[8] R.M. Wald, *General Relativity* (The University of Chicago Press, 1984).
[9] D. Pines, *The Many Body Problem, Lecture Notes and Reprint Volume*, edited by D. Pines (W.A.Benjamin Inc., 1962).
[10] A. Ottolenghi, "About a Possible Path Towards the Reverse Engineering of Quantum Mechanics," arXiv: quant-ph/1111.5215, (November 2011).
[11] G.N.Ord, "The Schrödinger and Dirac Free Particle Equations without Quantum Mechanics," Preprint, University of Western Ontario (1991).
[12] M.V. Berry, "Riemann's Zeta Function: a Model for Quantum Chaos?" in *Quantum Chaos and Statistical Nuclear Physics. Springer Lecture Notes in Physics*, Vol. 263, edited by T.H. Seligman and H. Nishioka (Springer-Verlag, 1986) pp. 1–17.
[13] S. Sachdev, "Beckenstein-Hawking Entropy and Strange Metals," arXiv: heph-th/1506.0111v4, (August 2015).
[14] F. Pastawski, B. Yoshida, D. Harlow, and J. Preskill, "Holographic Quantum Error-Correction Codes: Toy Models for the Bulk/Boundary Correspondence," arXiv: heph-th/1503.06237v2, (July 2015).
[15] D. de Carle, *Clock and Watch Repairing* (NAG Press, 2010).
[16] A.M. Turing, "The Chemical Basis of Morphogenesis," Philosophical Transactions of the Royal Society of London. Series B, Biological Sciences **Vol. 237**, 37–72 (1952).
[17] T.M. Apostol, *Modular Functions and Dirichlet Series in Number Theory* (Springer-Verlag, 1990).
[18] D. Mumford, *Tata Lectures on Theta I* (Birkhäuser Verlag, Basel., 1983).
[19] B. Riemann, "On the Number of Prime Numbers less than a Given Quantity (Über die Anzahl der Primzahlen unter einer gegebenen Grösse.)," Monatsberichte der Berliner Akademie (1859; 1998 English translation by D.R.Wilkins).
[20] H.J. Josephs, *Heaviside's Electric Circuit Theory* (Methuen & Co, London, 1950).
[21] A.S. Fokas, "A Novel Approach to the Lindelöf Hypothesis," arXiv: math.CA/1708.06607v4, (June 2018).
[22] F. Dyson, "Birds and Frogs," Notice of the AMS **56**, 212–223 (2009).
[23] M.V. Berry and J.P. Keating, "The Riemann Zeros and Eigenvalue Asymptotics," SIAM Review **41**, 236–266 (1999).

[24] G. Sierra and J. Rodrìguez-Laguna, "The H=xp Model Revisited and the Riemann Zeros," arXiv: math-ph/1102.5356v1, (February 2011).

[25] C.M. Bender, D.C. Brody, and M.P. Müller, "Comment on 'Comment' on ≪Hamiltonian for the Zeros of the Riemann Zeta Function≫," arXiv: quant-ph/1705.06767v1, (May 2017).

[26] A. Zewail, "Femtochemistry, Atomic-Scale Dynamics of the Chemical Bond Using Ultra-Fast Lasers," Chemistry Nobel Lecture, www.nobelprize.org (1999).

[27] M.A. Nielsen and I.L. Chuang, *Quantum Computation and Quantum Information* (Cambridge University Press, 2000).

[28] N. Wheeler, "Dirac Equation in 2-dimensional Spacetime," (2000), reed College Physics Department.

[29] E. Fermi, *Notes on Quantum Mechanics* (The University of Chicago Press, Chicago, 1954).

[30] G. Rash, *Probabilistic Models for Some Intelligence and Attainment Tests (1960/80)*, edited by Danish Institute for Educational Research (The University of Chicago Press, Copenhagen, 1980).

[31] F.Klein, *Mathematical Theory of the Top. Lectures Delivered on the Occasion of the Sesquicentennial Celebration of Princeton University* (Charles Scribner's Sons, New York, 1897).

[32] ICARUS Collaboration, "Measurement of the Neutrino Velocity with the ICARUS Detector at the CNGS Beam," arXiv: hep-ex/1203.3433v3, (March 2012).

[33] OPERA Collaboration, "Measurement of the Neutrino Velocity with the OPERA Detector in the CNGS Beam," arXiv: hep-ex/1109.4897v4, (July 2012).

[34] A.G. Cohen and S.L. Glashow, "Very Special Relativity," arXiv: hep-ph/0601236v1, (January 2006).

[35] A.Pais, *'Sottile è il Signore ...' La vita e la scienza di Albert Einstein (translation, 1982 book: 'Subtle is the Lord ...')* (Boringhieri, 1986).

[36] Various, "Grand Théorème de Fermat, 1641 - 1994," Quadrature, Ed.du Choix **N.22** (Été 1995).

[37] N. Elkies, "On $A^4 + B^4 + C^4 = D^4$," Mathematics of Computation **51**, 825–835 (1988).

[38] T. Paul, *Affine Coherent States and the Radial Schödinger Equation I. Radial Harmonic Oscillator and Hydrogen Atom* (Centre de Physique Theorique, Section 2, CNRS, Luminy, Marseille, France, 1984).

[39] Van der Waerden, *Sources of Quantum Mechanics* (North-Holland Publishing Co., Amsterdam, 1967).

[40] R. Angeloni, *Unity and Continuity in Niels Bohr's Phylosophy of Physics* (Leo S.Olschki, Firenze, 2013).

[41] B. Hoffmann, *The Strange Story of the Quantum* (Dover Publications, New York, 1947).

[42] E. Schrödinger, "The Final Affine Field Laws I," Proceedings of the Royal Irish Academy. Section A: Mathematical and Physical Sciences **Vol. 51 (1945-1948)**, 163–171 (1947).

[43] C.A. Fuchs and R. Schack, "Quantum-Bayesian Coherence: The No-Nonsense Version," arXiv: quant-ph/1301.3274v1, (January 2013).

[44] D.B. Rubin, "Estimating Causal Effects of Treatements in Randomized and NonRandomized Studies," Journal of Educational Psychology **66**, 688–701 (1974).

[45] The Big Bell Test Collaboration, "Challenging Local Realism with Human Choices," arXiv: quant-ph/1805.04431v1, (May 2018).

[46] N.D. Mermin, "Hidden Variables and the Two Theorems by John Bell," Review of Modern Physics **65**, 803–815 (1993).

[47] J. Pearl, *Causality* (Cambridge University Press, 2000).

[48] A.A. Belavin, B.Ya. Zel'dovich, A.M. Perelomov, and V.S. Popov, "Relaxation of Quantum Systems with Equidistant Spectra," Journal of Experimental and Theoretical Physics (JETP) **29**, 145–150 (1969).

[49] O. Costa de Beauregard, "Time Symmetry and the Einstein Paradox," Il Nuovo Cimento **Vol.42 B**, 41–64 (1977).

[50] J. Conway and S. Kochen, "The Free Will Theorem," arXiv: quant-ph/0604079v1, (April 2006).

[51] A. Ottolenghi, *Sur la Liaison Entre Volatilité Locale et Volatilité Implicite*, Internship Report. Available through Research Gate. To the best of my knowledge, unpublished. (BNP, Ingéniérie des Marchés, 1996).

[52] J.D. Norton, "The Dome: A Simple Violation of Determinism in Newtonian Mechanics." http://www.pitt.edu/ jdnorton/Goodies/Dome/ (2005).

[53] R.P. Feynman, "Simulating Physics with Computers," Int.J.Theor.Phys. **21**, 467 (1982).

[54] M.C. Berg, "The Double Cover of the Real Symplectic Group and a Theme from Feynman's Quantum Mechanics," International Mathematic Forum **Vol.7**, 1949–1963 (2012).

[55] Y. Couder, S. Protiere, E. Fort, and A. Boudaoud, "Dynamical Phenomena: Walking and Orbiting Droplets," Nature **437**, 208 (2005).

[56] S. Perrard, M. Labousse, M. Miskin, E. Fort, and Y. Couder, "Self-organization into Quantized Eigenstates of a Classical Wave-driven Particle," Nature communications **5**, ncomms4219 (2014).

[57] A. Eddi, *Marcheurs, Dualité Onde-particule et Mémoire de Chemin*, Ph.D. thesis, Université Paris-Diderot-Paris VII (2011).

[58] R. Brady and R. Anderson, "Why Bouncing Droplets are a Pretty Good Model of Quantum Mechanics," arXiv: quant-ph/1401.4356, (January 2014).

[59] M. Kontsevitch and D. Zagier, "Periods," Institut des Hautes Études Scientifiques (Mai 2011).

[60] J. Walker, "Drops of Liquid Can be Made to Float on the Liquid. What Enables Them to do So?" Sci.Am. **238**, 123–129 (1978).

[61] R. Rosa, "The Merli–Missiroli–Pozzi Two-Slit Electron-Interference Experiment," Physics in Perspective **14**, 178–195 (2012).

[62] Y. Couder and E. Fort, "Single-particle Diffraction and Interference at a Macroscopic Scale," Phys.Rev.Letters **97**, 154101 (2006).

[63] T. Beatus, T. Tlusty, and R. Bar-Ziv, "Burgers Shock Waves and Sound in a 2d Microfluidic Droplets Ensemble," Physical

review letters **103**, 114502 (2009).
[64] K. Batygin, "Schrödinger Evolution of Self-gravitating Discs," Monthly Notices of the Royal Astronomical Society **475**, 5070–5084 (2018).
[65] Z.K. Minev and al., "To Catch and Reverse a Quantum Jump Mid-flight," arXiv: quant-ph/1803.00545, (March 2018).
[66] G.N.Ord, "Schrödinger's Equation and Discrete Random Walks in a Potential Field," Annals of Physics **250**, 63–68 (1996).
[67] G.N.Ord and A.S.Deakin, "Classical Spin in a Potential Field," Int. Journal of Theoretical Physics **36**, 2013–2021 (1997).
[68] E.J. Gumbel, "Les Valeurs Extrêmes des Distributions Statistiques," Annales de l'IHP **5**, 115–158 (1935).
[69] A. Connes, "Trace Formula in Noncommutative Geometry and the Zeros of the Riemann Zeta Function," arXiv: math/9811068v1, (November 1998).
[70] G.N. Ord and A.S. Deakin, "Random Walks and Schrödinger Equation in 2+1 Dimensions," Journal of Physics A **30**, 819–830 (1997).
[71] B. Nagy and R. Strand, "Neighborhood Sequences in Diamond Grid - Algorithms with Four Neighbors," in *Lecture Notes in Computer Science. International Workshop on Combinatorial Image Analysis*, Vol. 5852, edited by P. Wiederhold and R.P. Baneva (Springer-Verlag, Berlin, Heidelberg, 2009) pp. 109–121.
[72] J.F. Sadoc and R. Mossseri, *Geometrical Frustration* (Cambridge University Press, 1999).
[73] P. Cartier, "A Mad Day's Work: from Grothendieck to Connes and Kontsevich, the Evolution of Concepts of Space and Symmetry," Bulletin (New Series) of the American Mathematical Society **Volume 38**, Pages 389–408 (2001).
[74] T. Sunada, "On the K_4 crystal," Seminar at the Isaace Newton Institute, University of Cambridge. http://www.newton.ac.uk/files/seminar/20070123143015301-150451.pdf (2015).
[75] R. Penrose, *The Road to Reality* (Vintage, 2005).
[76] H.W. Lin, M. Tagemark, and D. Rolnick, "Why Does Deep and Cheap Learning Work so Well?" arXiv: cond-mat/1608.08225v4, (August 2017).
[77] A. Ottolenghi, "Solutions Géneralisées pour l'Équation de Hamilton-Jacobi dans le cas d'Évolution," (1992), on Research Gate. Mathematics Diploma dissertation. English version: A.Ottolenghi and C.Viterbo *Variational Solutions of Hamilton-Jacobi Equations.* (1995). `www.math.ens.fr/~viterbo/Ottolenghi-Viterbo.pdf`. Unpublished.
[78] V.I. Arnold, *Huygens & Barrow, Newton & Hooke: Pioneers in Mathematical Analysis and Catastrophe Theory from Evolvements to Quasi-crystals* (Birkhäuser Verlag, Basel., 1990).
[79] A. Ottolenghi and J.P. Pouget, "Evidence of High Critical Temperature Charge Density Wave Transitions in the $(PO_2)_4(WO_3)_{2m}$ Family of Low Dimensional Conductors for $m \geq 8$," J.Phys.I (France) **6**, 1059 (1996).
[80] J. R. Busemeyer and P. D. Bruza, *Quantum Cognition and Decision* (Cambridge University Press, 2012).
[81] M. Rees, "One Hundred Years of Complex Dynamics," Proc.Math.Phys.Eng.Sci. (Proc. A) The Royal Society (2016).
[82] A.L. Baker, *Elliptic Functions* (J. Wiley & Sons, New York, 1890).
[83] F. Lemmermeyer, *Reciprocity Laws. From Euler to Eisenstein.* (Springer-Verlag, Berlin, Heidelberg, New York, 1991).
[84] L.C. Washington, *Elliptic Curves. Number Theory and Cryptography* (CRC Press, 2008).
[85] L.V. Alfhors, *Lectures on Quasiconformal Mappings* (American Mathematical Society, Providence, Rhode Island, 1966).
[86] J.M. Feigenbaum, "Quantitative Universality for a Class of Nonlinear Transformations," Journal of Statistical Physics **Vol.19**, 25–52 (1978).
[87] B.B. Mandelbrot, *Fractal Aspects of the Iteration of* $z \to \lambda z(1-z)$ *for Complex* λ *and* z, Tech. Rep. (IBM T.J. Watson Research Center; available on Harvard University website, 1980).
[88] R. Brooks and J.P. Matelski, "The Dynamics of the 2-Generator Subgroups of PSL$(2,\mathbb{C})$," Proceedings of the 1978 Stony Brook Conference on Riemann Surfaces and Related Topics (1980).
[89] R. Penrose and W. Rindler, *Spinors and Space-time* (Cambridge University Press, 1984).
[90] A. Ottolenghi, "Une Definition Géometrique des Applications Quasi-conformes," (April 1992), on Research Gate. Dissertation for the Mathematics Master course in Conformal and Quasi-Conformal Mappings by A.Douady. Unpublished.
[91] S. Marmi, "An Introduction to Small Divisors Problems," arXiv: math/0009232v1, (September 2000).